427 | April 1983

SCHRIFTENREIHE SCHIFFBAU

K. Eggers und S.D. Sharma

Festkolloquium zur Emeritierung von Karl Wieghardt

TUHH
Technische Universität Hamburg-Harburg

Festkolloquium zur Emeritierung von Karl Wieghardt

K. Eggers, S.D.Sharma **,** Hamburg, Technische Universität Hamburg-Harburg, 1983

Schriftenreihe Schiffbau
Schwarzenbergstraße 95c
D-21073 Hamburg

http://www.tuhh.de/vss

INSTITUT FÜR SCHIFFBAU DER UNIVERSITÄT HAMBURG

Bericht Nr. 427

Festkolloquium zur Emeritierung von Karl Wieghardt

K. Eggers

S.D. Sharma

Hamburg, April 1983

VORWORT

Am 31. März 1982 wurde Professor Karl Wieghardt emeritiert, nachdem er an unserem Institut fast über die ganze Zeit seit der Gründung im Jahre 1952 gewirkt hatte. Aus diesem Anlaß wurde ein Festkolloquium durchgeführt, bei dem ein großer Kreis von Freunden und ehemaligen Schülern versammelt war.

Wir hatten acht Kollegen aus aller Welt zu Vorträgen über Themen aus dem Bereich der maritimen Hydrodynamik eingeladen. Dabei war aber vorerst nicht an eine gemeinsame Veröffentlichung der Reihe dieser Beiträge gedacht. Da jedoch vier Vorträge bereits in Manuskriptform vorlagen, folgten wir einem mehrfach geäußerten spontanen Wunsch, die Arbeiten in gedruckter Form zu sammeln. Die restlichen Arbeiten werden anderwärts erscheinen, soweit sie sich in der vorliegenden Form für eine Veröffentlichung eignen. So sind die theoretischen Ausführungen von Professor T.Y. Wu über lange Wellen auf flachem Wasser, für welche sich überraschend Zusammenhänge mit dem Bericht von Professor J.V. Wehausen über experimentelle Untersuchungen aufzeigten, inzwischen in erweiterter Form auf dem 14ten Symposium on Naval Hydrodynamics in Ann Arbor vorgetragen worden und werden in den dortigen Proceedings zu finden sein. Andererseits konnte die nicht nur optisch sehr farbige Darstellung von Professor J.N. Newman über seine Durchsegelung des Nordatlantiks aus drucktechnischen Gründen nicht einbezogen werden.

Hamburg, im März 1983 Die Herausgeber

PREFACE

Professor Karl Wieghardt retired from office on March 31st, 1982 after nearly thirty years of service in our Institute starting soon after its inauguration in 1952. To celebrate this event an "informal" colloquium had been organized, which was attended by a large number of his friends and former students.

Eight colleagues from all over the world followed our invitation and contributed lectures on various topics within the broad field of marine hydrodynamics.
We had not originally intended to publish formal proceedings, but the ready availability of four manuscripts has encouraged us to meet the spontaneous desire of several participants to study the material in writing.
The remaining lectures will either appear in print elsewhere or are, unfortunately, not amenable to adequate reproduction on paper.
Thus the theoretical exposition of Professor T.Y. Wu on long waves in shallow water, which incidentally turned out to be closely complementary to the experimental investigations reported by Professor J.V. Wehausen, has been subsequently presented in extended form at the 14th ONR Symposium on Naval Hydrodynamics at Ann Arbor in August '82 and will appear in due course in its Proceedings. On the other hand, Professor J.N. Newman's colorful slide-show on his sailing cruise across the North Atlantic had to be omitted for purely graphical reasons.

Hamburg

March, 1983 The Editors

Festkolloquium

anläßlich der Emeritierung von

Professor Dr. rer. nat. Karl Wieghardt

am Montag, dem 29. März 1982,
im Institut für Schiffbau der Universität Hamburg

P r o g r a m m

9.00 - 9.30 h Ansprachen

Prof. Hansjörg Petershagen, Direktor des Instituts für Schiffbau
Prof. Hansjörg Sinn, Senator für Wissenschaft und Forschung
Dr. Peter Fischer-Appelt, Präsident der Universität Hamburg

9.30 - 12.30 h Vorträge (Vorsitz: Prof. Klaus Eggers)

Über die inkompressible Potentialströmung im Staupunkt spitzer Körper
Prof. Klaus Oswatitsch, Technische Universität Wien

Ships in Very Shallow Water
Prof. John V. Wehausen, University of California, Berkeley

Kaffeepause

The Science and Art of Wave Forecasting
Prof. Klaus Hasselmann, Max-Planck-Institut für Meteorologie, Hamburg

Nonlinear Long Waves
Prof. Theodore Y. Wu, California Institute of Technology, Pasadena

Imbiß im Institut

14.00 - 17.00 h Vorträge (Vorsitz: Dr. Som D. Sharma)

Calculation of Ship Frictional Resistance Increase due to Surface Roughness
Dr. Eiichi Baba, Mitsubishi Heavy Industries Ltd., Nagasaki

Design of Devices for Improving the Wake Flow into the Propeller Plane
Dr. George E. Gadd, National Maritime Institute, Feltham

Kaffeepause

On the Characterization of Complex Flows
Dr. Jürgen Kux, Universität Hamburg

A Sailing View of the North Atlantic
Prof. J. Nicholas Newman, Massachusetts Institute of Technology, Cambridge

Begrüßung durch den Direktor des Instituts,
Herrn Prof. Petershagen

Meine sehr verehrten Damen, meine Herren !

Zum Kolloquium aus Anlaß der Emeritierung von Professor Dr. rer. nat. Karl Wieghardt darf ich Sie in unserem Institut sehr herzlich begrüßen. Herr Senator Sinn ist verhindert; ich darf aber Herrn Staatsrat Bilstein herzlich begrüßen, und ebenfalls begrüße ich Herrn Dr. Fischer-Appelt, und ich danke Ihnen, daß Sie es möglich gemacht haben, trotz Ihres immer sehr knappen Terminplanes hier zu sein und einige Begrüßungsworte zu uns zu sprechen. Ich darf dies wohl auch über den heutigen Anlaß hinaus als ein Zeichen Ihres Interesses an der Arbeit unseres Instituts deuten. Mein besonderer Gruß gilt auch den Vortragenden des heutigen Tages. Ein wissenschaftliches Kolloquium ist sicherlich die dem heutigen Anlaß am besten entsprechende Art der Veranstaltung, und so danke ich vor allem auch Ihnen für Ihren Beitrag zur Gestaltung dieses Tages.

Erlauben Sie mir nun einige Grußworte an unsere ausländischen Gäste.

I welcome our foreign guests and especially our foreign lecturers. I thank you for your readiness to present lectures on this special occasion which will surely make this colloquium a success.

Bevor ich nun das Wort weitergebe, darf ich sagen, daß wir im Anschluß an die Begrüßung eine kurze Pause machen werden. Danach wird Herr Kollege Eggers die Leitung des eigentlichen Kolloquiums übernehmen.

Darf ich nun zunächst Sie, Herr Staatsrat Bilstein, bitten.

Ansprache von Herrn Staatsrat Bilstein
als Vertreter des Präses der Behörde für Wissenschaft
und Forschung, Prof. H. Sinn

Meine sehr verehrten Damen und Herren,
lieber Herr Wieghardt !

Ich überbringe Ihnen sehr gern die besten Wünsche des Senats und der Bürger unserer Stadt.
Von meinem Vorredner ist schon darauf hingewiesen worden, daß der Präses der Behörde für Wissenschaft und Forschung, Herr Senator Sinn, verhindert ist. Er ist zur Zeit in Bonn. Dort tagt wieder eines der vielen Gremien, die sich mit dem Thema Hochschulbau beschäftigen. Sie werden wissen, soweit Sie Hamburger oder Deutsche sind, möglicherweise aber auch unsere ausländischen Kollegen, daß dies ein in der Bundesrepublik Deutschland ungemein interessierendes Thema ist, und daß in den letzten Tagen dazu einige Vorentscheidungen im Wissenschaftsrat getroffen wurden, die gerade für die Stadt Hamburg von besonderem Interesse sind, und daß soeben heute die letzte Runde in Bonn eingeläutet wird. Der Präses bedauert seine Abwesenheit von diesem Kolloquium sehr. Das drückt sich darin aus, daß ich noch heute morgen von ihm einen Anruf aus Bonn erhielt.

Wie wichtig ein funktionsgerechter Hochschulbau ist, haben Sie, verehrter Herr Wieghardt, im Laufe der Geschichte dieses Instituts sozusagen hautnah erfahren. Die Anfänge Ihres Instituts, so habe ich mir heute morgen noch sagen lassen, lagen vor 30 Jahren in einem Gebäude im Hinterhof der Ingenieurschule am Berliner Tor, bis zu Beginn der sechziger Jahre mit den jetzigen Gebäuden bessere räumliche Voraussetzungen geschaffen wurden.

In einer vergleichbaren Situation ist zur Zeit noch die Technische Universität Hamburg-Harburg, zwar nicht in einem Hinter-

hof, aber doch in einem angemieteten, wenn auch funktional brauchbaren Gebäude. Für unsere ausländischen Gäste darf ich anmerken, daß die Technische Universität Hamburg-Harburg wohl vermutlich die letzte Hochschulneugründung in diesem Jahrhundert in der Bundesrepublik sein wird. Die Zielsetzung dieser Technischen Universität, die im Süden Hamburgs gebaut wird, ist es, das naturwissenschaftliche Defizit, das das Land Hamburg, wie allgemein ganz Norddeutschland aufweist, zu verringern bzw. zu beseitigen. In dem bisher angemieteten Gebäudekomplex dieser neuen Universität arbeiten bereits 17 Professoren mit ihren Mitarbeitern, und in wenigen Wochen wird das erste TU-eigene Gebäude, das Technikum, übergeben werden.

Meine Damen und Herren, insbesondere auch für die Schiffstechnik - einen Forschungsschwerpunkt der TU Harburg - wird es in diesem Gebäude weitere gute Arbeitsmöglichkeiten geben. Ich glaube, das dürfte für ein fachkundiges Auditorium eine gute Nachricht sein.

Die bisherigen Anfangserfolge dieser neuen Universität zeigen Parallelen zum Institut für Schiffbau: Wenn persönliches Engagement vorhanden ist, lassen sich Mängel - ich meine insbesondere räumliche Mängel -, wenn auch mit großer Mühe, überwinden.

Meine Damen und Herren, ich habe kurz auf das bisherige strukturelle Defizit Norddeutschlands hingewiesen. Bei dieser Pauschalität gilt es, Einschränkungen zu machen. Neben einigen Abteilungen der Fachbereiche Physik und Chemie ist das Institut für Schiffbau die einzige technisch-naturwissenschaftliche Einrichtung, die im Rahmen der Universität Hamburg bisher bestand. Man hat dabei etwas weniger respektvoll, dafür aber treffend, von Ihrem Institut als einem "Zoo" von vielen Gebieten gesprochen. Fächer der Mathematik gehören zu ihnen genauso wie verschiedene Gebiete der Physik neben den klassi-

schen ingenieurwissenschaftlichen Bereichen.
Was an Ihrem Institut bereits vorhanden und eingespielt ist, wird mit der TU Hamburg-Harburg seine adäquate Ausweitung erhalten: Die Erfahrungen, die eine so interdisziplinäre Einrichtung wie die Ihre sammeln konnte, werden für das Funktionieren dieser neuen Hochschule wie für ihre Zusammenarbeit mit den anderen Hochschulen in Hamburg wertvolle Hinweise geben können. Denn wenige wissenschaftliche Einrichtungen in Hamburg sind so ausgeprägt auf Zusammenarbeit mit mehreren anderen Hochschulen ausgerichtet wie Ihr Institut. Es wäre schön gewesen, wenn die Unterzeichnung der Verträge zur Umsiedlung der bisher in Hannover lokalisierten schiffstechnischen Bereiche wie geplant in diesen Tagen hätte stattfinden können. Doch wird diese eher äußerliche Terminsache sich verschmerzen lassen; entscheidend ist, für Hamburg wie für Ihr Institut, daß die Konzentration dieser Bereiche in Hamburg gute und bessere Arbeitsbedingungen und -möglichkeiten erwarten läßt.

Lassen Sie mich, meine Damen und Herren, bevor ich schließe, noch einmal ein Wort des Dankes an Sie, Herr Wieghardt, richten. Dank für die 30jährige Tätigkeit an verantwortlicher Stelle des Instituts, mit der Sie seit den Jahren des Wiederaufbaues in Lehre, Forschung und wissenschaftlicher Dienstleistung entscheidendes zur jetzigen Stellung der Einrichtung beigetragen haben - sei es im Rahmen der alten "math-nat-Fakultät", sei es in der formal größeren organisatorischen Selbständigkeit der Jahre seit 1970. Für Hamburg schließt der Dank besonders mit ein, was Ihren Beitrag betrifft zur Berechnung, Konzeption und Dimensionierung bei der Belüftung im U-Bahn-Bau, vor allem aber beim Elbtunnel. Das ist für mich geradezu prototypisch für das, was mit "wissenschaftlicher Dienstleistung" für die Gesellschaft zu bezeichnen ist.

In zwei Jahren wird das traditionelle Symposium des "Office of Naval Research" in Hamburg stattfinden - sicher kein

alltägliches Ereignis. Es ist für mich aber auch willkommener Anlaß, Ihnen für Ihre Bereitschaft zu danken, auch weiterhin für die wissenschaftlichen Einrichtungen in Hamburg tätig zu sein und ihre Belange in internationalen Gremien, gesützt auf Ihre Erfahrung, zu vertreten.

Ich wünsche Ihnen, sehr geehrter Herr Wieghardt, persönlich dazu allen Erfolg, dem Symposium einen guten Verlauf !

Ansprache von Herrn Dr. Fischer-Appelt,
Präsident der Universität Hamburg

Ladies and Gentlemen !

It is indeed a great pleasure and honour for me to welcome you, the great family of shipbuilders and naval architects, at this fine Institute of Naval Architecture this morning. It is very early in the morning for everybody and especially for those who had official business or private undertakings to attend last night. Nevertheless, you are used to beginning rather early and I am glad to be with you again this morning.

This is a colloquium in honour of Professor Wieghardt on the occasion of his retirement. Professor Wieghardt was born in 1913 in Vienna. But he was brought up in Dresden where his father was appointed Professor at the Technical University. You, Professor Wieghardt, later began to study mechanical engineering and advanced physics in that city. Your special interest in advanced physics brought you later on to Göttingen, where you worked with Professor Prandtl, the famous master of mechanics and flow research. In Göttingen you completed your doctorate and became a research worker in the Kaiser-Wilhelm-Institut, a forerunner of the Max-Planck-Institut. During the time you spent at this research institute you also completed your habilitation. After the Second World War you worked in the Admirality Research Laboratory in England from 1949 to 1952. It was, I suppose, a unique international experience for you especially so short time after the Second World War. You helped to bridge the gap between England and Germany after this war. In 1952 you were offered a position as an assistant at the Hamburg Institut für Schiffbau which you finally accepted after you could no longer resist the pressure and charm of Professor Weinblum who strongly encouraged you to come to Hamburg. This decision

was certainly not an easy one for you. You left a very large laboratory and exchanged it for an institute which in those days was a rather desolate place in a backyard. But with the aid and support of the faculty of mathematics and science of this university and the German Research Foundation, the Institut für Schiffbau of Hamburg University became well known and highly esteemed among similar institutions throughout the world. The presence of the leading experts in this field here today, from this country and abroad, is sufficient evidence of this fact. You, Professor Wieghardt, have had a decisive share in it. Although several professorships were offered to you by other universities, you remained a devoted member of this Institute here in Hamburg. Thank you especially for this. You were not only respected by experts in your field all over the world, but you also enjoyed the reputation of a good teacher among your students. And some of your pupils followed your example and became well-known teachers and researchers themselves. You are now retired. But you must certainly enjoy and be proud to know that your work will be continued by your colleagues and your pupils.

Together with all of us here, as President of the University of Hamburg, I thank Professor Wieghardt today as one of the founding fathers of this institute. You will have my support and, I think, the support of all responsible persons and bodies of the Hamburg University in your future work. I say this also looking to the future because I believe Naval Architecture and all the other topics related to this field will probably have a very great future in Hamburg. So when our colleagues from Hannover join us and we establish a new institute at the Technical University of Hamburg-Harburg, it will be one of the major institutes of Naval Architecture and will provide a solid basis for cooperation within the greater area of Hamburg. Naval Architecture has a good tra-

dition in Hamburg and is matched by other related studies. Marine research is one of the strongholds of our university, and at the moment we are trying to establish a new special research area that will be called "Oceanic Processes". In this effort the departments of geophysics, geology and mineralogy will work together. We hope to establish this new special research area which, together with the already existing Research Areas 98 (Marine Technology) and 94 (Interaction between the Ocean and the Atmosphere), will be able to carry out very promising projects to the benefit of us all. Our future is in the sea !

Es ist für mich, lieber Herr Wieghardt, ein ganz großes Vergnügen und ein wenig auch ein Abschied mit einem Hauch von Trauer, daß ich Ihnen heute - ich werde dies nachher tun - die Urkunde anläßlich Ihrer Emeritierung überreiche. Zwölf Jahre, die wir in Hamburg zusammen gewirkt haben, sind vielleicht in Ihrem Leben ein kurzer Abschnitt, in meinem schon ein längerer. Jahre, die uns hier gemeinsam in Hamburg verbunden haben, haben uns öfter zusammengeführt - in Ihrer Arbeit, zuweilen auch in meiner Arbeit - und am Ende in gemeinsamer Arbeit, die uns verbindet in Erkenntnis neuen Wissens und seiner Vermittlung zum besten unserer Studenten und im weiteren Sinne aller Bürger nicht nur unserer Gesellschaft. Dieses Stück Internationalität, das die Universität verkörpert, das zu ihren wesentlichen Bedingungen, ja Lebensbedingungen gehört, hat dieses Institut für Schiffbau stets sich angelegen sein lassen. Es ist eben eine große Familie der Schiffbauer, die rund um die Welt alle Institute dieses schönen Faches verbindet. Daß heute so viele Kollegen aus Ost und West, aus Nord und Süd hier versammelt sind, um Sie zu feiern, das erfüllt sicher nicht nur Sie allein mit Stolz, sondern auch die Universität weiß dies zu danken und, wenn möglich, zurückzugeben. Ich wünsche Ihnen noch viele fruchtbare Jahre der Zusammenarbeit mit Ihren Kollegen und ein Stückchen Gelassenheit, wohl auch im Kreise Ihrer so reizenden Familie.

Antwort von Herrn Prof. Wieghardt

Meine Damen und Herren !

"Zwei Seelen wohnen, ach, in meiner Brust". - Das kommt daher, daß wir ja zwei Gehirne haben. Das alte, das wir schon hatten, als wir noch Reptilien waren. Das neue entwickelte sich tumorartig erst vor einer halben Million Jahre, merkwürdigerweise nur beim Menschen. In diesem neocortex sitzen die ratio und die Logik, und die sagen mir - als Schiffshydrodynamiker - ganz deutlich, daß ich heute weit über Verdienst geehrt werde, um mehrere Nummern zu sehr.

Andrerseits, im alten Gehirn, da hausen die Gefühle, und zwar auch die warmen und heißen Gefühle, die nicht von des Gedankens Blässe angekränkelt sind. Und die sagen mir eitlem, alten Männchen: Ist das nicht wunderbar !
Und in der Tat, es ist schöner als der schönste Wunschtraum, den ich mir selber hätte ausdenken können.

Deshalb kann ich - trotz aller Bedenken - Ihnen allen nur sehr herzlich danken. Allen Institutsangehörigen und Studenten für die freundschaftliche Zusammenarbeit über viele Jahre lang, bei manchen bis fast 30 Jahre lang. (Ich meine jetzt Institutsangehörige, nicht Studenten.) Ebenso warm danke ich den Veranstaltern dieses Kolloquiums und allen Rednern und Freunden und Kollegen, die von nah und fern gekommen sind.

Die inkompressible Strömung am Staupunkt schlanker Spitzen

Klaus Oswatitsch

1. Einleitung

Die Untersuchung sei auf stationäre inkompressible Potentialströmung beschränkt. Bei den geläufigen Theorien für nicht angestellte schlanke Profile, Rotationsrümpfe oder Flügel wird mit Quellbelegungen der Körperachse oder Körpersymmetrie-Ebene gearbeitet. Die vereinfachten Randbedingungen führen dabei an Profil-, Körper- oder Flügelspitzen zu einem sprunghaften Beginn der Quellbelegung. Dieser hat jedoch eine logarithmische Singularität für die Geschwindigkeit an der Spitze zur Folge. Die Geschwindigkeit wird am Belegungsbeginn nicht Null sondern negativ logarithmisch unendlich, vgl. etwa [1], S.443 und S.458.

Dieser Fehler beruht darauf, daß nicht die Quellbelegung an der Körperspitze sprunghaft beginnt, sondern daß sich dort die Strömungsrichtung sprunghaft ändert. Wenn der skizzierte Fehler auch nicht gravierend ist, so erscheint es doch unbefriedigend, daß der Staupunkt selbst bei einer Theorie schlanker Körper falsch wiedergegeben wird. Die Begegnung dieses Mangels soll im folgenden kurz dargelegt werden.

Stark vergrößert entspricht die Umgebung einer Körper- oder Flügelspitze einer Kegelspitze. In Ermangelung eines Längenmaßes kann die Strömungsrichtung auf Strahlen durch die Kegelspitze als konstant angenommen werden. Diese Eigenschaft hat die inkompressible Strömung mit der reinen Überschallströmung noch gemeinsam. Während bei letzterer aber auch der Geschwindigkeitsbetrag auf Strahlen durch die Spitze konstant ist, nimmt er bei inkompressibler Strömung mit einer positiven Potenz des Abstandes von der Spitze zu. Diese Eigenschaft tritt schon an der Keilspitze, also bei der ebenen Strömung zutage, einer Strömung, die man mittels konformer Abbildung völlig beherrscht. Sie ist keinesfalls auf schlanke Spitzen beschränkt,

wird uns aber besonders zur Lösung unserer Aufgabe dienen.

2. Separationsansätze

Die Geschwindigkeitskomponenten seien durch ein Potential dargestellt:

$$u = \Phi_x, \quad v = \Phi_y, \quad w = \Phi_z \tag{1}$$

wobei das Potential der Laplacegleichung genügt:

$$\Phi_{xx} + \Phi_{yy} + \Phi_{zz} = 0 . \tag{2}$$

Die Spitze der Kegel liege stets im Koordinatenursprung. Die Abszisse sei die Kegelachse und

$$r = \sqrt{x^2 + y^2 + z^2} \tag{3}$$

der Abstand von der Spitze.

Für den Kreiskegel, der zunächst behandelt werden soll, seien Winkelvariable eingefügt, Bild 1:

$$\xi = x/r = \cos\beta . \tag{4}$$

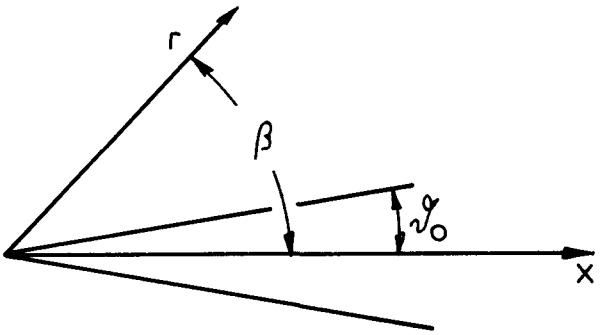

Bild 1

Folgender Separationsansatz erweist sich als zweckmäßig:

$$\Phi = r^{1+\nu} \cdot F(\xi) \tag{5}$$

mit ν als einer Konstanten, die mit dem halben Öffnungswinkel θ_o des Kreiskegels in Verbindung gebracht werden wird.

Der Ansatz (5) in (2) eingeführt, ergibt für $F(\xi)$ die Legendresche Differentialgleichung:

$$(1 - \xi^2)\, F_{\xi\xi} + (1+\nu)(2+\nu)\, F = O \ . \tag{6}$$

Auf dem Körper und auf der Anströmlinie, der negativen x-Achse, muß die Normalableitung des Potentials, d.i.

$$\Phi_\beta = r^{1+\nu} \cdot F_\xi \sin\beta$$

verschwinden. Das führt zu den Randbedingungen:

$$\begin{aligned} &\beta = \theta_o \neq o : F_\xi = O \ , \\ &\beta = \pi \ : \quad F_\xi \quad \text{beschränkt.} \end{aligned} \tag{7}$$

Auf der Kegelerzeugenden ist der Geschwindigkeitsbetrag W gleich Φ_r :

$$\beta = \theta_o : \ W = (1+\nu) r^\nu F \ . \tag{8}$$

Zwei Lösungen von (6) sind leicht zu finden. Die Parallelströmung in x-Richtung:

$$\theta_o = O : \nu = O \ , \quad F = B\, \xi \ . \tag{9}$$

Bei dieser ist die Randbedingung, $\Phi_\beta = O$, auf der gesamten x-Achse erfüllt. $F_\xi = B \neq O$ führt daher zu keinem Widerspruch.

Die zweite Lösung ist die senkrecht angeströmte Platte, also der Kegel mit

$$\theta_o = \pi/2 : \nu = 1, \ F = B(1-3\xi^2) \ .$$

In allen Fällen der reinen Kegelströmung bleibt in Φ und folglich in F eine multiplikative Konstante, in den Beispielen B, unbestimmt.

Die Beziehung zwischen ν , der r-Potenz der Geschwindigkeit an der Oberfläche, Gl. (8), und dem halben Kegelöffnungswinkel θ_o wurde von Leuteritz und Mangler [2] durch numerische Integration von Gl. (6) für einen weiten Bereich von θ_o gewonnen. R. Schwarzenberger [3] hat mittels funktionentheoretischer Methoden eine Entwicklung von ν nach θ_o hergeleitet, von der die ersten Glieder lauten:

$$\nu = \frac{1}{2}\,\theta_o^2 + \frac{1}{2}\,\theta_o^4 \ln\frac{\theta_o}{2} + \frac{11}{24}\,\theta_o^4 + \ldots \quad . \tag{10}$$

Für einen Kegel allgemeiner Querschnittsform bedarf es zweier Winkelvariabler. Es sei

$$\xi = x/r, \quad \eta = y/r, \quad \zeta = z/r \quad . \tag{11}$$

Von den neuen Variablen sind nur zwei unabhängig, denn es gilt:

$$\xi^2 + \eta^2 + \zeta^2 = 1 \quad . \tag{12}$$

Im folgenden werden ξ und ζ als Unabhängige gewählt. Der Separationsansatz schreibt sich dann:

$$\Phi = r^{1+\nu} \cdot F(\xi,\zeta) \quad . \tag{13}$$

Für die Komponenten gilt nach Zwischenrechnung:

$$\begin{aligned} u &= \Phi_x = r^\nu \left[(1+\nu)\xi\, F + (1-\xi^2)F_\xi - \xi\zeta\, F_\zeta\right]; \\ v &= \Phi_y = r^\nu \eta \left[(1+\nu)F - \xi\, F_\xi - \zeta\, F_\zeta\right]; \\ w &= \Phi_z = r^\nu \left[(1+\nu)\zeta\, F - \xi\zeta\, F_\xi + (1-\zeta^2)F_\zeta\right] \quad . \end{aligned} \tag{14}$$

Man bestätigt leicht, daß die Strömungsrichtung u:v:w unabhängig von r ist. Das Einführen des Ansatzes (13) in Gl. (2) führt nach Zwischenrechnung in Verallgemeinerung von Gl. (6) zur partiellen Differentialgleichung:

$$\begin{aligned} &(1-\xi^2)\, F_{\xi\xi} - 2\xi\zeta\, F_{\xi\zeta} + (1-\zeta^2)\, F_{\xi\zeta} - \\ &\quad - 2\xi\, F_\xi - 2\zeta\, F_\zeta + (1+\nu)(2+\nu)\, F = 0 \quad . \end{aligned} \tag{15}$$

Da zunächst noch keine Richtung ausgezeichnet ist, würde sich formal dieselbe Gleichung im Variablenpaar ξ, η oder η, ζ ergeben.

Zum Aufbau kegeliger Strömungsfelder müßten nun geeignete partikuläre Lösungen der Differentialgleichungen (15) gefunden werden. Dies ist jedoch nicht einfach, weshalb ein zweiter Weg zur Lösung unserer Aufgabe beschritten werden soll.

3. Methode mit der logarithmischen Geschwindigkeit

Da die Umströmung der Keilspitze mit Hilfe der konformen Abbildung leicht lösbar ist, liegt es nahe, sich für die Lösung unserer Aufgabe an der ebenen Strömung zu orientieren. Mit den Symbolen von Bild 1, angewendet auf den Keil, findet man nach Zwischenrechnung als Realteil des komplexen Potentials:

$$\Phi = B\, r^{1+\nu} \cos\left[(1+\nu)(\beta - \pi)\right] \tag{16}$$

mit den Komponenten

$$\begin{aligned} u &= (1+\nu)\, B\, r^{\nu} \cos \nu(\beta - \pi) \ ; \\ v &= (1+\nu)\, B\, r^{\nu} \sin \nu(\beta - \pi) \ . \end{aligned} \tag{17}$$

Daraus folgt für den Geschwindigkeitsbetrag W und den Strömungswinkel θ :

$$\begin{aligned} \ln W &= \nu \ln r + \ln (1+\nu)\, B \ ; \\ \theta &= \nu\, (\pi - \beta) \ . \end{aligned} \tag{18}$$

Man erkennt, daß die negative x-Achse Stromlinie ist:

$$\beta = \pi \ : \ \theta = 0 \ ,$$

Aus der Randbedingung:

$$\beta = \theta_0 \ : \ \theta = \theta_0 \tag{19}$$

folgt:

$$\nu = \frac{\theta_o}{\pi - \theta_o} \,. \tag{20}$$

Das Variablenpaar $\ln W$, θ erfüllt wie das Variablenpaar u,v die Cauchy-Riemannschen Differentialgleichungen. Bei ebener Strömung können daher beide Paare gleichberechtigt als abhängige Veränderliche verwendet werden. Während jedoch v im Staupunkt nicht springt, ist dies bei θ sehr wohl der Fall.

Die skizzierte Lösung gilt bei ebener Strömung für beliebige halbe Öffnungswinkel des Keiles. Für schlanke Keilspitzen kann ν als Störparameter aufgefaßt werden, wobei dann θ_o im Nenner von Gl. (20) gegen π in erster Ordnung vernachlässigt werden kann. Auch an der Entwicklung von Schwarzenberger, Gl. (10), ist zu erkennen, daß ν als Störparameter bei Kreiskegeln angesehen werden kann. Damit geht Hand in Hand, daß gem. Gl. (9) für ungestörte Parallelströmung $\nu = 0$ ist.

Während aber der Störparameter im Separationsansatz sowie in den Gln. (17) im Exponenten wie im Argument der Funktion auftritt, erscheint er im Variablenpaar Gl. (18) ausschließlich als Faktor, wie man es sich bei einer Entwicklung nach Störparameter wünscht. Das Auftreten von ν im Argument des Logarithmus in der oberen Gl. (18) ist bedeutungslos, weil $(1 + \nu)B$ durch eine neue, frei wählbare Konstante ersetzt werden kann.

Es liegt daher nahe, es auch bei räumlicher Strömung mit ähnlichen Abhängigen zu versuchen.

Um bei achsensymmetrischer Strömung die Einführung zusätzlicher Symbole zu vermeiden, sei dort in der Ebene $z = 0$ als Repräsentations-Achsenschnitt gearbeitet. Im neuen Variablenpaar findet man dann folgendes Gleichungssystem:

$$\begin{aligned} z = 0: \quad & \frac{\partial \ln W}{\partial x} + \frac{\partial \theta}{\partial y} + \frac{1}{y} \sin\theta \cos\theta = 0 \,; \\ & \frac{\partial \ln W}{\partial y} \qquad \frac{\partial \theta}{\partial x} + \frac{1}{y} \sin^2\theta \qquad = 0 \,. \end{aligned} \tag{21}$$

Die Gleichungen sind exakt, leider aber nicht mehr in θ linear.

Bei allgemein räumlicher Strömung müssen zwei Komponenten des Strömungswinkels eingeführt werden. Es sei:

$$\operatorname{tg}\theta_1 = v/u\ , \qquad \operatorname{tg}\theta_2 = w/u \tag{22}$$

mit folgender Beziehung zum Winkel der Strömung mit der x-Achse.

$$\operatorname{tg}\theta = \sqrt{v^2 + u^2}/u = \sqrt{\operatorname{tg}^2\theta_1 + \operatorname{tg}^2\theta_2}\ . \tag{23}$$

Es seien nun kleine Strömungswinkel $\operatorname{tg}\theta_1$ und $\operatorname{tg}\theta_2$ vorausgesetzt. Nach Zwischenrechnung erhält man folgendes Gleichungssystem, das nun aber nur Glieder bis einschließlich quadratischen Termen in den Abhängigen enthält:

$$\begin{aligned}
&\frac{\partial \ln W}{\partial x} + \frac{\partial \operatorname{tg}\theta_1}{\partial y} + \frac{\partial \operatorname{tg}\theta_2}{\partial z} = 0\ ; \\
&\frac{\partial \ln W}{\partial y} - \frac{\partial \operatorname{tg}\theta_1}{\partial x} - \operatorname{tg}\theta_2 \frac{\partial \operatorname{tg}\theta_2}{\partial y} + \operatorname{tg}\theta_1 \frac{\partial \operatorname{tg}\theta_2}{\partial z} = 0\ ; \\
&\frac{\partial \ln W}{\partial z} - \frac{\partial \operatorname{tg}\theta_2}{\partial x} - \operatorname{tg}\theta_1 \frac{\partial \operatorname{tg}\theta_1}{\partial z} + \operatorname{tg}\theta_2 \frac{\partial \operatorname{tg}\theta_1}{\partial y} = 0\ .
\end{aligned} \tag{24}$$

Die erste Gleichung, die der Kontinuitätsbedingung entspricht, ist bis einschließlich quadratischer Glieder noch linear. Die beiden anderen Gleichungen sind es aber nur bei ebener Strömung, etwa bei $\partial/\partial z = 0$ und $\operatorname{tg}\theta_2 = 0$.

4. Lösung für den schlanken Kreiskegel

Bei der Lösung des Systems (21) für schlanke Kreiskegel ist zu beachten, daß $\ln W$ wohl proportional zum Störparameter ν und damit gemäß Gl. (10) proportional zu θ_o^2 ist, daß aber das gleiche auch für θ gilt. Der Term mit $\sin^2\theta$ erscheint deshalb in Körpernähe als von derselben Größenordnung wie der Term mit $\ln W$. Im Sinne einer Entwicklung nach dem Störparameter ν handelt es sich jedoch bei $\sin^2\theta$ um einen quadratischen Term in ν .

Das Glied kann also für die linearen Glieder in ν gestrichen werden. Dieser zunächst überraschend und vielleicht bedenklich anmutende Schluß wird nachträglich noch gerechtfertigt. Es empfiehlt sich ferner, θ durch $\operatorname{tg}\theta$ zu ersetzen. Das System (21) erhält damit in erster Näherung einer Entwicklung nach ν die Form:

$$\begin{aligned} &\frac{\partial \ln W}{\partial x} + \frac{\partial \operatorname{tg}\theta}{\partial y} + \frac{1}{y}\operatorname{tg}\theta = 0 ; \\ &\frac{\partial \ln W}{\partial y} - \frac{\partial \operatorname{tg}\theta}{\partial x} = 0 \end{aligned} \tag{25}$$

Durch Einführen eines "Potentials" Ω :

$$\Omega_x = \ln W , \quad \Omega_y = \operatorname{tg}\theta \tag{26}$$

erhält man schließlich die vertraute Gleichung:

$$\Omega_{xx} + \Omega_{yy} + \frac{1}{y}\Omega_y = 0 . \tag{27}$$

Die gesuchte Lösung muß in den Koordinaten homogen erster Ordnung und in y symmetrisch sein. Die einzige Lösung, die diesen Forderungen genügt, ist:

$$\begin{aligned} &\Omega = \nu \; x \ln\left[(\sqrt{x^2 + y^2} - x) + \sqrt{x^2 + y^2}\right] ; \\ &\ln W = \nu \ln r \,(1 - \cos\beta) ; \\ &\operatorname{tg}\theta = \nu \operatorname{cot}\beta/2 \end{aligned} \tag{28}$$

mit β von Gl. (4).

Aus der Randbedingung (19) folgt:

$$\nu = \operatorname{tg}\theta_o \cdot \operatorname{tg}\theta_o/2 = \frac{1}{2}\operatorname{tg}^2\theta_o + .. = \frac{1}{2}\theta_o^2 + .. , \tag{29}$$

im Einklang mit der Entwicklung (10). Daraus folgt für den Kegel und seine Anström-Stromlinie:

$$\beta = \theta_o \;:\; W = W_o [r \cdot \mathrm{tg}^2\, \theta_o /2\,]^{\nu} \;;$$
$$\beta = \pi \;:\; W = W_o [2\,r\,]^{\nu} \;. \qquad (30)$$

Die in Gl. (27) berücksichtigte additive Konstante von $\ln W$ ist in Gl. (30) als eine in ihrer Größe zunächst freie multiplikative Geschwindigkeit W_o eingeführt.

Im Gegensatz zur Keilströmung Gl. (18) wächst W am Kegel und an der Anström-Stromlinie nicht mehr mit demselben Faktor vor der Potenz r^{ν} an. Die ebene Strömung ist ja im Gegensatz zur achsensymmetrischen Strömung gegenüber einer Drehung um die z-Achse invariant.

Mit Hilfe der gefundenen Lösung läßt sich nun auch die Separationsfunktion $F(\xi)$ von Gl. (5) bestimmen.

Ganz allgemein gilt nach Zwischenrechnung:

$$\Phi_r = (1+\nu) r^{\nu} F = W\,(\cos\beta + \mathrm{tg}\,\theta\, \sin\beta) \;.$$

Mit der Lösung (28) und der Variablen ξ von Gl. (4) folgt daraus:

$$(1+\nu)\; F\;(\xi) = W_o\;(1-\xi)^{\nu}\;[\xi + \nu\;(1+\xi)\,] + \ldots \qquad (31)$$

Man überzeugt sich leicht, daß die Lösung (31) die Legendresche Gleichung (6) bis einschließlich Gliedern ν^1 erfüllt. Damit bestätigt sich die Vernachlässigung des Terms $\sin^2\theta /y$ im System (21) bis zu einer Entwicklung erster Ordnung im Störparameter ν als berechtigt. Für $\nu = 0$ liefert Gl. (30) die Parallelströmung Gl. (9).

5. Einbetten der Spitzenströmung in die Rumpfumströmung

Das Einbetten der Keilströmung in die Strömung um spitze Profile ist beispielsweise in [1] (S.476 ff) wiedergegeben. Das Einbetten der Kegelumströmung sei am Beispiel des vorderen Stau-

punktes eines spitzen Rotationsrumpfes von kleinem Dickenverhältnis τ gezeigt. Ein solcher stellt sich gemäß der vereinfachten Theorie, vergl. etwa [1] (S.452 ff), für $0 < x$ wie folgt dar:

$$W/u_\infty = 1 + \frac{1}{2} \operatorname{tg}^2 \theta_0 \ln (x \operatorname{tg}^2 \theta_0/4) + \frac{\tau^2}{16} E(x) . \qquad (32)$$

u_∞ ist die Anströmgeschwindigkeit, $E(x)$ ist eine in der Staupunktsumgebung endliche Funktion von der Größenordnung der Einheit. Der Logarithmus ergibt den in der Einleitung erwähnten falschen Staupunktswert. Gl. (32) läßt sich in der gleichen Näherung auch schreiben:

$$W/u_\infty = \left[1 + \frac{1}{2} \operatorname{tg}^2 \theta_0 \ln \left(\frac{x \operatorname{tg}^2 \theta_0}{4} \right) \right] \cdot \left[1 + \frac{\tau^2}{16} E(x) \right] + \ldots .$$

Eine nähere Untersuchung zeigt, daß der erste Klammerausdruck die mangelhafte Staupunktsströmung darstellt und durch einen der ersten Zeile von Gl. (30) entsprechenden Ausdruck zu ersetzen ist, mit dem Ergebnis, für $0 \quad x$:

$$W/u_\infty = \left[x \frac{\operatorname{tg}^2 \theta_0}{4} \right]^{\frac{1}{2} \operatorname{tg}^2 \theta_0} \cdot \left[1 + \frac{\tau^2}{16} E(x) \right] , \qquad (33)$$

worin $E(x)$ dieselbe Funktion wie jene von Gl. (32) darstellt.

Es ist bekannt, daß die Geschwindigkeitsverteilung (32) trotz ihres unbefriedigenden Wertes in $x = 0$, in nächster Umgebung von $x = 0$ bereits sehr gut ist. Das liegt daran, daß es für eine Basis b mit einer kleinen Potenz ν folgende Entwicklung gibt:

$$b^\nu = 1^{\nu \ln b} = 1 + \nu \ln b + \frac{1}{2} (\nu \ln b)^2 + \ldots \qquad (34)$$

In unserem Falle ist $\nu = \operatorname{tg}^2 \theta_0/2$ und $b = x \operatorname{tg}^2 \theta_0/4$.

Ein Maß für die Genauigkeit von Gl. (32) kann man dadurch erhalten, daß man den Ort des Staupunktes dieser Gleichung bestimmt. Man erhält für $W = 0$:

$$x = \frac{4}{\tg^2 \theta_o} \; 1^{-2/\tg^2 \theta_o}$$

Andererseits kann man eine Staupunktsumgebung gem. Gl. (33) dadurch definieren, daß man den Ort bestimmt, an dem die Geschwindigkeit auf die halbe Anströmgeschwindigkeit abgesunken ist. Für $W/u_\infty = 1/2$ in Gl. (30) erhält man näherungsweise:

$$x = \frac{4}{\tg^2 \theta_o} \; 2^{-2/\tg^2 \theta_o} \quad .$$

In beiden Fällen ist x in Bruchteilen der Körperlänge gemessen. Bei einem halben Öffnungswinkel von $\theta_o = 10^o$ erhält man im ersten Fall $x = 1{,}5 \cdot 10^{-26}$, im zweiten Fall $x = 5{,}6 \cdot 10^{-18}$, also Dimensionen, bei denen selbst bei großen Körpern die Kontinuitätsphysik verlassen wird.

6. Lösung für flache Kegel

Flache Kegel sind von Interesse, weil sie in der Umgebung der Spitze nicht angestellter gepfeilter Flügel auftreten. Für die Berechnung ihrer Umströmung seien die Gln. (24) linearisiert. Dann kann analog zu Gl. (26) ein "Potential" eingeführt werden:

$$\Omega_x = \ln W \,, \quad \Omega_y = \tg \theta_1 \,, \quad \Omega_z = \tg \theta_2 \,, \tag{35}$$

das der Laplacegleichung genügt:

$$\Omega_{xx} + \Omega_{yy} + \Omega_{zz} = 0 \,. \tag{36}$$

Es ist zweckmäßig, den Winkel

$$\tg \gamma = z/x \tag{37}$$

in der Kegelebene $y = 0$, Bild 2, einzuführen. $\gamma = \Lambda$ sei die Vorderkante des Kegels.

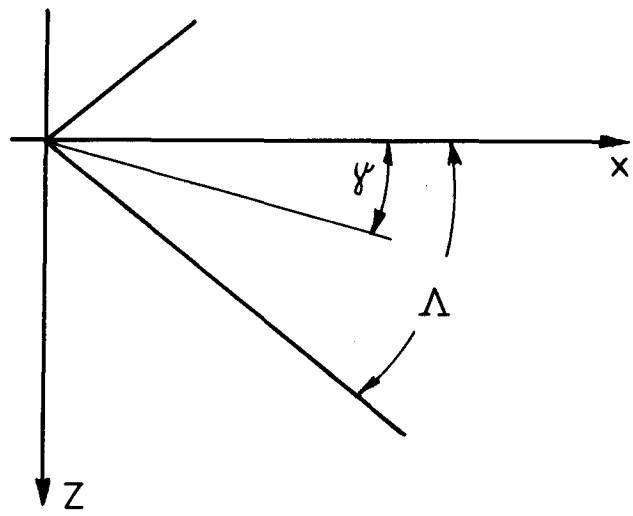

Bild 2

Die Lösung muß nun aus Pretikulärlösungen aufgebaut werden. Für die Quellbelegung eines Strahles $\gamma = \lambda$ findet man:

$$\Omega_p = (x \cos\lambda + z \sin\lambda) \ln [r - \cos\lambda + z \sin\lambda)] + r \; . \quad (38)$$

Es handelt sich um eine Verallgemeinerung des Potentials von Gl. (28) für $\lambda \neq o$, wobei der Störparameter ν zunächst noch weggelassen wurde.

Werden x und z wie folgt dargestellt

$$\begin{aligned} x &= \sqrt{x^2 + y^2} \cos\gamma = \sqrt{r^2 - y^2} \cos\gamma \; ; \\ z &= \sqrt{x^2 + y^2} \sin\gamma = \sqrt{r^2 - y^2} \sin\gamma \; , \end{aligned} \quad (39)$$

so erhält man für die Ableitungen von Ω_p nach Zwischenrechnung die Form:

$$\begin{aligned} \Omega_{px} &= \frac{d}{d\lambda} \left\{ \sin\lambda \ln [r - \sqrt{r^2 - y^2} \cos(\lambda-\gamma)] \right\} \; ; \\ \Omega_{py} &= \frac{y}{r - \sqrt{r^2 - y^2} \cos(\lambda-\gamma)} \; ; \\ \Omega_{pz} &= - \frac{d}{d\lambda} \left\{ \cos\lambda \ln [r - \sqrt{r^2 - y^2} \cos(\lambda-\gamma)] \right\} . \end{aligned} \quad (40)$$

Die Lösung setzt sich wie bei Singularitätenmethoden immer aus einem Integral über Partikulärlösungen mit entsprechenden Quellbelegungen $q(\lambda)$ zusammen:

$$\Omega = \int_{-\Lambda}^{+\Lambda} q(\lambda)\ \Omega_p\ d\lambda \quad . \tag{41}$$

Dies gilt sowohl für Ω wie auch für seine Ableitungen, Gl.(35). Nur Ω_y macht eine gewisse Ausnahme, weil Ω_{py} für $y \to 0$ überall verschwindet außer an der Stelle $\gamma = \lambda$. Daraus leitet sich eine Beziehung zwischen der Quellbelegung und $\operatorname{tg}\theta_1$ ab, nämlich:

$$q(\gamma) = \frac{1}{2\pi} \operatorname{tg}\theta_1(\gamma) \quad . \tag{42}$$

Die Herleitung soll hier nicht in den Einzelheiten vorgerechnet werden.

Bei einem flachen Kegel dürfen die Werte von $\ln W$ und $\operatorname{tg}\theta_2$ auf dem Kegelmantel in der angestrebten Näherung jenen auf der Projektionsebene $y = 0$ gleichgesetzt werden. Und man erhält unter der Voraussetzung, daß ein in z symmetrischer Kegel vorliegt

$$q(\lambda) = q(-\gamma), \tag{43}$$

auf $y = 0$ das Ergebnis:

$$\begin{aligned} \ln W &= \frac{1}{2\pi} \int_{-\Lambda}^{+\Lambda} \operatorname{tg}\theta_1(\lambda) \cos\lambda\ d\lambda \cdot \ln r\ + \\ &\quad + \frac{1}{2\pi} \int_{-\Lambda}^{+\Lambda} \operatorname{tg}\theta_1 \frac{d}{d\lambda}\left\{\sin\lambda\ \ln[1-\cos(\lambda-\gamma)]\right\}\ d\lambda\ ; \\ \operatorname{tg}\theta_2 &= \frac{1}{2\pi} \int_{-\Lambda}^{+\Lambda} \operatorname{tg}\theta_1(\lambda) \frac{d}{d\lambda}\left\{\cos\lambda\ \ln\left[1-\cos(\lambda-\gamma)\right]\right\}\ d\lambda \quad . \end{aligned} \tag{44}$$

Es sei besonders darauf hingewiesen, daß der in der dritten Gl. (40) auch für $y = 0$ auftretende Ausdruck mit $\ln r$ nur unter der Symmetrie-Bedingung (43) verschwindet. Das heißt, daß $\operatorname{tg} \theta_2$ bei Kegeln, die nicht zur Ebene $z = 0$ symmetrisch sind, wie $\ln W$, auch von r abhängt. Die Strömungsrichtung ist in einem solchen Falle auf Strahlen durch die Kegelspitze nicht mehr konstant und der Separationsansatz (Gl. 13) folglich nicht mehr zielführend. Dies mag mit dem Anstelleffekt zusammenhängen. Bei Anstellung rutscht der Staupunkt von der Spitze weg.

7. Beispiele für flache Kegel

Das mathematisch einfachste Beispiel bietet die konstante Quellbelegung, gem. Gl. (42) also:

$$- x \operatorname{tg} \Lambda \leq z \leq + x \operatorname{tg} \Lambda \; : \; \operatorname{tg} \theta_1 = \text{konst.}$$

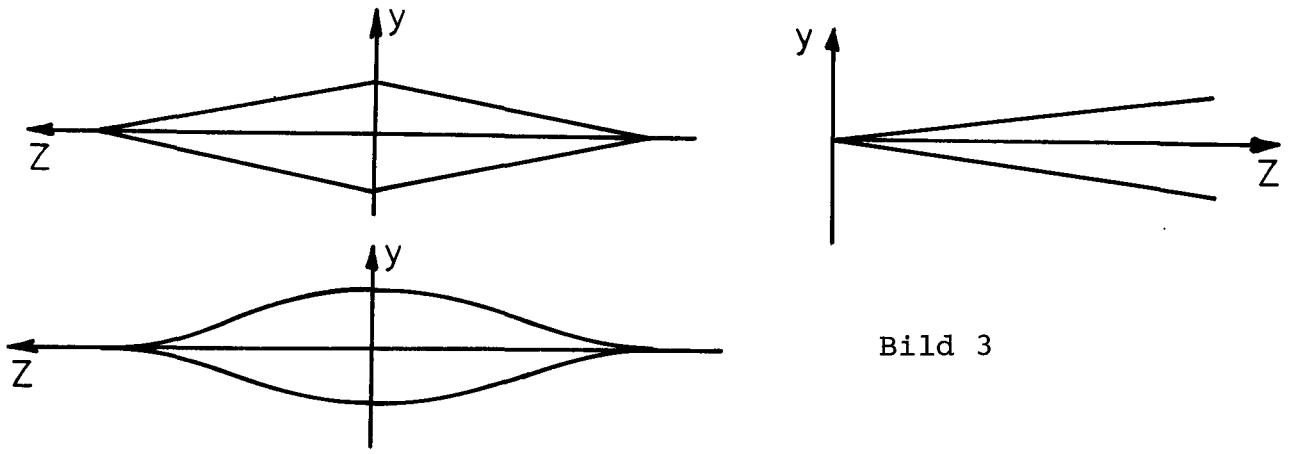

Bild 3

Es entspricht dem Kegel mit Rhombusquerschnitt, Bild 3. Aus den Gln. (44) folgt für diesen auf $y = 0$:

$$\begin{aligned} W/W_o &= r^{\nu} \left[|\cos \Lambda - \cos \gamma| \right]^{\nu} \\ \operatorname{tg} \theta_2 &= \nu \cot \Lambda \ln \left[\sin \frac{\Lambda+\gamma}{2} \sin \frac{|\Lambda \gamma|}{2} \right] , \end{aligned} \tag{45}$$

mit

$$\nu = \frac{1}{\pi} \operatorname{tg} \theta_1 \sin \Lambda \; . \tag{46}$$

Der Störparameter ν geht wie erwartet für $\Lambda = \pi/2$ in jenen für ebene Strömung, Gl. (20), über. Für starke Pfeilung, also kleines Λ, entspricht der Wert von ν der Flächenregel, wie ein Vergleich mit Gl. (20) zeigt.

Der Rhombuskegel weist aber nicht nur bei $r = 0$ einen Staupunkt auf, sondern bei $\gamma = \Lambda$, also an der Vorderkante, eine Staulinie. Dies ist nach den Ergebnissen der vereinfachten Flügeltheorie nicht überraschend. Die letztere weist an der Vorderkante eine logarithmische Singularität auf. Physikalisch erklärt sich der Effekt dadurch, daß die Strömung bei Überschreiten der Rhombuskante einen Knick erfährt. Leider versagt dort aber auch die Theorie kleiner Strömungswinkel. Gemäß der unteren Gl. (45) wird $\operatorname{tg}\theta_2$ bei $\gamma = \Lambda$ logarithmisch unendlich.

Definiert man die Staupunktsumgebung ähnlich wie an der Spitze etwa als jenen Bereich, in dem bei $r = 1$, $W/W_o < 1/2$ wird, so erhält man für den Rand des Bereiches

$$\sin\frac{|\Lambda-\gamma|}{2} = \frac{1}{2\sin\Lambda}\,2^{-1/\nu}\;; \qquad (47)$$

$$\operatorname{tg}\theta_2 = \cot\Lambda\,[\ln 2 + \nu \ln(2\sin^2\Lambda)]$$

An der unteren Gl. (47) ist zu erkennen, daß die Entwicklung für $\operatorname{tg}\theta_2$ am Staupunkt mit ν^0 und nicht, wie bei der Linearisierung der Gln. (24) angenommen, bei ν^1 beginnt.

Der Staupunktsbereich, also das Gebiet des Versagens der linearen Theorie, ist allerdings wieder verschwindend klein. Für $\operatorname{tg}\theta_1 = 0{,}10$ und $\Lambda = \pi/4$ findet man mit Gl. (46) und (47):

$$\sin\frac{|\Lambda-\gamma|}{2} = 3\cdot 10^{-14}\,.$$

Das Problem der Staukante fällt weg, wenn ein Stromlinienknick an der Vorderkante vermieden wird, wie das beim Cosinuskegel von Bild 3 der Fall ist. Mit $\tau/2 = \operatorname{tg}\theta_1(0)$ findet man für die halbe Dicke h dieses Kegels für:

$$- \pi/4 \leqq \lambda \leqq \pi/4 \quad : \quad h = \frac{\tau}{2} \, x \, (2 \cos^2 \lambda - 1)^2 \quad ; \qquad (48)$$

$$\operatorname{tg} \theta_1 = h_x = \frac{\tau}{2} \cos 2\lambda \, (2 + \cos 2\lambda - 2 \cos^2 2\lambda) \, .$$

Die Berechnung der zugehörigen Strömung ist zwar elementar, aber etwas umständlich. Der Störparameter ν ist dagegen mit der ersten Gl. (44) leicht zu bestimmen:

$$\nu = \frac{1}{2\pi} \int_{-\Lambda}^{+\Lambda} \operatorname{tg} \theta_1 (\lambda) \cos \lambda \, d\lambda = \frac{10 \sqrt{2}}{21 \pi} \frac{\tau}{2} \, .$$

Er unterscheidet sich kaum von jenem des Rhombuskegels gleichen Mittelschnittes und gleicher Pfeilung.

8. Zusammenfassung

Zur Berechnung der Strömung schlanker Spitzen werden zwei Wege beschritten. Der eine geht von Separationsansätzen aus, der andere vom Logarithmus der Geschwindigkeit und dem Strömungswinkel als abhängige Veränderliche. Die zweite Methode erweist sich vorläufig für kleine Störungen der Strömungsrichtung als erfolgreicher, versagt aber an geknickten Kegelkanten. Die Staugebiete sind bei schlanken Körpern stets verschwindend klein, nämlich jenseits der Gültigkeit der Kontinuumsmechanik. Dennoch dürften die Ergebnisse im Hinblick der Vervollständigkeit der Theorie sinnvoll sein. Eine Weiterentwicklung des Verfahrens mit den Separationsansätzen scheint, gestützt auf die Ergebnisse mit der zweiten Methode, möglich und wünschenswert.

Schrifttum

[1] Oswatitsch, K.: Grundlagen der Gasdynamik, Springer, Wien, 1976

[2] Leuteritz, R. - W. Mangler: Die symmetrische Potentialströmung gegen einen Kreiskegel, Bericht 45/A/03 der AVA, Göttingen, 1.2.1945

[3] Schwarzenberger, R.: Die symmetrische Potentialströmung gegen Kreiskegel, DLR Mitt. 68-27, November 1968

Ships in Very Shallow Water

by

De-bo Huang, O.J. Sibul and J.V. Wehausen

The work reported here is a continuation of that described earlier in Schiffstechnik (Sibul et al., 1979). Although the phenomenon described in that paper seemed to be adequately explained, both qualitatively and quantitatively, for the most part, there was one set of data taken in very shallow water where the proposed theory failed completely. It is to this situation that we address ourselves here.

First we summarize briefly the parts of the earlier paper relevant to the present work. We also refer to it for the motivation of the investigation. A ship model was attached rigidly to the towing carriage, wave gauges were fixed to the carriage, both ahead and to the side of model, the carriage was set into motion rather abruptly, and the resulting waves were recorded. Instead of the transient wave record that we had anticipated, we found a slowly decaying almost periodic wave. Let u be the model speed, h the water depth, and T_e the period of encounter. Then it was found that gT_e/u depended upon $u/\sqrt{gh}$ but not upon the hull form, length of model or particular nature of the start. A form for the curve gT_e/u against $u/\sqrt{gh}$ was obtained by assuming that the disturbance generated by the abrupt start could be analyzed as a Cauchy-Poisson initial-value problem, using linearized theory. The predicted curve fitted remarkably well with the measured values over part of the curve and the discrepant points could be explained by wall reflection. Figures 1 and 2 show typical wave records and plots of gT_e/u against $u/\sqrt{gh}$.

As remarked above, this explanation failed completely when the water was very shallow, in this case about 0.5 ft. Figure 3, reproduced from the earlier paper, shows this failure. What

Figure 3 does not show is the remarkable qualitative difference in the wave patterns for very shallow-water and for moderately deep water. In the case of moderately deep water the waves generated by the abrupt start that were overtaking the model were hardly visible, although certainly measurable. In the case of very shallow water, for values of $u/\sqrt{gh} > 0.7$ and < 1.3 visible waves spanning the tank, approximately two-dimensional waves, propagate down the tank ahead of the model. The longer the run, the more of them appear.

Before showing any data from our own experiments I should like to show some relevant results that have been obtained in studies of initial-value problems for the Korteweg-de Vries (KdV) equation. The graphs in Figure 4 are taken from a paper by Hammack and Segur (J. Fluid Mech. 65 (1974), 289-314) and show both measured wave records (solid lines) and calculated values (points) for various initial disturbances in a tank with shallow water (5 cm). Unfortunately the tank was not long enough to allow the final asymptotic behavior to develop. Figure 5 shows qualitatively, but as a snapshot rather than a time record, the predicted behavior after a sufficiently long time. This is taken from a course of lectures given by Segur at the International School of Physics "Enrico Fermi", Varenna, Italy, July 1980. What one sees are, in this case, two humps moving ahead, these followed by a longish downward-sloping region, and finally a trailing region of waves of gradually decreasing wave length that are slowly decaying in amplitude and also modulated. The leading humps, above the still-water level, are called "solitons", the trailing waves, the "radiated" waves.

We now turn to our own measurements. Two types of wave records were made. In one, three wave gauges were fixed in the tank as shown in the top part of Figure 6; in the other, the three gauges were attached to the towing carriage just ahead of the model in the arrangement shown in the lower half of Figure 6. Three types of run were made with the gauges fixed in the tank, ones of length 20 ft, 45 ft and 70 ft. The longest runs stopped about 15 ft short of the last gauges. The model was generally started up rather abruptly, but this did not appear to be neces-

sary for generating the observed results. The model itself was a model of a Series 60, block 80 hull, but the hull shape has rather little to do with the observed phenomenon. With the gauges fixed to the carriage only long runs were usually made.

In order not to overwhelm you with data, records will be shown only for Fr = $U/\sqrt{gh}$ = 0.9 and 1.1. Similar results were observed for values of Fr ranging from 0.8 to just below 1.2. At Fr = 1.2 and above wave breaking began, but even then the tank wave records were similar up to Fr = 1.35. Carriage wave records of solitons could not be obtained for Fr $\leqq$ 1.30, for the carriage moved faster than the solitons.

It is evident from inspection of the wave records taken from the fixed gauges that we are observing wave patterns very similar to these predicted by the KdV equation for asymptotic behavior of initially humped-up water. There are, however, some special aspects of these data. One very striking aspect is the almost perfect two-dimensionality of the solitons as they move down the tank ahead of the model, a surprising occurrence in the view of the three-dimensionality of the source of the waves, i.e., the model. This happens very quickly. In some of the runs even the first few trailing radiated waves appear to be almost two-dimensional. It seems reasonable to suppose that this observed two-dimensionality must be connected with tank width and would not occur in a sufficiently wide tank. Further experiments to study this phenomenon are planned.

The physical situation is different from the one that led to Hammack and Segur's results shown in Figures 4 and 5, for there is now a moving boundary, i.e., the model. This has produced an effect not accounted for by the usual initial-value problem for the KdV equation. If one examines the wave records for the different lengths of run, it is evident that more solitons are generated as the run becomes longer. This leads one to conjecture that the motion does not approach a steady state, but that solitons will continue to be generated as long as the model keeps moving. In such a case one might expect that eventually solitons of equal amplitude would be generated and

move off ahead of the model. This, however, appears to contradict a theorem stating that two solitons of equal amplitude cannot propagate in the same direction. The experimental data do not really throw much light on this situation. In some cases the individual solitons do appear to be of about equal amplitude, in others they definitely get smaller as one goes back, perhaps tending toward a limit but not reaching it. The phenomenon needs further investigation, both experimental and analytical.

If one examines the data from the longer runs, one can see that a shelf of water seems to be building up ahead of the model and to extend across the tank. The elevation seems to be approximately proportional to Fr - 0.7 for Fr > 0.7 .

Although a graph of gT_e/u against $u/\sqrt{gh}$ can be prepared, it is not clear that it is really significant until we can determine the parameters determining the periodicity, either by experiment or by theory. This a problem that will be examined in the future.

One may ask if the observed phenomenon has any practical significance in ship-model testing or in ship operation. In the case of model testing for resistance, it certainly must have an effect if a steady state is never reached. The consequences of not being aware of this can be left to one's imagination. As far as ship operation is concerned, one can envisage a situation where a ship is moving up a narrow channel of shallow depth and sending out ahead of it solitons moving at velocities considerably greater than that of the ship and possibly damaging shore installations before the ship is even in sight. An interesting problem for maritime lawyers. We suspect, however, that at present the chief interest is scientific, we present it as such, and hope to have more to report in the near future.

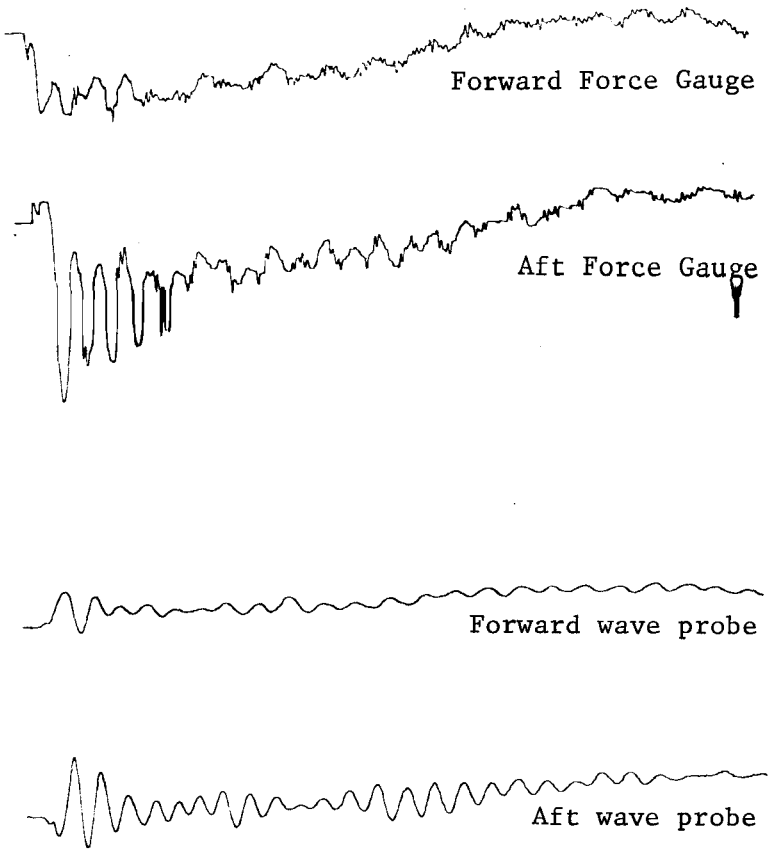

Figure 1

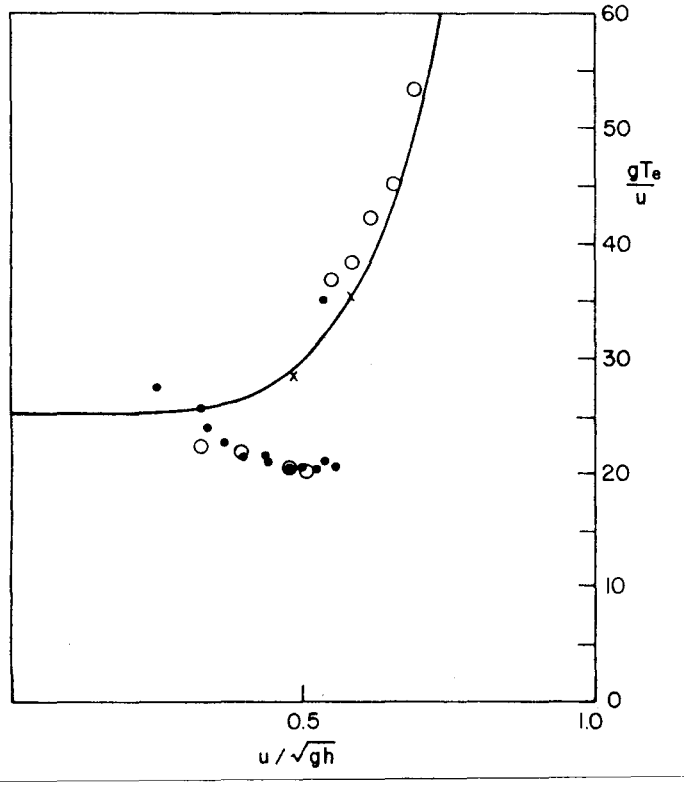

• Series 60; C_B = 0.80

o Series 60; C_B = 0.60

X Series 60; C_B = 0.80, measured 6 inches ahead of model

Figure 2-1

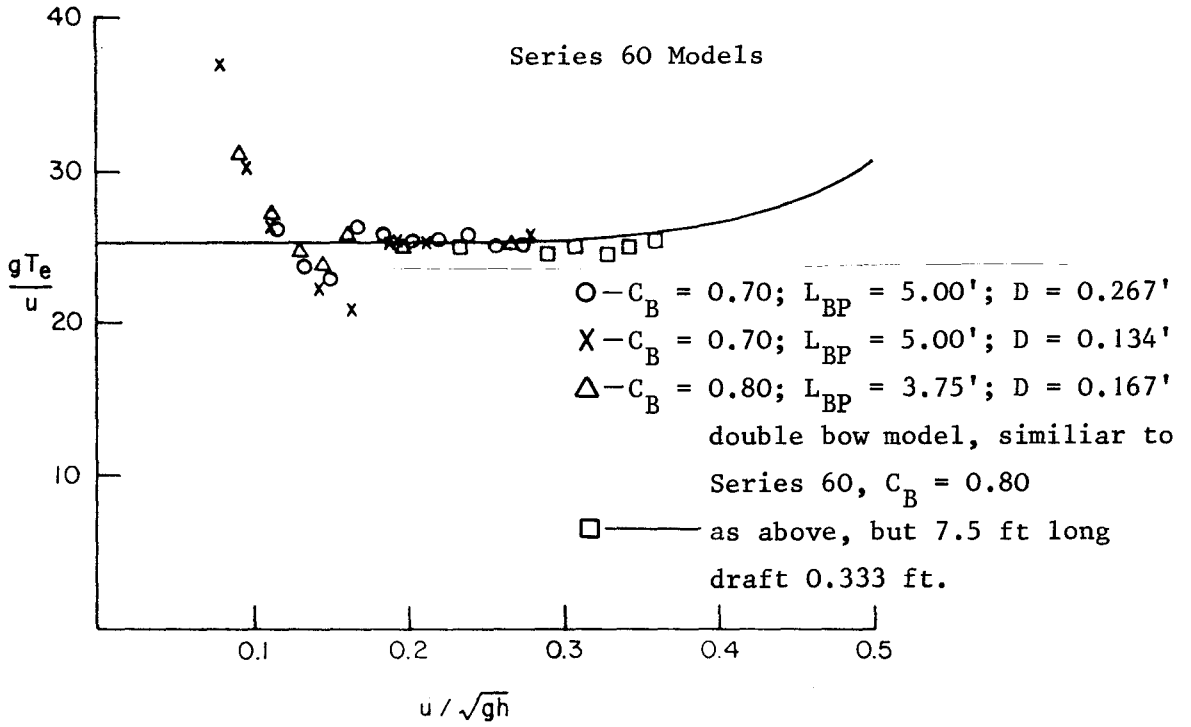
Series 60 Models
40
30
20
10
$\frac{gT_e}{u}$
O—C_B = 0.70; L_{BP} = 5.00'; D = 0.267'
X—C_B = 0.70; L_{BP} = 5.00'; D = 0.134'
Δ—C_B = 0.80; L_{BP} = 3.75'; D = 0.167'
double bow model, similiar to
Series 60, C_B = 0.80
□——— as above, but 7.5 ft long
draft 0.333 ft.
0.1
0.2
0.3
0.4
0.5
$u/\sqrt{gh}$

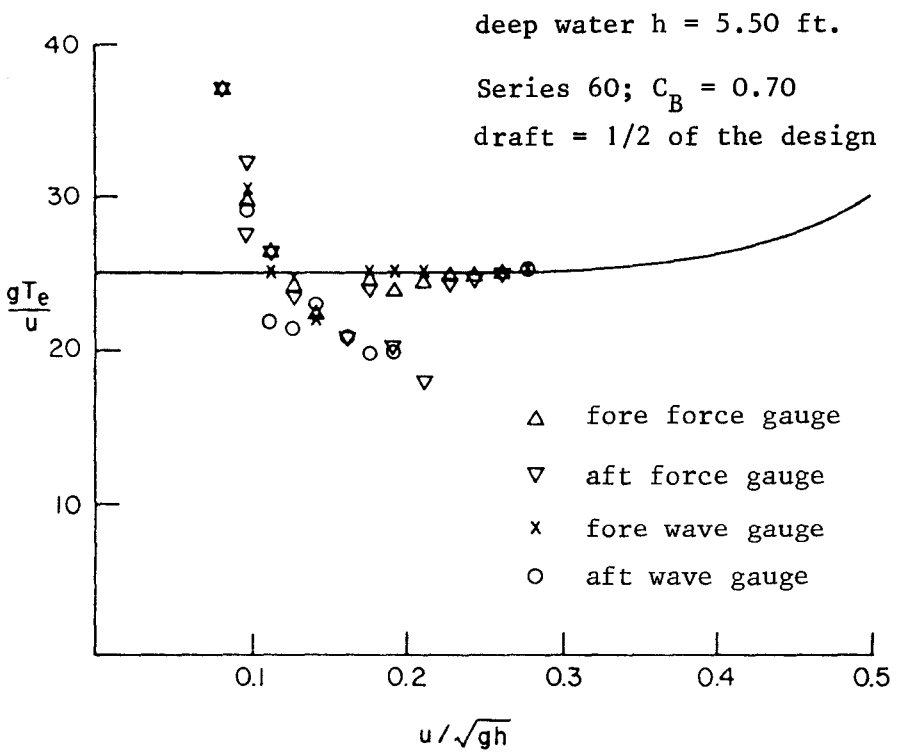
deep water h = 5.50 ft.
Series 60; C_B = 0.70
draft = 1/2 of the design
40
30
20
10
$\frac{gT_e}{u}$
Δ fore force gauge
∇ aft force gauge
x fore wave gauge
O aft wave gauge
0.1
0.2
0.3
0.4
0.5
$u/\sqrt{gh}$

Figure 2-2

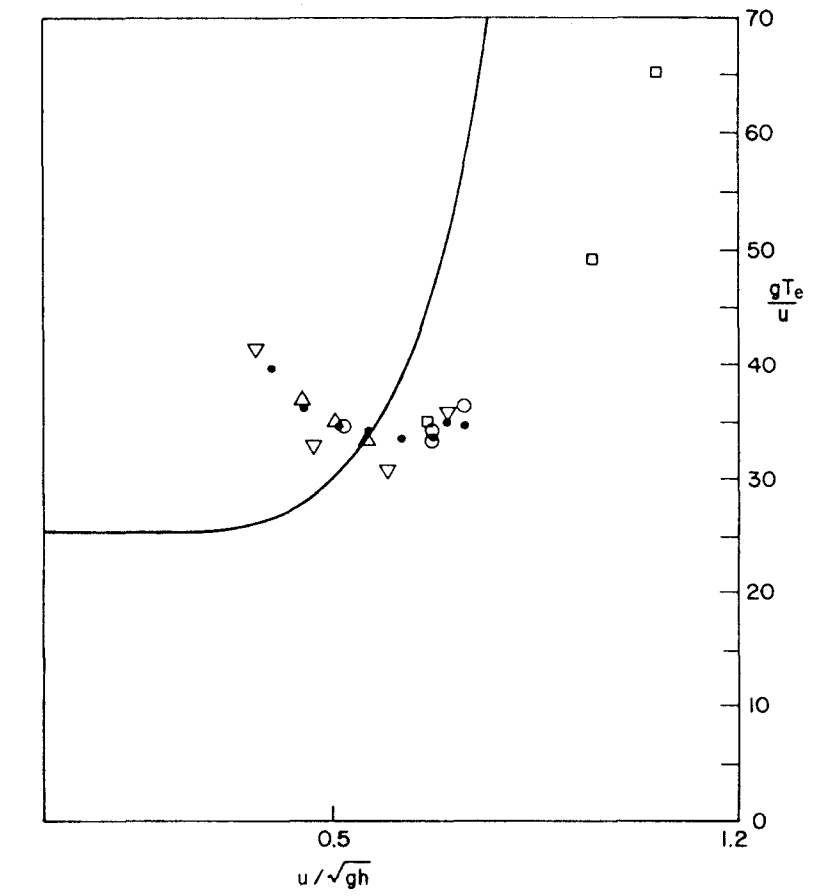

- ○ h = 0.520'; hump 2.5' long; C_B = 0.60
- • h = 0.520'; hump 2.5' long; C_B = 0.80
- △ h = 0.520'; hump 8.0' long; C_B = 0.80
- □ h = 0.500'; const. depth C_B = 0.60
- ▽ h = 0.616'; const. depth C_B = 0.80

Figure 3

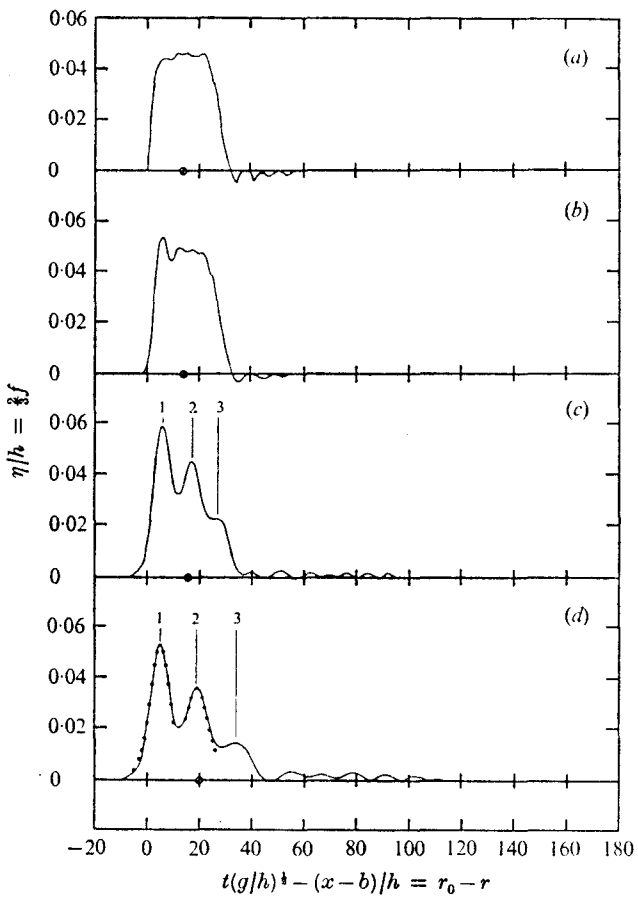

V = 30.5 cm^3/cm, N = 3, d_s/h = 700

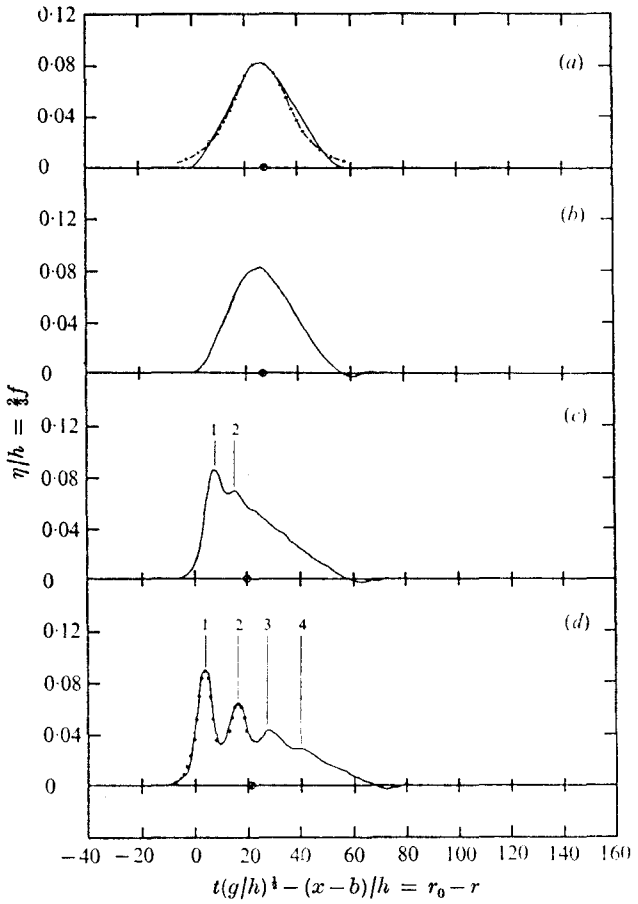

V = 61 cm^3/cm, N = 4, d_s/h = 680

—+— $f = 0.12\ \mathrm{sech}^2\{0.069(r_0 - r)\}$

Figure 4-1 Experimental wave systems after Hammack + Segur (1974)

h = 5 cm, b = 61 cm

——— measured profiles

● soliton profiles computed using (11)

◓ location of centroid

(a) $(x-b)/h$ = 0 (b) $(x-b)/h$ = 20

(c) $(x-b)/h$ = 180 (d) $(x-b)/h$ = 400

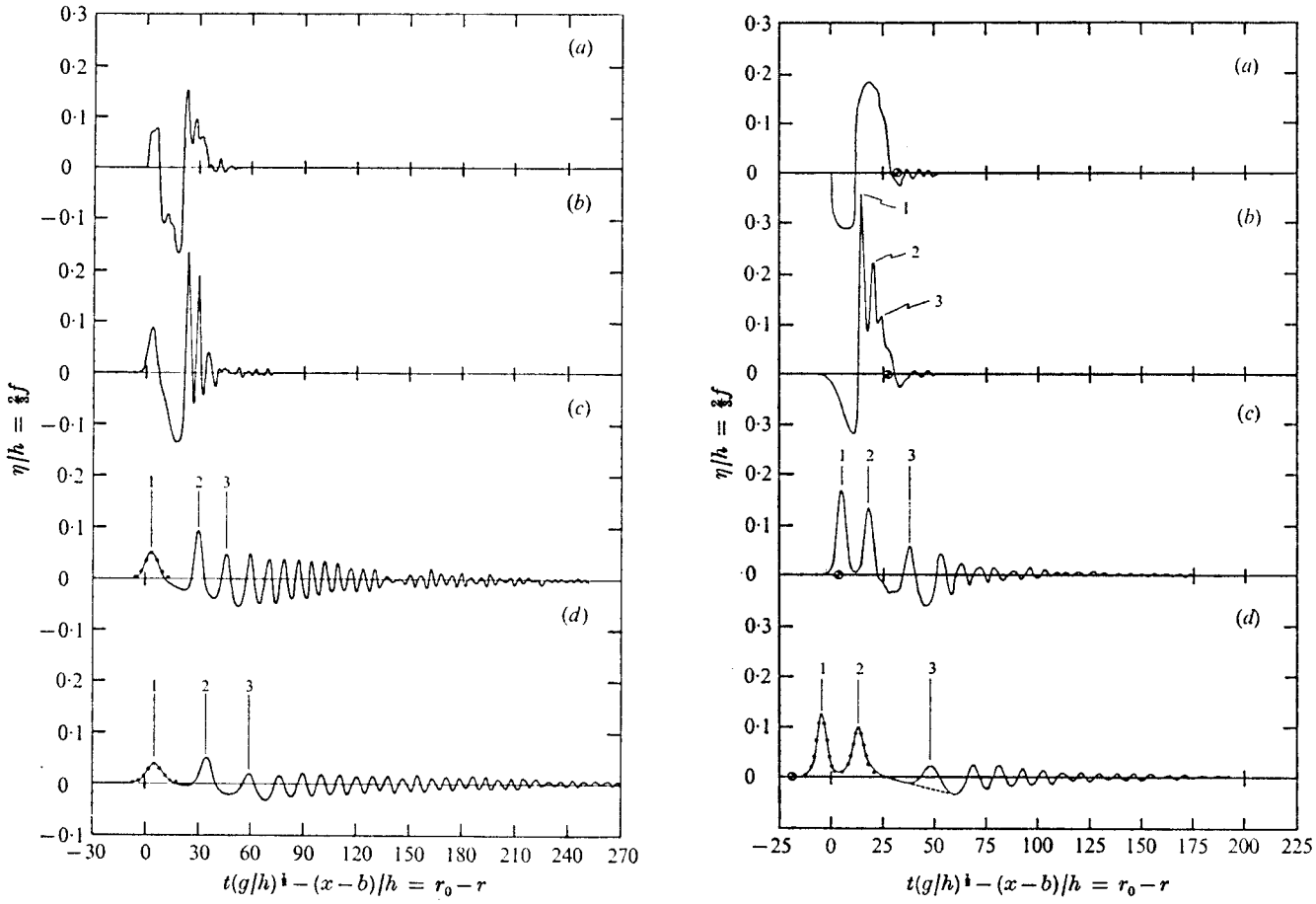

$V = 0$, $d_s/h = 220$

$V = 30.5$ cm^3/cm, $d_s/h = 260$

------ hypothetical position of the leading portion of the tail

◕ location of centroid

Figure 4-2 Experimental wave systems after Hammack + Segur (1974)

$h = 5$ cm, $b = 30.5$ cm, $N = 3$

——— measured profiles

● soliton profiles computed using (11)

(a) $(x-b)/h = 0$ (b) $(x-b)/h = 20$

(c) $(x-b)/h = 200$ (d) $(x-b)/h = 400$

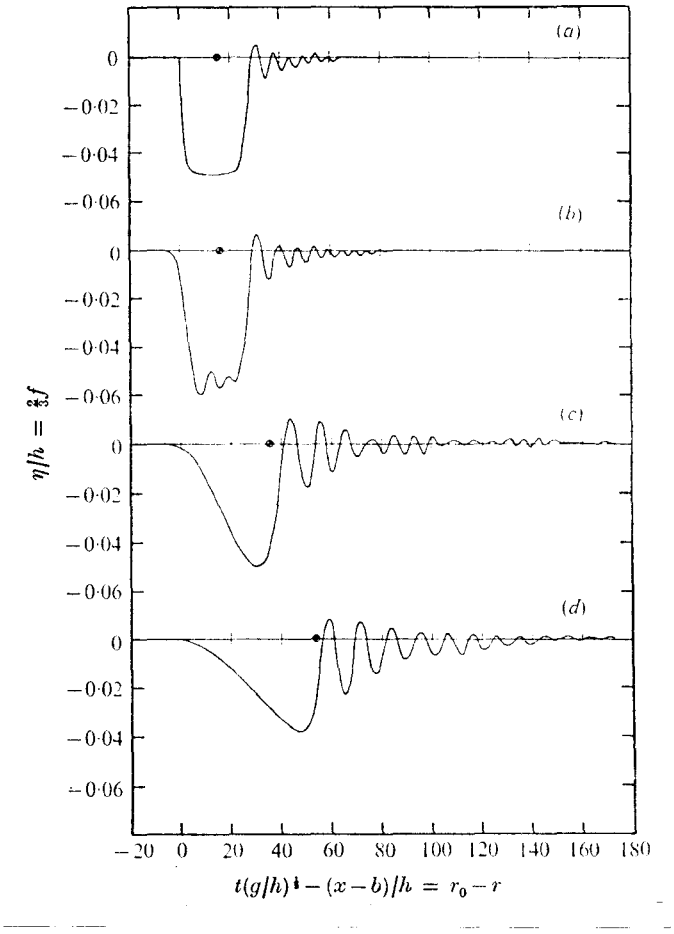

b = 61 cm, N = 0, d_s/h = 600

(c) $(x-b)/h$ = 180

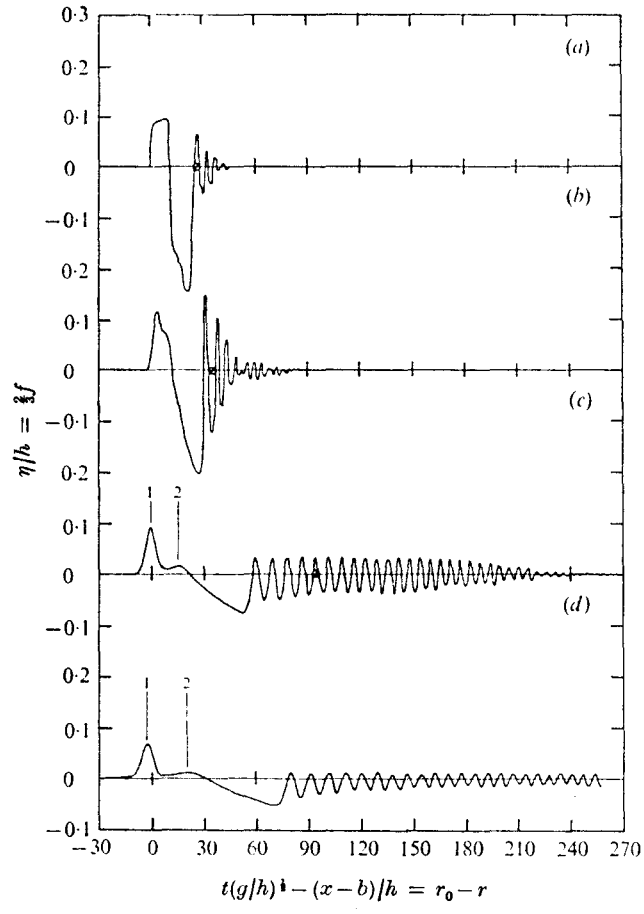

b = 30.5 cm, N = 1, d_s/h = 110

(c) $(x-b)/h$ = 200

Figure 4-3 Experimental wave systems after Hammack + Segur (1974)

h = 5 cm, V = -30.5 cm^3/cm,

——— measured profiles

◕ location of centroid

(a) $(x-b)/h$ = 0 (b) $(x-b)/h$ = 20

(d) $(x-b)/h$ = 400

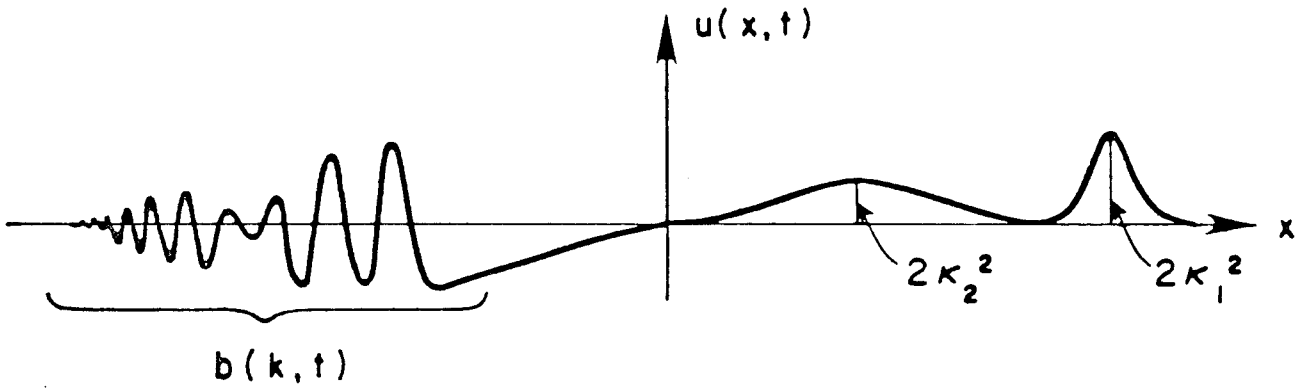

Figure 5

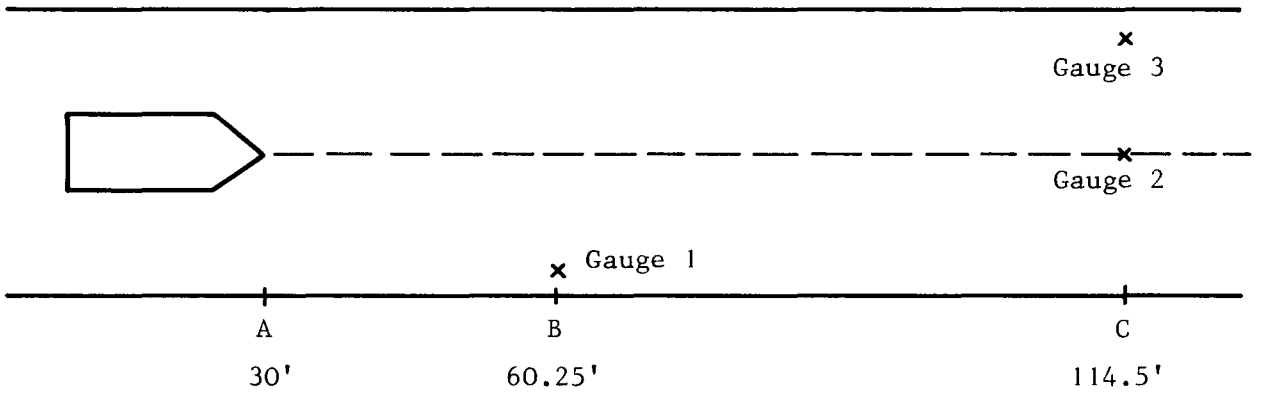
Gauge 3
Gauge 2
Gauge 1
A
B
C
30'
60.25'
114.5'

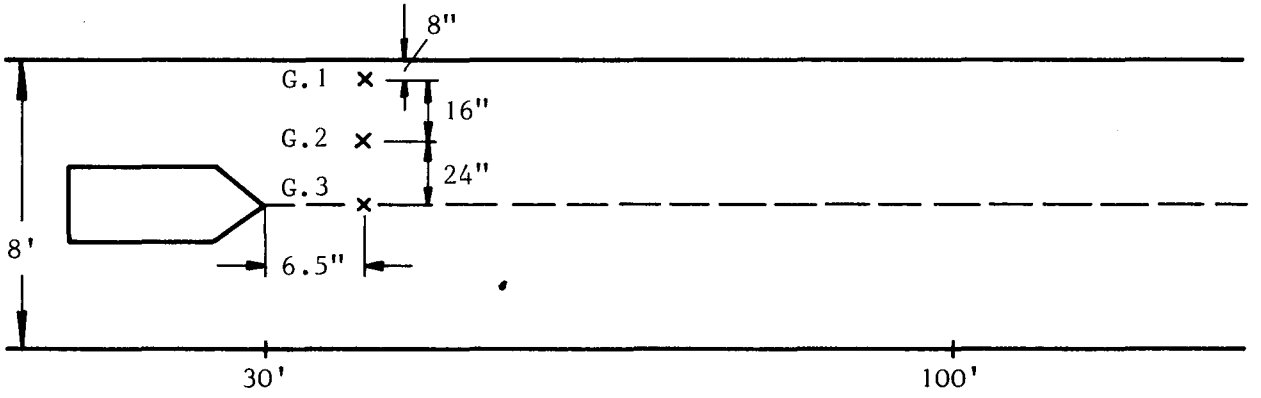
8"
G.1
16"
G.2
24"
G.3
8'
6.5"
30'
100'

Figure 6

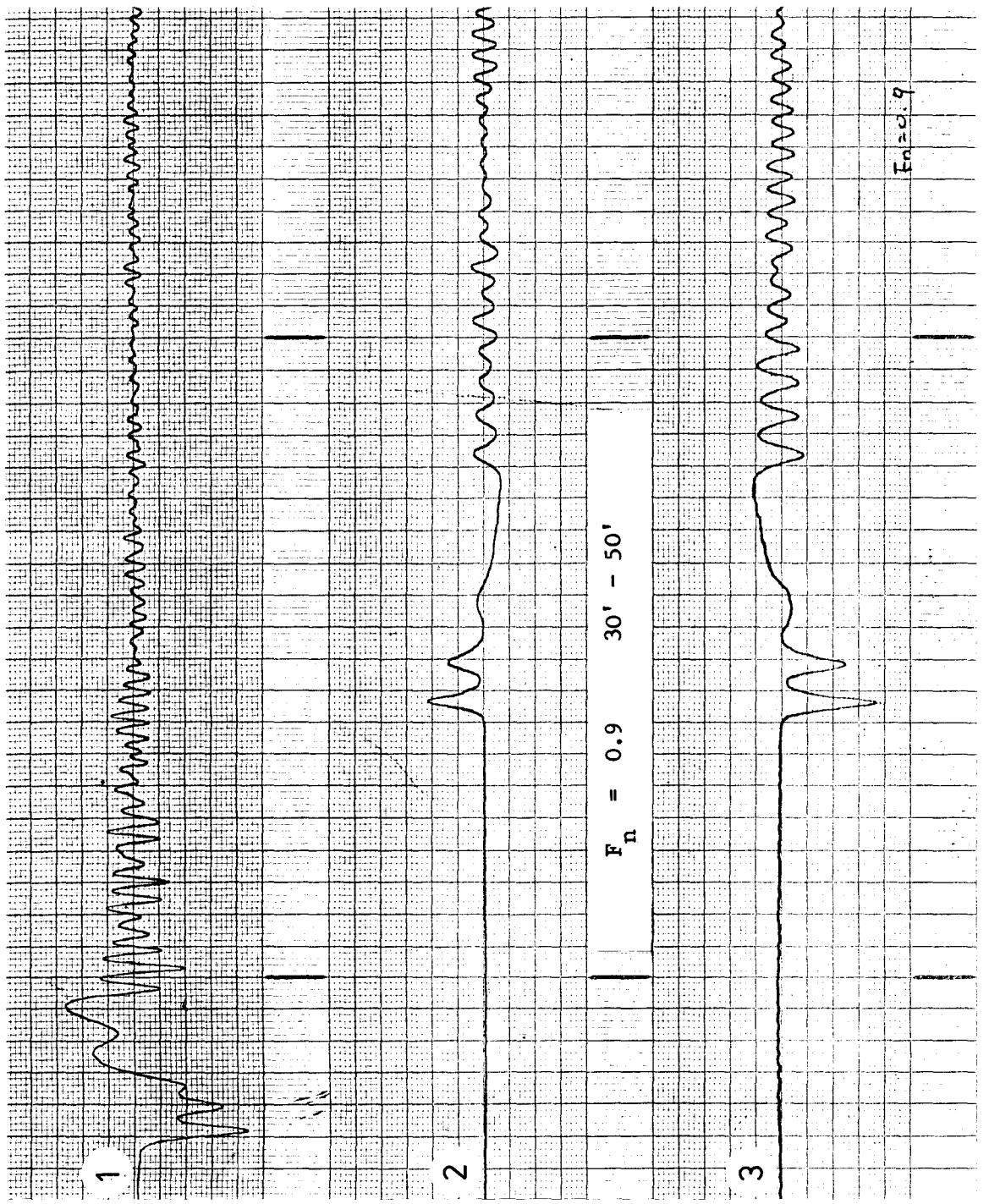

Figure 7-1

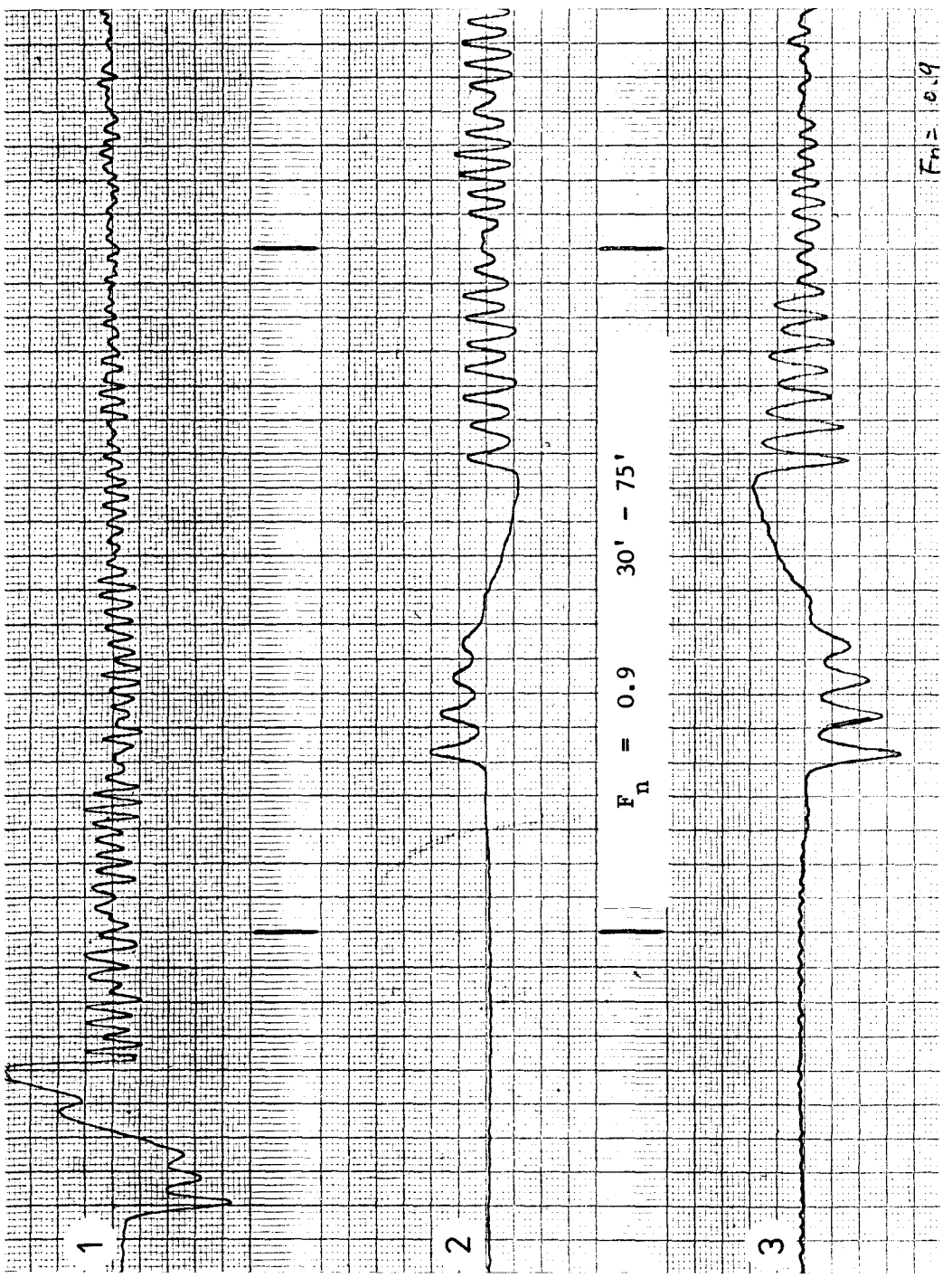

Figure 7-2

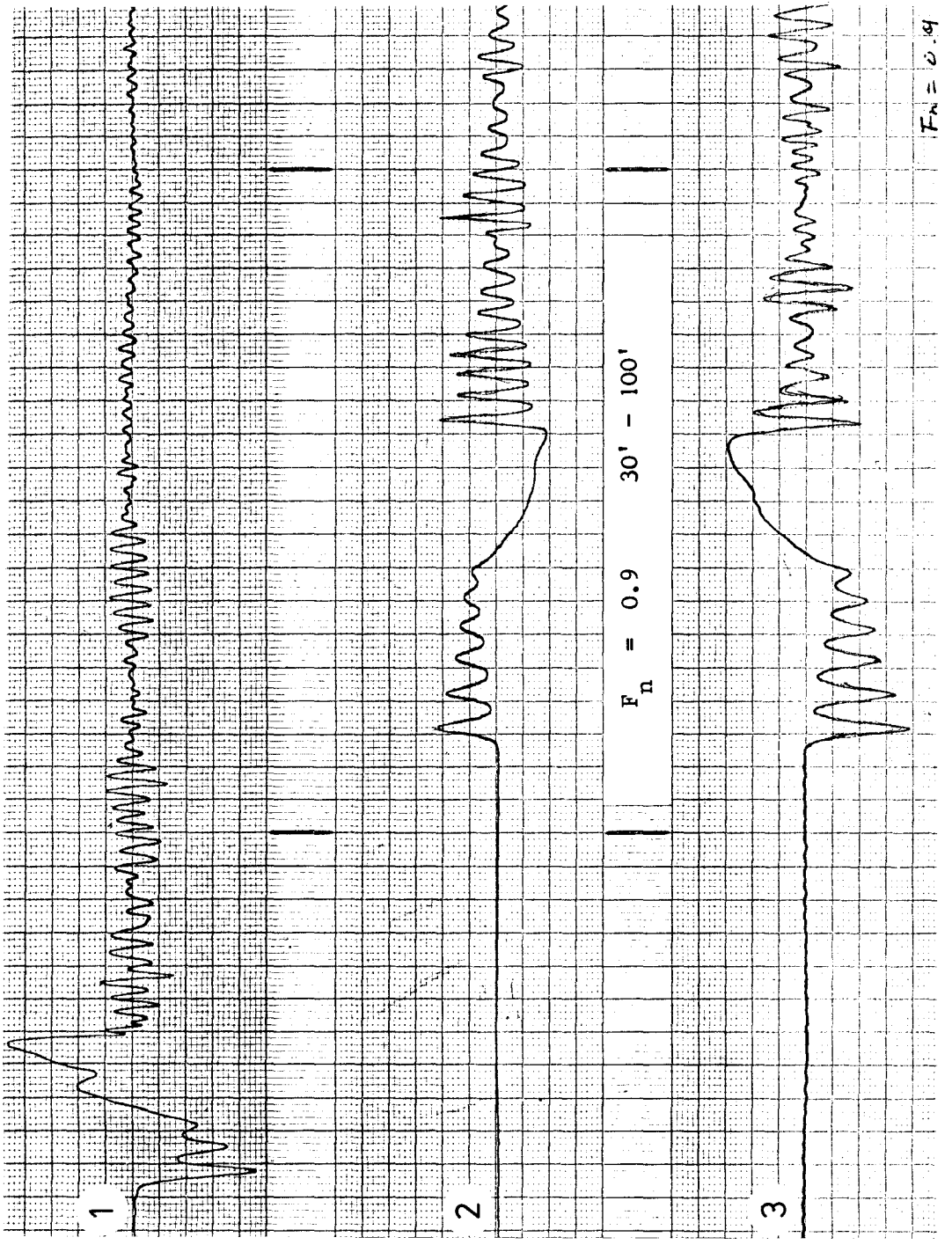

Figure 7-3

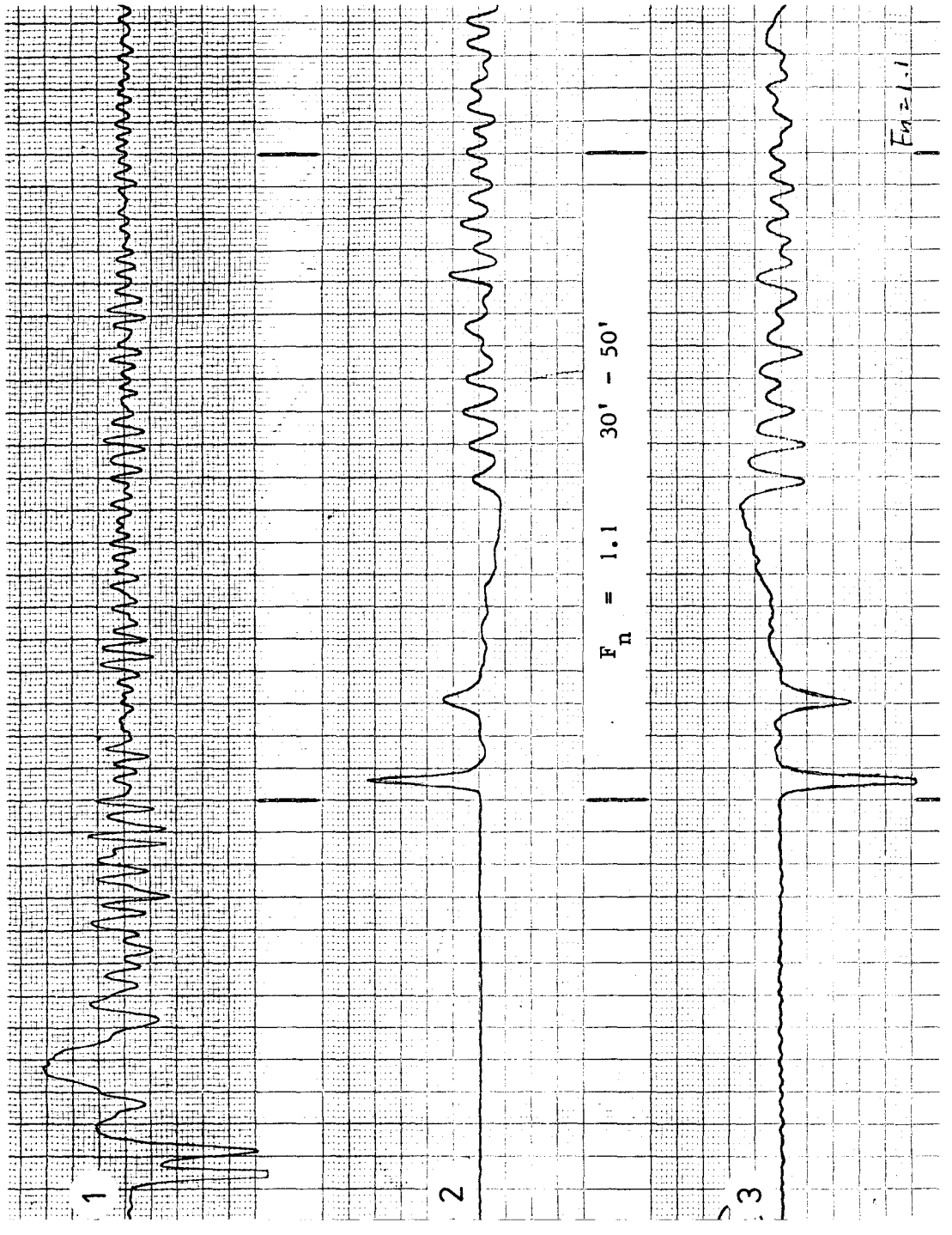

Figure 8-1

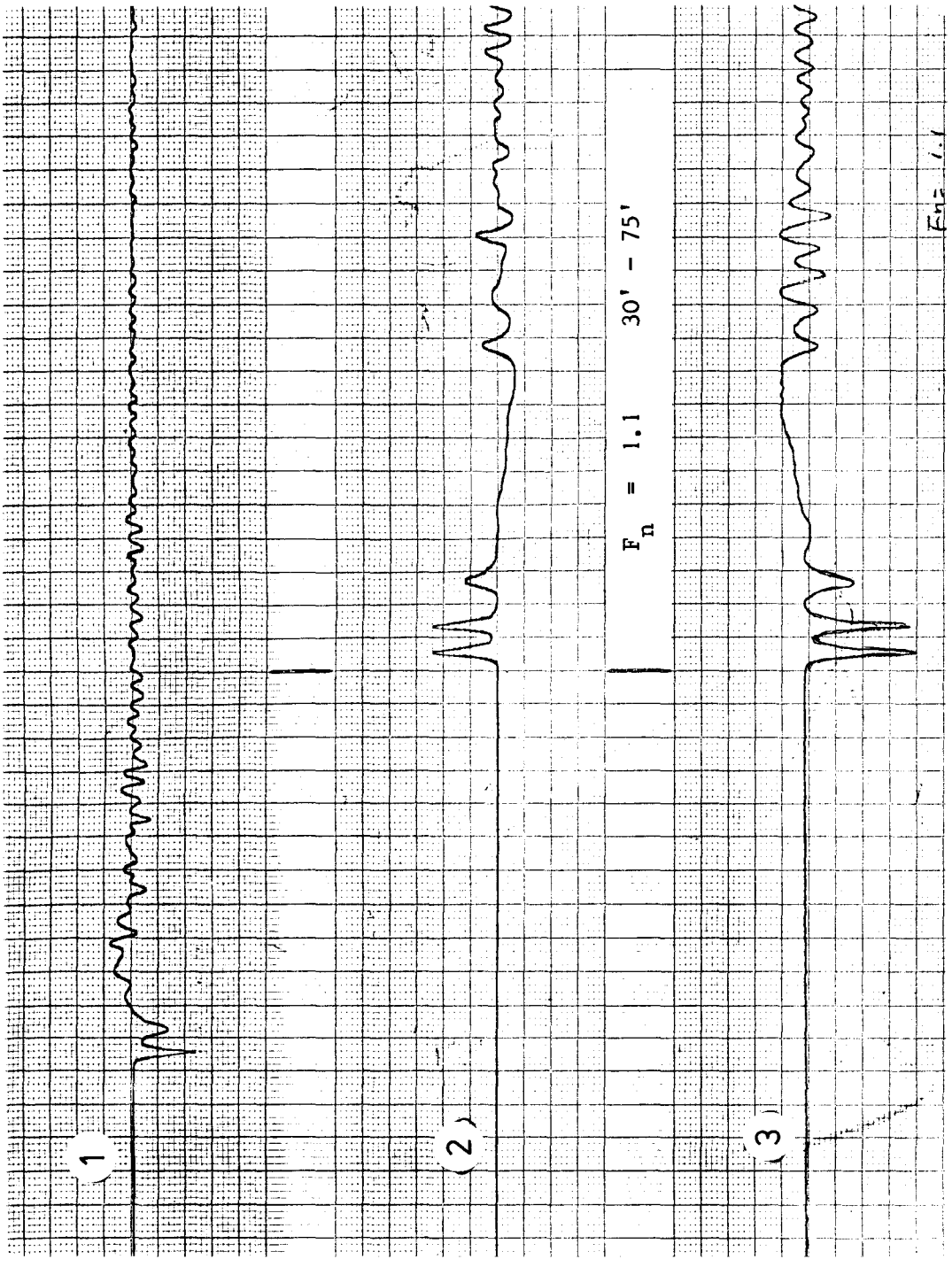

Figure 8-2

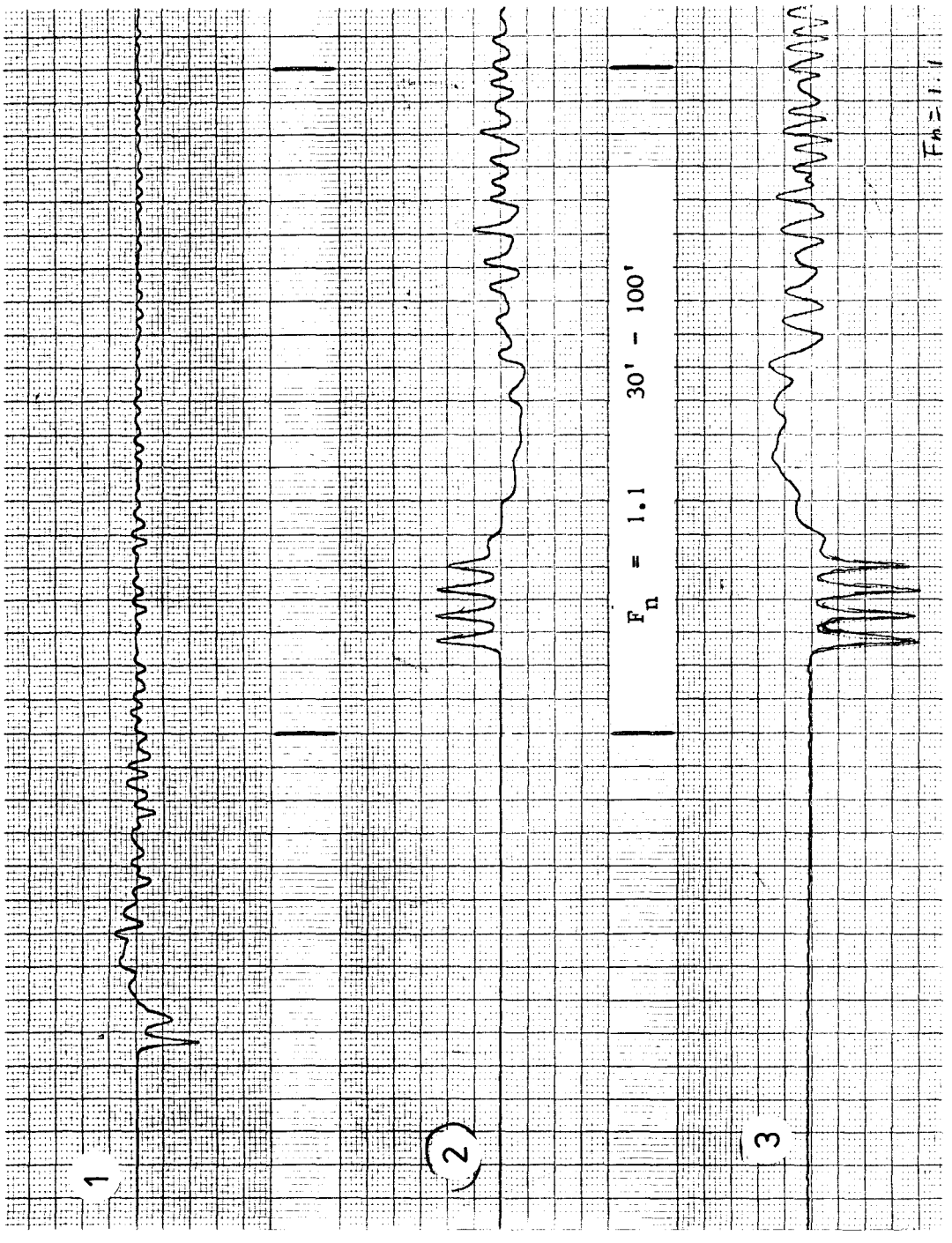

Figure 8-3

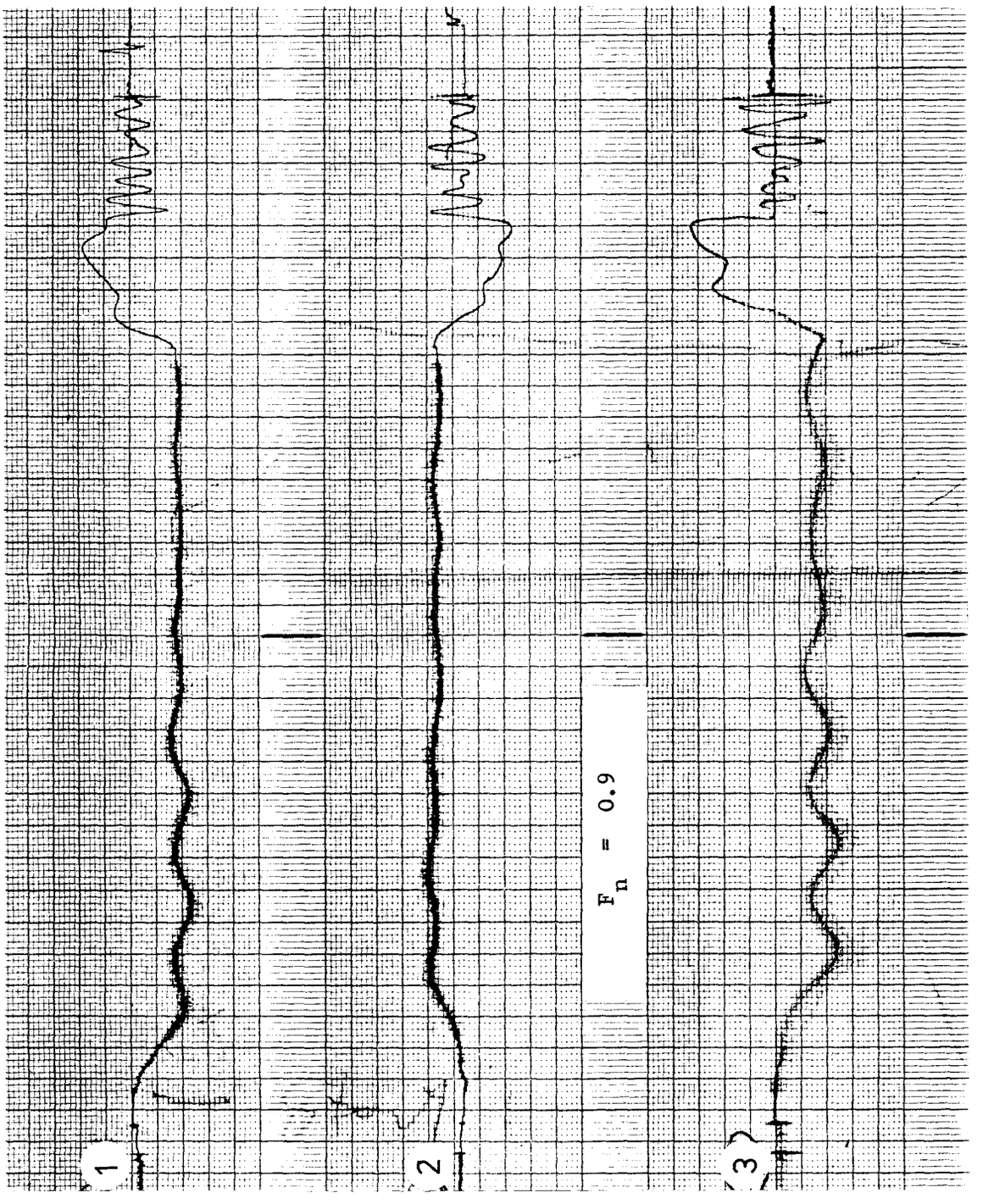

Figure 9-1

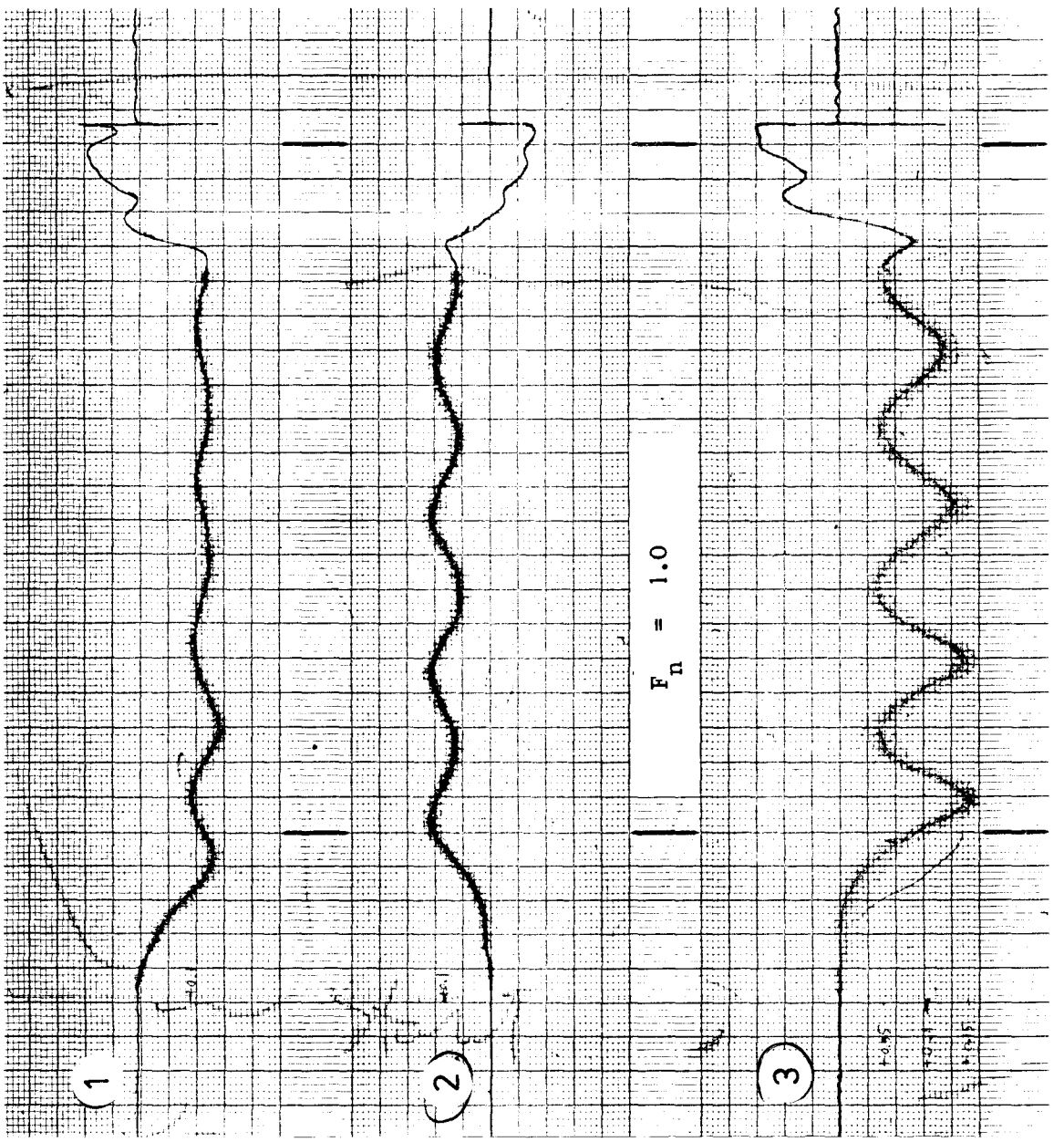

Figure 9-2

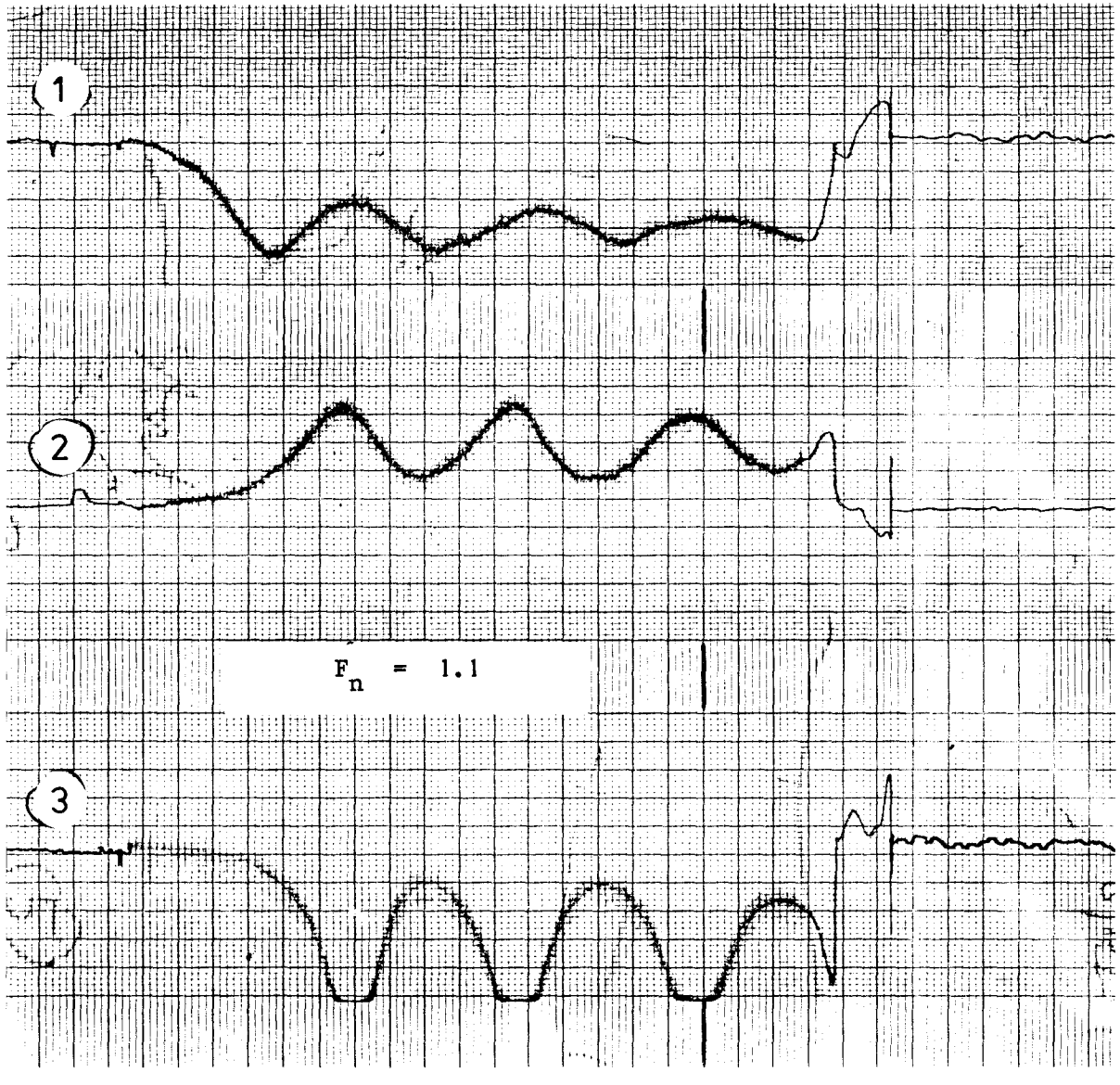

Figure 9-3

Approximate Calculation of Ship Frictional Resistance Increase due to Surface Roughness

by E. Baba and K. Tokunaga *

1. Introduction

Hull roughness is an important factor to the propulsive performance of a ship in operation. Therefore, in the days of uprising fuel oil cost, prediction of frictional resistance characteristics due to hull roughness has become one of the major topics in ship hydrodynamics.

In the past, efforts have been made in finding relationship between roughness geometry and frictional resistance increase [1),2)]. However, a clear cut prediction method of frictional resistance for irregular rough surface has not been developed yet.

In the recent years it becomes possible to determine roughness function of full-scale hull roughness. For instance, Karlsson developed a wind tunnel floating element drag measurement technique and gave roughness function data for replicas of roughened ship plates.[3)] Musker and Lewkowicz developed a method to transfer copies of ship-hull roughness onto the inside a pipe-line, and gave roughness function data.[4)]

The usage of such roughness function determined by use of replica of full-scale hull roughness seems to be a direct and reliable method for the resistance prediction.

---

* Nagasaki Experimental Tank, Nagasaki Technical Institute Mitsubishi Heavy Industries, Ltd.

In accordance with the development of efficient procedure in determining roughness function by use of replica, it may become possible to represent hull roughness by a combination of various roughness functions which are determined from replicas taken from various parts of hull surface.

Making use of such roughness functions we may predict ship frictional resistance increase based on boundary layer theory for rough surface.

As far as the theory for rough surface is concerned, three-dimensional theory for ship form has not been developed yet. At present, a ship is replaced by a flat plate with the same length and speed. Then two-dimensional turbulent boundary layer theory for rough surface is used. Further, hull roughness is represented by a single roughness function for the sake of convenience.

It has not been clarified yet to what extent this approximation can predict frictional resistance increase for ship forms, especially for full ship forms which deviate largely from flat plate.

In the present study a two-dimensional boundary layer theory for roughened surface is applied to potential streamlines over the hull surface of a full ship so as to take into account the longitudinal pressure gradients along the streamlines, and the calculated results were compared with those calculated by replacing a ship with a flat plate in order to know the effect of pressure

gradient. In this calculation the roughness functions provided by Karlsson for full-scale ship were used.

The calculated frictional resistance increase by the present method was compared with extrapolated values from tank tests of flat plates covered with conventional paints of various roughness. In the extrapolation from model-scale to full-scale Sasajima and Himeno's scaling law of frictional resistance for rough surface was used.[5)]

Finally, calculations were made for a combination of different roughness functions over a ship hull. And then the interference effects of upstream roughness on the downstream local frictional resistance was discussed.

2. Outline of the theory

In 1969 Uberoi applied a two-dimensional turbulent boundary layer theory to the streamlines over smooth hull surface and calculated viscous resistance of a ship for the first time.[6)]

In the present study the same method was applied to calculate turbulent boundary layer for rough surface so as to take into account the influence of the longitudinal pressure gradients along the streamlines. In this calculation, therefore, neither the crossflow nor the streamline convergence was taken into account for the sake of simplicity.

Streamlines and pressure distribution over the hull surface were calculated by the potential theory.

Calculations of boundary layer parameters on each streamline are based on the following equations.

Momentum integral equation was used as the basic equation, viz.,

$$\frac{d\theta}{ds} = \frac{C_f'}{2} - (H+2).\frac{\theta}{U}\frac{dU}{ds} \qquad (1)$$

and entrainment equation was used as the auxiliary equation.

$$\frac{d}{ds}(\delta-\delta^*) = F(H_{\delta-\delta^*}) - \frac{\delta-\delta^*}{U}\frac{dU}{ds} \qquad (2)$$

where $F(H_{\delta-\delta^*})$ is the Head's entrainment function.

Relationship between Head's entrainment function F and shape factor H is common to both smooth and roughened surfaces.

As the skin friction law for smooth and roughened surface, Clauser's formula was used:[7)]

$$\sqrt{\frac{2}{C_f'}} = 5.6 \log_{10}\frac{U\delta^*}{\nu} + 4.3 - \frac{\Delta U_1}{U_*} + \frac{\Delta U_2}{U_*} , \qquad (3)$$

where $\Delta U_1/U_*$ is the roughness function, which was approximated by a function of U_*K/ν:

$$\frac{\Delta U_1}{U_*} = C_o + C_1 R_k + \sum_{i=2} C_i \,(\ell n R_k)^{\,i-1} \qquad (4)$$

$R_k = U_* K/\nu$, and C_o, C_1, C_i are constants which are determined so as to fit the experimental values of $\Delta U_1/U_*$. This function is alterable depending on the location over the hull surface. For smooth surface $\Delta U_1/U_* = 0$.

$\Delta U_2/U_*$ represents the contribution of pressure gradient to velocity defect law,

$$\frac{\Delta U_2}{U_*} = 1.253\ (G-6.7) \qquad G \geq 6.7,$$
$$= 0.404\ (G-6.7) \qquad G < 6.7, \tag{5}$$

where

$$G = \sqrt{\frac{2}{C_{f'}}} \cdot \frac{H-1}{H}$$

Equations (1) and (2) can be integrated simultaneously by Runge-Kutta-Gill method with the skin friction coefficient being determined numerically at each step from equations (3) to (5) by iterative method.

3. Calculation of frictional resistance increase of a full-scale ship

3.1 Calculation for a full ship form of $C_b = 0.84$

Two-dimensional theory for rough surface explained in the previous section was applied to the potential streamlines over a full ship form with the following principal particulars:

Lpp = 220 m , Cb = 0.84 , Lpp/B = 5.96 , B/d = 2.62

Fig.1 shows the body plan where framelines are expressed by a modified Lewis form. The calculations were made on thirteen potential streamlines over the hull surface. Some of them are shown in the body plan.

In the calculation of frictional resistance for rough surfaces, four different roughness functions prepared by Karlsson[3] were used, since they are mathematically expressed in a form of the expression (4) in the previous section. Rough surfaces and roughness functions prepared by Karlsson are shown in Appendix 1.

Table 1 shows the results of calculations made by the present method. For reference, calculations were also made when the ship is replaced by a flat plate with the same length and speed as done by Karlsson[3] and Grigson[8].

The frictional resistance increase calculated along streamlines gives a little higher values than those of flat plate calculation. The present results are a little lower than those read off the charts prepared by Karlsson for flat plate.

3.2 Effect of pressure gradient

In the previous section only a small difference was observed between the frictional resistance increase based on calculations along streamlines and flat plate.

In order to know the effect of pressure gradient a comparison was made of boundary lager parameters by use of Karlsson's rough surface NO.3. Fig.2 shows the comparison of boundary layer parameters, local skin friction coefficient C_f, shape factor H and momentum thickness θ/L for both methods. It is clear that the flat plate calculation gives rather monotonous change of these parameters. On the other hand, the calculation along streamline shows an influence of pressure gradient.

For the consideration of local characteristics of flow around a ship due to roughness, the present method of calculation may give more rational information. However, the integrated values, that is the total skin friction resistance for both methods come close together as is the case for smooth hull surface.

4. Relation between ΔC_f and surface roughness

4.1 Resistance test data of flat plates with various surface roughness

In the previous section calculations of frictional resistance increase due to surface roughness were made by use of roughness functions corresponding to full-scale ships.

In the present section attempts were made to compare these calculated results with existing towing test data of flat plates whose surfaces were treated by use of conventional paints for ship hull surface.

At present, following test results are available to the present authors:

	Method of test	Length of test plate	Test speed
Todd[9]	Towing test of planks	6.4 m	<7.13 m/sec
Townsin et al.[10]	Flume test of plates	1.0 m	7.50 m/sec
Present authors	Towing test of flat plates.	3.0 m	<9.0 m/sec

These experimental data were extrapolated to full-scale condition by making use of Sasajima and Himeno's scaling law of frictional resistance due to surface roughness.[5]

$$\Delta C_{fs} = \Delta C_{fm} \cdot \left(\frac{C_{fs}}{C_{fm}}\right)^2 \qquad (6)$$

with roughness Reynolds number UK/ν = constant.

This formula can be applied to any kind of roughness provided that $UK/\nu < 1\times10^3$.

The validity of this formula was examined by the authors by use of 7m and 4.2m geosims whose surfaces were artificially roughened.[11] In Appendix 2 a summary of the examination is shown.

In the followings extrapolated values from model tests to a ship of 220 m in length at 15 Knots are shown.

Todd's data (Plank length=6.4m, speed=7.13m/sec)

Kinds of paint	Peak to valley height	$10^3\Delta C_{fm}$	$10^3\Delta C_{fs}$
Hot plastic	508 μm*	0.900	0.347
Anticorrosive	76	0.240	0.093
Cold plastic	51	0.040	0.015
Zin chromate	54	0.040	0.015

$\Delta C_{fs} = (C_{fs}/C_{fm})^2 \Delta C_{fm} = 0.386\Delta C_{fm}$ based on Schoenherr line.

*Reading from the roughness recordings shown in Fig.11(a) to (d) of ref.(9).

Townsin et al.'s data (Plate length = 1.0 m, Speed = 7.50 m/sec)

MAA Roughness	Drag at U = 7.5 m/sec	$10^3 C_{fm}$	$10^3\Delta C_{fm}$	$10^3\Delta C_{fs}$
Smooth	3.33 kg	2.903		
46 μm	3.80	3.313	0.410	0.084
54	3.70	3.225	0.322	0.066
351	4.70	4.097	1.195	0.243
113	4.20	3.661	0.758	0.155
415	5.20	4.533	1.630	0.332
95	3.96	3.452	0.549	0.112
654	5.65	4.925	2.022	0.412
136	4.25	3.705	0.802	0.164

C_{fm} for smooth surface is close to Hughes friction line.

$\Delta C_{fs} = 0.204\ \Delta C_{fm}$ based on Hughes friction Line.

Baba and Tokunaga (Plate length = 3.0^{m}, Speed = 7.60^{m}/sec)

Test arrangement is shown in Fig.3. Water temperature = 14.0°C.
$U_{model} = U_{ship} \times (\nu_{model}/\nu_{ship}$ at 15°C) = 7.60 m/sec.

MAA Roughness	$10^3 C_{fm}$	$10^3 \Delta C_{fm}$	$10^3 \Delta C_{fs}$
Schoenherr friction line	2.638		
96 μm	2.815	0.177	0.055
48	2.600	-0.038	-0.012
35	2.670	0.032	0.010
128	2.855	0.217	0.067
241	3.330	0.692	0.213

$\Delta C_{fs} = 0.308\ \Delta C_{fm}$ based on Schoenherr line.

*Resistance was determined from the difference of resistance measured at two different drafts (0.5m and 0.3m) of the plates so as to eliminate the effect of spray resistance, wind resistance of supporting apparatus and other experimental errors.

4.2 Comparison of calculated ΔC_f with experimental data

In Fig.4 extrapolated experimental data of Todd, Townsin et al. and the present authors are plotted versus mean apparent amplitude α, which is defined as the mean of peak to valley heights in 50mm interval as proposed by BSRA. In this figure ΔC_f read off Karlsson's charts which were prepared based on flat plate calculation and the present authors' calculations which were made along streamlines by use of Karlsson's roughness functions are shown.

Notwithstanding that the methods of resistance measurements are different, experimental data come close together after the application of Sasajima and Himeno's scaling law. Further, calculated ΔC_f are also close to the experimental data. The plotted data seem to be proportional to the mean apparent amplitude. This is an important result for practical purpose to know quickly the order of magnitude of ΔC_f versus roughness height.

Nextly, equivalent sand roughness height was sought by use of Nikuradse-Schlichting resistance diagram for sand-roughened plate [12].

Readings from Nikuradse-Schlichting resistance diagram

L/Ks	Ks	α (MAA)		$10^3\Delta C_f$ at $UL/\nu=1.43\times10^9$
	(L=220m)	α=4Ks	α=5Ks	
2×10^6	110 μm	440 μm	550 μm	0.35
1.5×10^6	147	587	735	0.44
1×10^6	220	880	1100	0.66
7.5×10^5	293	1172	1465	0.80

As shown in this figure it was found that the plotted data approximately correspond to the sand roughness height Ks in between $\frac{1}{4}\alpha$ and $\frac{1}{5}\alpha$.

For reference, in this figure 1978 ITTC correlation formula:

$$10^3 \Delta C_f = 105 \left(\frac{\alpha}{L} \right)^{\frac{1}{3}} - 0.64$$

is also shown. This formula was derived based on the analyses of a number of ship trials and their model experiments. Therefore, effects of structural roughness and other factors related to full-scale trials are included. The comparison of this correlation formula with the data prepared in the present study may give an idea about the order of magnitude of these effects which were not considered in the present study.

It is noted that the rate of increase of ΔC_f in the present study with respect to the mean apparent amplitude α is less than that of ITTC correlation formula.

5. Calculation for a combination of different hull roughnesses

In this section calculations were made for two hypothetical combinations of hull roughness by use of roughness functions prepared by Karlsson.[3)]

Rough Surface No.3 (roughest surface in Karlsson's data) was applied to the fore body of a ship and rough surface No.1 (Corresponds to hull roughness of a newly built ship) was applied to the aft body, and then, in the reverse order, rough surface No.1 was applied to the first half length and rough surface No.3 to the aft body.

Calculations were made along the potential streamlines for the same hull form as used in Section 3.
Calculated results are shown in Table 2.

Table 2 Frictional resistance increase for a combination of different hull roughness

Ship length 220 m ship speed 15 Knots Reynolds No. 1.43×10^9

Surface No. for fore body	Surface No. for aft body	Increment of frictional resistance $\Delta C_f \times 10^3$
No.3	No.1	0.312
No.1	No.3	0.334

From Table 2 it is observed that the case where Rough surface No.3 is in the forebody gives a little lower value of ΔC_f than the case where the Rough surface No.1 is in the forebody.

Fig.5 shows a comparison of local skin friction coefficients for both cases. From the figure it is observed that due to larger roughness in the forward part the local skin friction coefficient in the after part is almost comparable with smooth hull. On the other hand, Rough surface No.1 produces resistance increase due to its surface roughness when it is in the forward part, and Rough surface No.3 does not have a big influence of the boundary layer of forward part because of high roughness of surface No.3.

It is recognized that there is an effect of upstream roughness to the local skin friction to the neighbour in the downstream part. A similar result has been shown by Townsin et al. in their recent paper.[13] Fig.6 shows are of calculated examples quoted from the paper. Experimental studies to confirm this theoretical prediction is worthwhile for the examination of the validity of the theory used in the present study.

6. Concluding remarks

In the present paper approximate calculations of frictional resistance increase due to surface roughness were made by use of the roughness functions corresponding to the actual hull surfaces. The results were compared with the experimantal data extrapolated by use of Sasajima and Himeno's scaling law of frictional resistance of rough surface. A good correlation of the various data was obtained when they were plotted with respect to the mean apparent amplitude.

In accordance with the development of an efficient procedure in determining roughness function for full-scale hull roughness, the present method of calculation may serve as a practical means to predict ship frictional resistance due to hull surface roughness.

It is left for the future study to investigate into the effect of cross flow and streamline convergence on frictional resistance increase. Effect of roughness on flow separation along the hull surface and its effect on the free-surface phenomena should also be investigated. A preliminary study on the separation problem has been made by Musker and Lewkowicz[4].

7. Acknowledgements

The authors wish to express their deep appreciation to Dr. H. Tanibayashi, manager of Resistance and Propulsion Laboratory, Nagasaki Experimental Tank, MHI and Mr. T. Nagamatsu of the laboratory for their stimulating and encouraging discussions. Thanks are also due to Dr. R.L. Townsin for his instructive discussions.

8. References

(1) Sasajima, H. and Yoshida, E., Frictional Resistance of Wavy Roughened Surface, International Shipbuilding Progress. Vol.2, No.13, 1955.

(2) Sasajima, H., Terao,T., Yoko,K., Nakato,M. and Ogawa,A., Experimental investigation into roughness of hull surface and increase of skin frictional resistance, Journal of the Society of Naval Architects of Japan, Vol.117, June 1965.

(3) Karlsson, R.I., The effect of irregular surface roughness on the frictional resistance of ships, Proceedings of International Symposium on Ship Viscous Resistance, SSPA Göteborg, 1978.

(4) Musker,A.L. and Lewkowicz,A.K., The effect of ship hull roughness on the development of turbulent boundary layers, Proceedings of International Symposium on Ship Viscous Resistance, SSPA Göteborg, 1978.

(5) Sasajima,H., and Himeno,Y., Scale correction for roughness effect, Journal of the Society of Naval Architects of Japan, No.118, 1965.

(6) Uberoi,S.B.S., Viscous resistance of ships and ship models, Hydro-OG Aerodynamik Laboratorium, Report No. Hy-13, 1969.

(7) Clauser,F.H., Turbulent Boundary Layers in Adverse Pressure Gradients, Journal of the Aeronautical Science, 1954.

(8) Grigson, CWB, Drag coefficients of a range of ship surfaces, International Symposium on Advances in Marine Technology, Trontheim 1979.

(9) Todd,F.H., Skin Friction Resistance and the Effects of Surface Roughness, Trans. of the Society of Naval Architects and Marine Engineers, Vol.59,1951.

(10) Townsin,R.L., Byrne,D., Milne,A., and Svensen,T., Speed, Power and Roughness: The Economics of Outer Bottom Maintenance, Trans. of the Royal Institution of Naval Architects, Vo.122, 1980.

(11) Baba,E. and Tokunaga,K., Study of Local Roughness Effect on Ship Resistance for Effective Cleaning and Protection of Hull Surface, Shipboard Energy Conservation, 1980.

(12) Schlichting,H., Boundary Layer Theory,Pergamon Press,1955.

(13) Townsin,R.L., Milne,A. and Medhurst,J.S., The Differential maintenance of outer bottom hull surfaces, IMAEM Congress, Trieste 1981.

Table 1 Frictional resistance increase for a full form of 220 m at 15 kn

Karlsson's rough surfaces			$10^3 \times \Delta C_f$		
surface Number	Peak to valley height (μm) in 52.5mm length	RMS amplitude (μm)	Calculations along Streamlines	Calculations for Flat plate	
				Karlsson	Authors
1	132	31	0.122	0.135	0.109
2	344	65	0.213	0.256	0.197
3	825	183	0.520	0.616	0.491
4	154	29	0.092	0.105	0.080

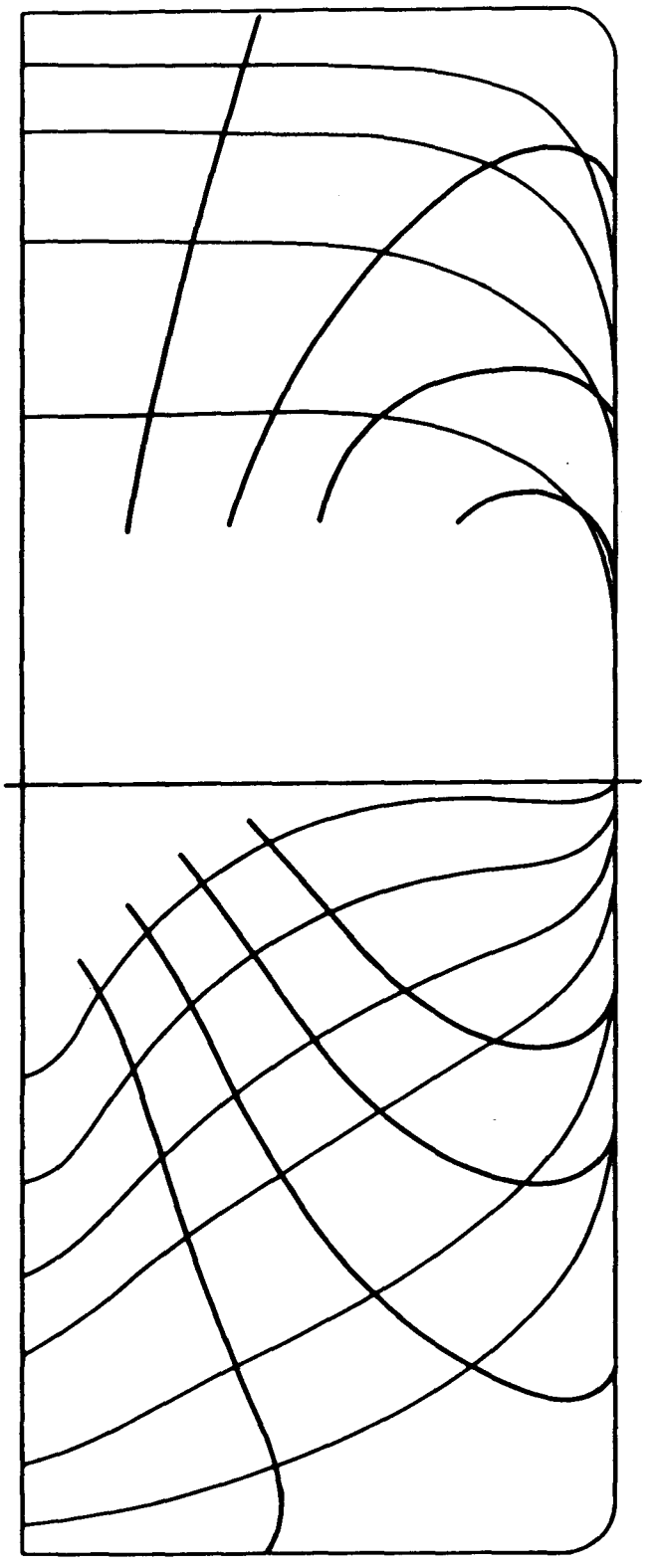

Fig. 1 Body plan and potential streamlines

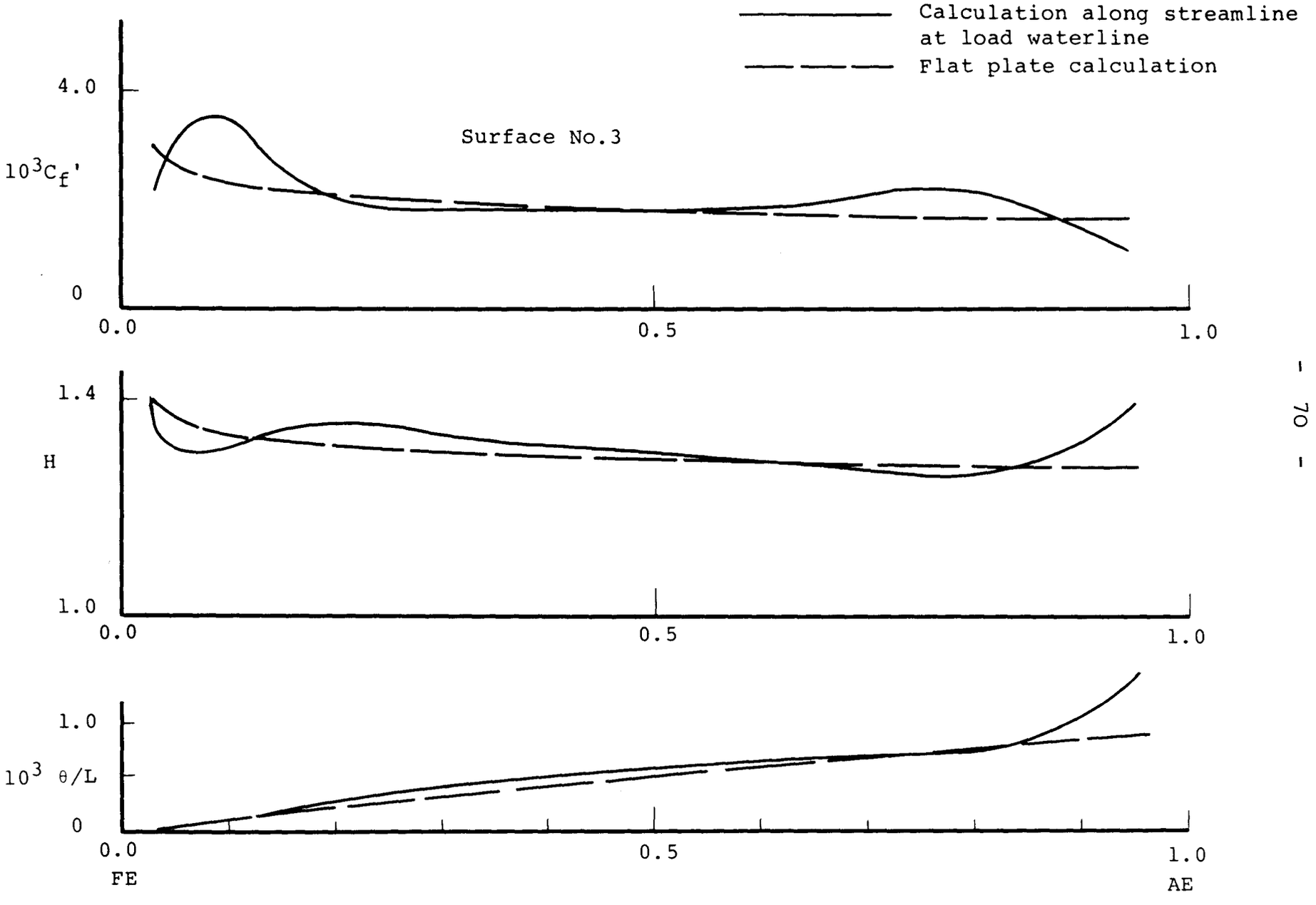

Fig. 2 Effect of pressure gradient on boundary layer parameters for rough surface

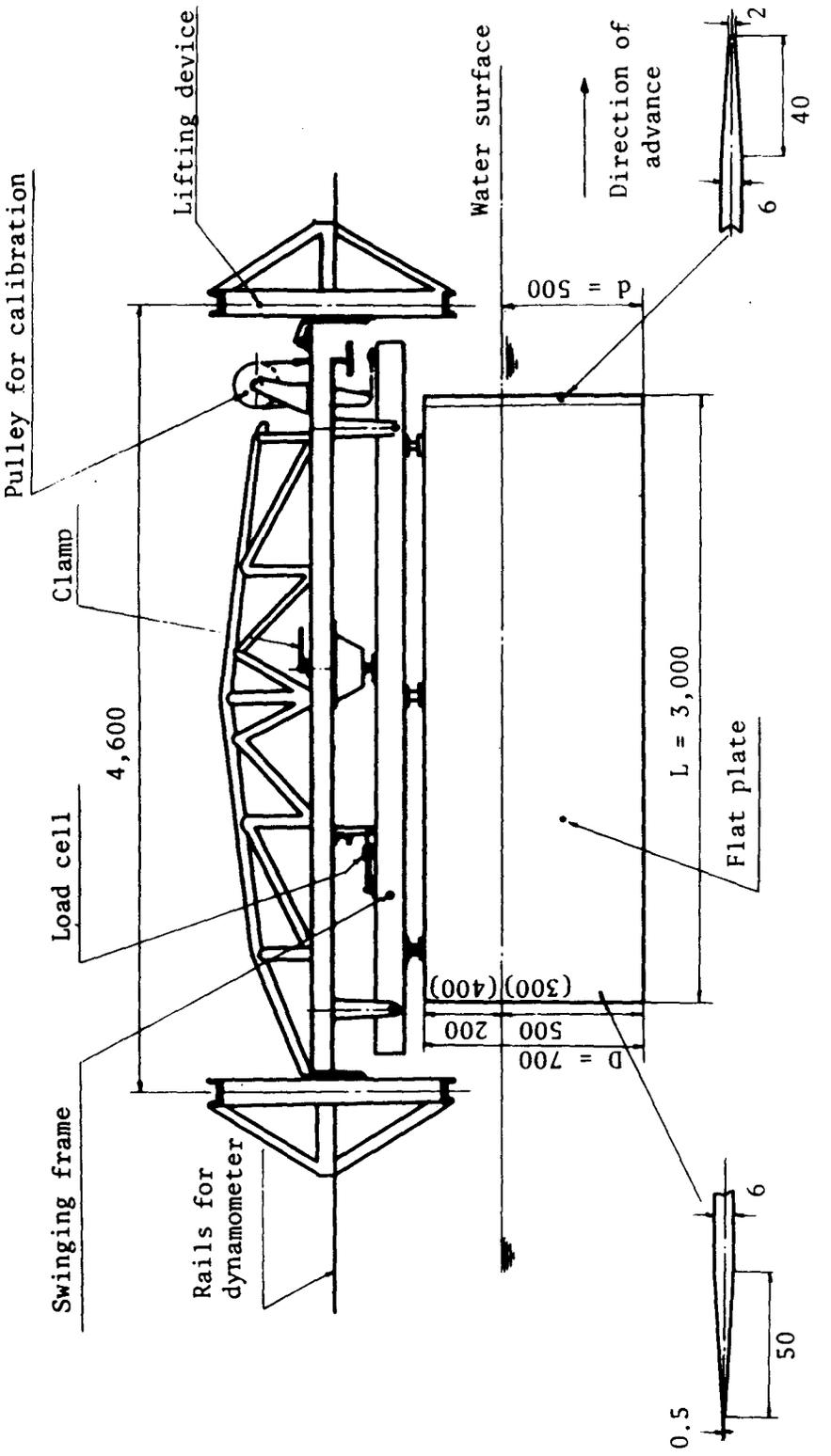

Fig.3 Arrangement of test apparatus for 3 m flat plate resistance test

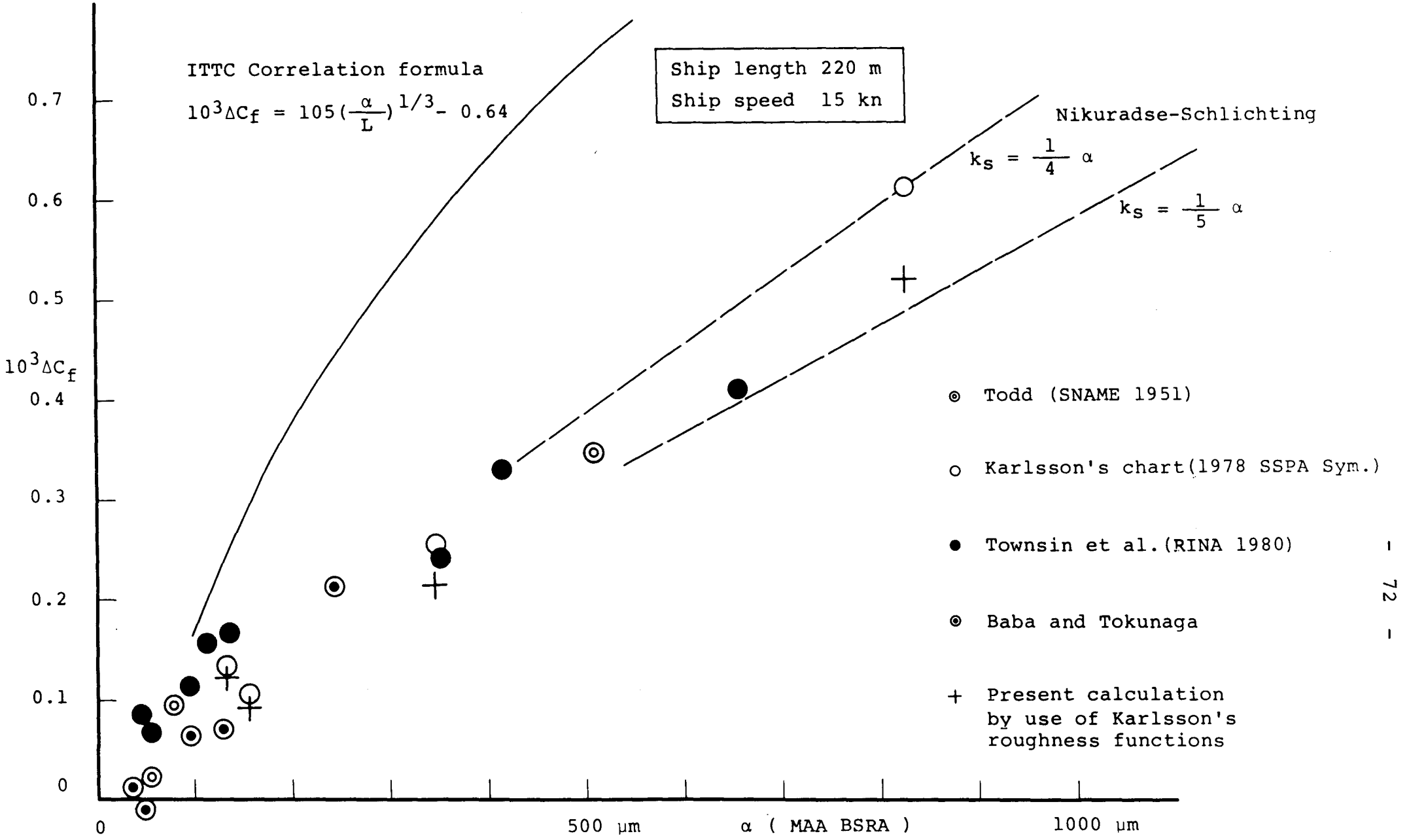

Fig.4 Relatinship between ΔC_f and roughness height

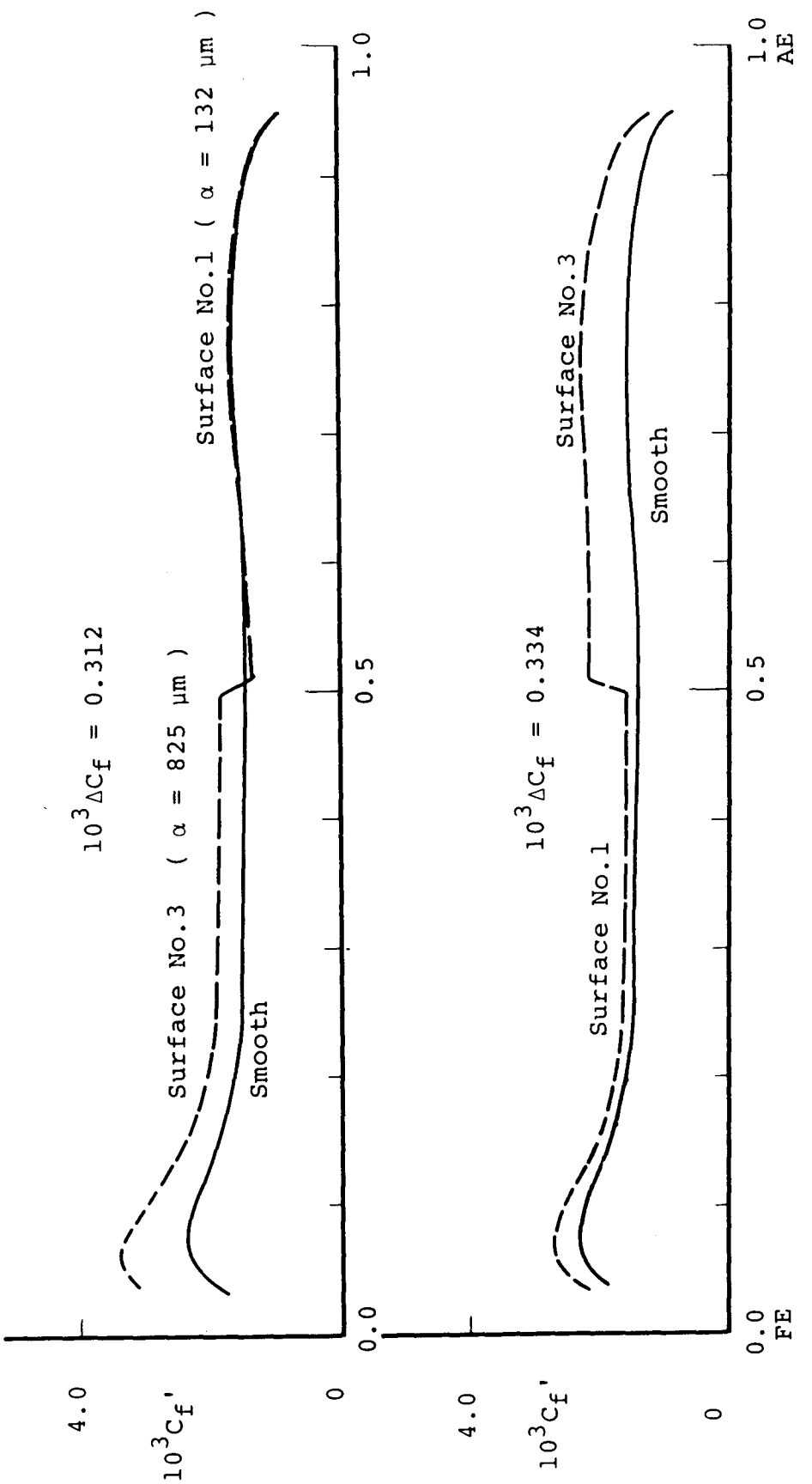

Fig. 5 Combination of different surfaces

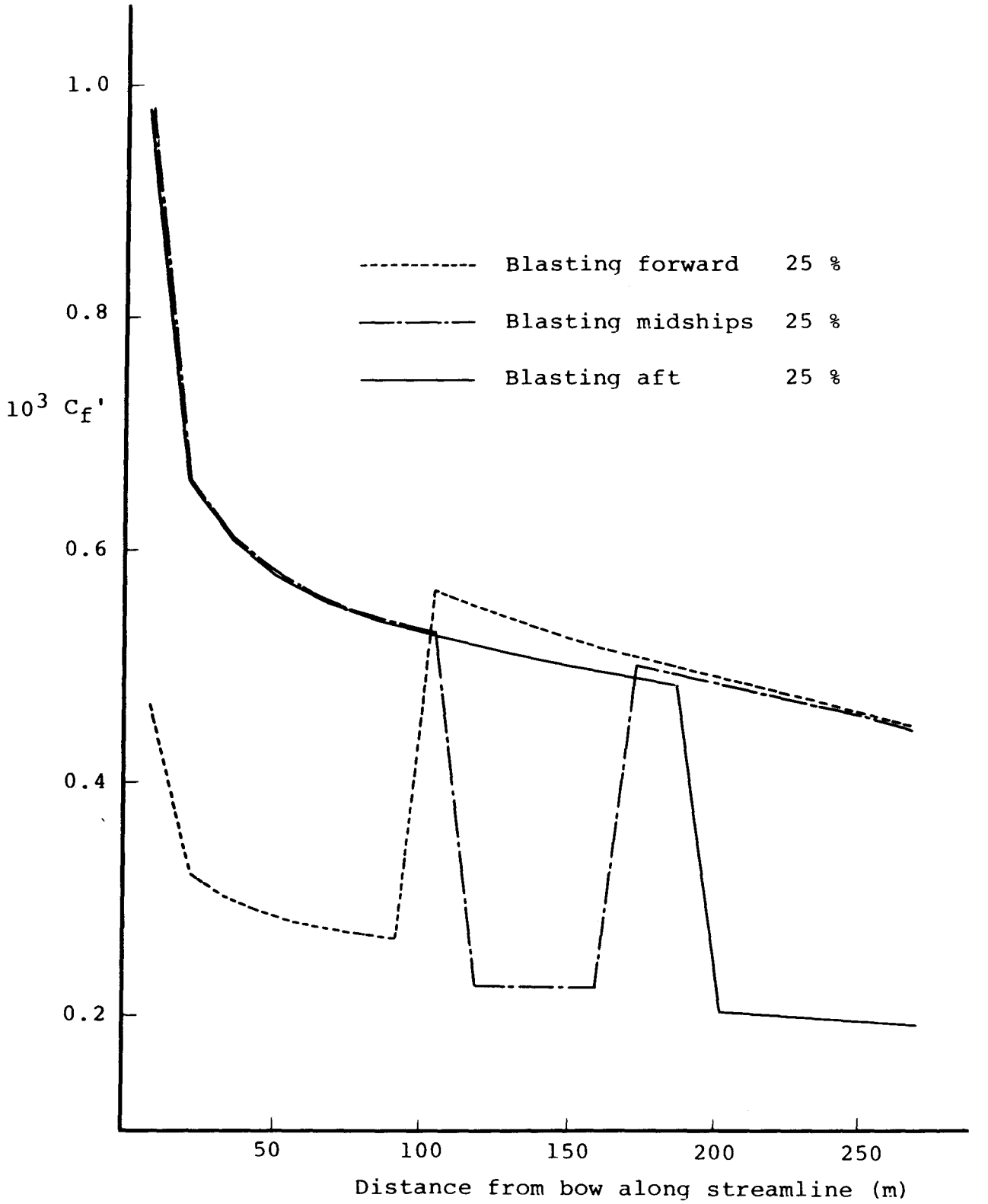

Fig.6 Distribution of local skin friction coefficient with different hull treatment
(Townsin et at. IMAEM CONGRESS, TRIESTE 1981)

Appendix 1 Karlsson's roughness data from ref.(3)

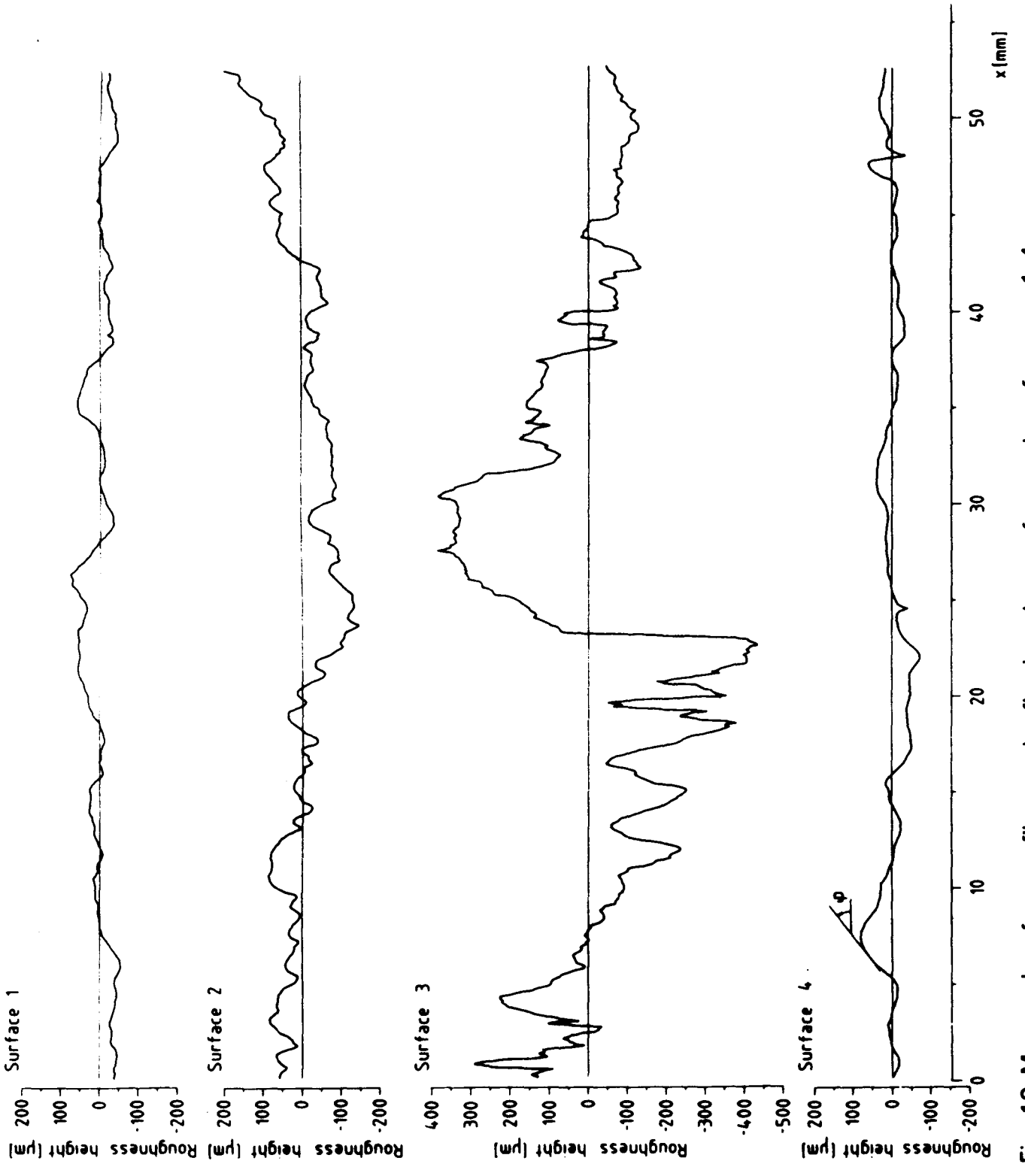

Fig. 10 Measured surface profiles on the floating element for rough surfaces no 1–4

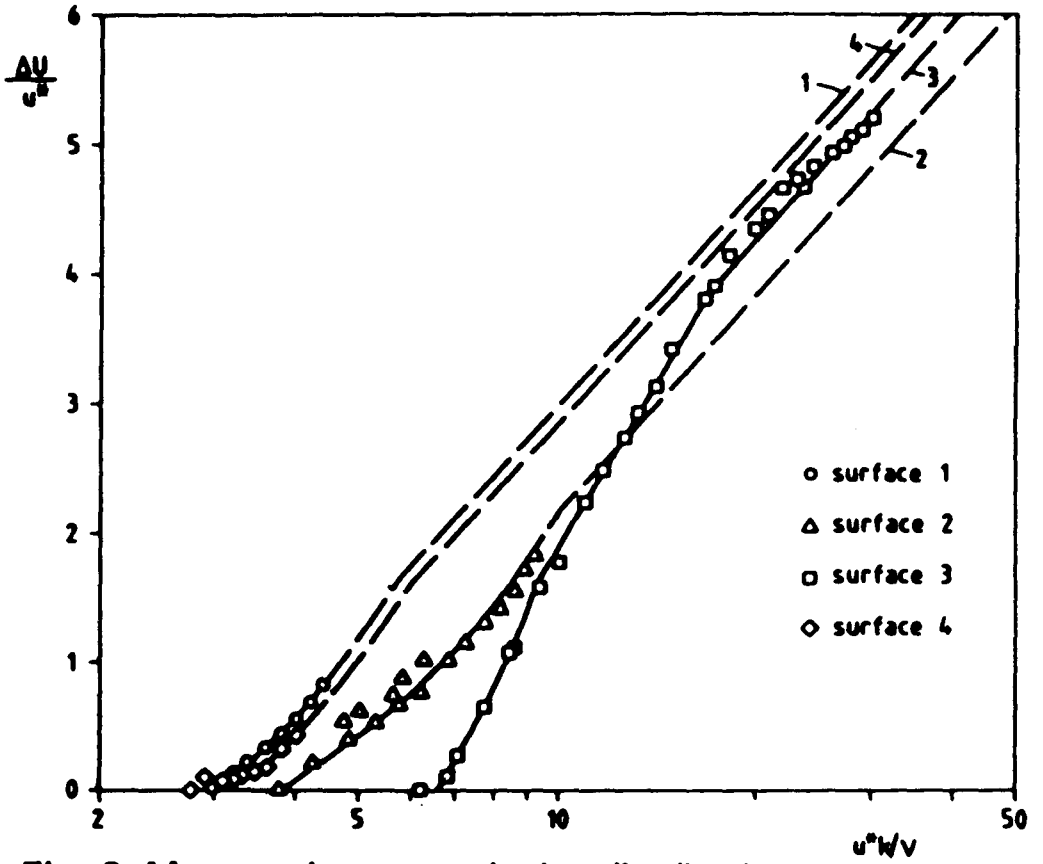

Fig. 9 Measured mean velocity distributions at station 7 (on the floating element) for different free-stream velocities on rough surface no 3

Table 1. Analytical description and extrapolation of measured roughness functions for rough surfaces no 1 - 4.

Surface 1: σ_y = 31 μm	Surface 2: σ_y = 65 μm
$\frac{\Delta U}{u^*} = 0$; $0 \leq R_k \leq 3.05$,	$\frac{\Delta U}{u^*} = 0$; $0 \leq R_k \leq 3.8$,
$\frac{\Delta U}{u^*} = 0.6(R_k - 3.05)$; $3.05 < R_k \leq 5.7$,	$\frac{\Delta U}{u^*} = 0.35(R_k - 3.8)$; $3.8 < R_k \leq 10$,
$\frac{\Delta U}{u^*} = 2.44 \ln R_k - 2.65$; $R_k > 5.7$.	$\frac{\Delta U}{u^*} = 2.44 \ln R_k - 3.45$; $R_k > 10$.
Surface 3: σ_y = 183 μm	Surface 4: σ_y = 29 μm
$\frac{\Delta U}{u^*} = 0$; $0 \leq R_k \leq 6.6$,	$\frac{\Delta U}{u^*} = 0$; $0 \leq R_k \leq 3.3$,
$\frac{\Delta U}{u^*} = 0.6(R_k - 6.6)$; $6.6 < R_k \leq 9.0$,	$\frac{\Delta U}{u^*} = 0.6(R_k - 3,3)$; $3.3 < R_k \leq 6.0$,
$\frac{\Delta U}{u^*} = 3.8 \ln R_k - 6.9$; $9.0 < R_k \leq 17$,	$\frac{\Delta U}{u^*} = 2.44 \ln R_k - 2.75$; $R_k > 6.0$.
$\frac{\Delta U}{u^*} = 2.44 \ln R_k - 3.05$; $R_k > 17$.	

Appendix 2 Examination of Sasajima and Himeno's scaling law for rough surface resistance from ref.(11)

Table 6. Examination of scaling law of resistance increase due to roughness

Sasajima and Himeno's formula: $\Delta C_{f2} = \Delta C_{f1} [C_{f2\ smooth} / C_{f1\ smooth}]^2$ with vk/ν = constant					
Suffix 1: 4.2^m model, Suffix 2: 7^m model, k = 0.8 mm $C_{fi} = 0.455/(\log vL/\nu)^{2.58}$ (i=1,2), Water temp. 21.7°C					
	7 m model Reynolds No. 4.2m model	3.723×10^6 2.234	5.584 3.350	7.445 4.467	9.307 5.584
Roughness cond.	vk/ν	415	623	830	1038
rough smooth 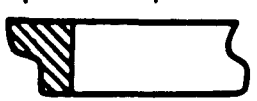 $SS2\frac{1}{2}$	(1) ΔC_{f1}	0.00227	0.00245	0.00252	0.00281
	(2) $(C_{f2}/C_{f1})^2$	0.8376	0.8415	0.8442	0.8463
	(1)x(2) predicted ΔC_{f2}	0.00190	0.00206	0.00213	0.00238
	(3) measured ΔC_{f2}	0.00134	0.00191	0.00228	0.00237
	(1)x(2)/(3)	1.42	1.08	0.93	1.00
 SS5	(1) ΔC_{f1}	0.00457	0.00501	0.00543	0.00577
	(1)x(2)	0.00383	0.00422	0.00451	0.00488
	(3)	0.00311	0.00409	0.00458	0.00472
	(1)x(2)/(3)	1.23	1.03	0.98	1.03
 $SS7\frac{1}{2}$	(1) ΔC_{f1}	0.00656	0.00749	0.00786	0.00848
	(1)x(2)	0.00549	0.00630	0.00664	0.00718
	(3)	0.00450	0.00595	0.00665	0.00678
	(1)x(2)/(3)	1.22	1.06	1.00	1.06
	(1) ΔC_{f1}	0.00895	0.01064	0.01320	0.01532
	(1)x(2)	0.00750	0.00895	0.01114	0.01299
	(3)	0.00657	0.01017	0.01150	0.01218
	(1)x(2)/(3)	1.14	0.88	0.97	1.06

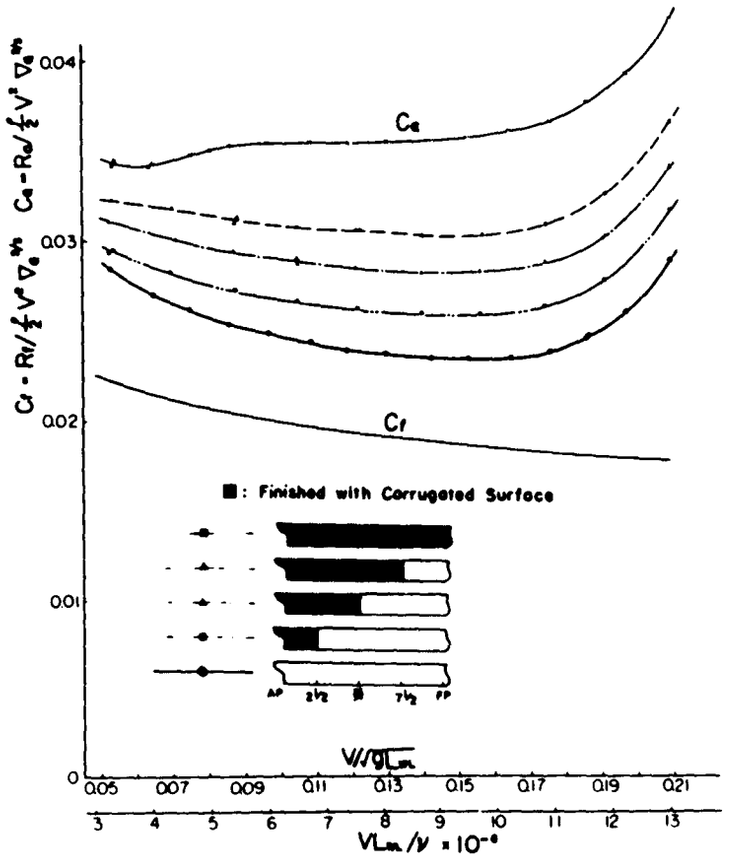

Fig. 10 Total resistance coefficient of 7 m tanker model with corrugated surface

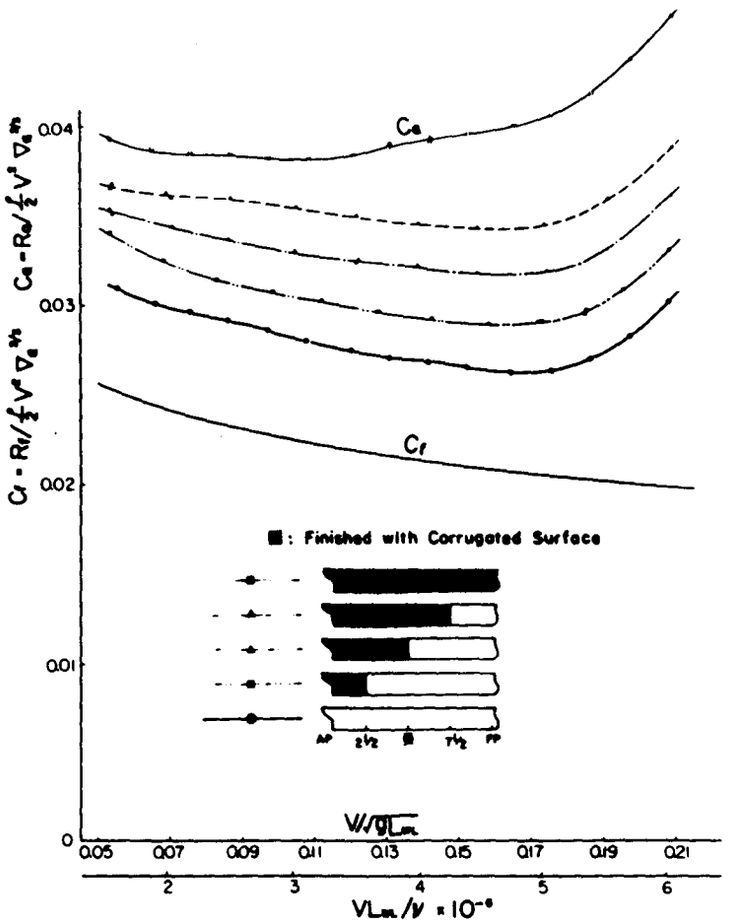

Fig. 11 Total resistance coefficient of 4.2 m tanker model with corrugated surface

Design of devices for improving the wake flow into the propeller plane

G.E. Gadd

This paper relates to the serious problems which may arise if the boundary layer development over the hull leads to an unsatisfactory wake in the propeller plane. Such problems occur most commonly, perhaps, with single screw merchant ship forms as dealt with in this paper. They can also arise however with twin screw warship forms if the wake shadows from bossings or shaft support brackets are excessive. For both types of ship the result of unsatisfactory wake flow can be vibration and noise, possibly causing fatigue damage to the ship, as well as annoyance and discomfort to the crew, with, in the case of warships, unacceptable levels of radiated noise.

Ways of avoiding propeller excited vibration

The best way of avoiding propeller excited vibration is by careful design of the stern to ensure that there are no local regions of unduly low speed in the flow entering the propeller disc. Sometimes however designs which it had been thought would be acceptable turn out not to be so in practice, and it is then necessary to devise a cure. In such cases for single screw ships a successful cure has often been effected by attaching a large fin above the propeller. This however is a major structure involving considerable cost and difficulty in its manufacture and attachment to the hull.

Flow deflectors

A much cheaper alternative method of curing the problem, applicable either to single screw ships or to twin screw ships

with bossings, is to fit flow deflectors. In the two full scale cases with which the NMI has been concerned to date, /7/ these have been relatively small cambered aerofoils welded to the hull (fig. 13). In the first such case these deflectors made a considerable improvement and in the second they cured the problem completely. However the positioning of such deflectors is critical to their success, and in the cases just quoted this was only achieved after making initial full scale trials with less successful arrangements. There is therefore a need to devise reliable model technique for determining an optimum arrangement of flow deflectors before fitting these to the full scale ship.

The present paper describes some experiments relating to the second (the most successful) case mentioned above. It was hoped to develop a technique such that it could have been predicted from the results obtained that the deflectors would work on the full scale. Then the same technique could be used in any future case which may arise, enabling a successful arrangement to be fitted to the ship straight away and avoiding the need for full scale experimentation.

The reasons why towing tank tests with scaled flow deflectors are unreliable

The stern in the case considered tended to the bulbous type. This made it especially difficult to determine the best deflector arrangement by tests on ordinary towing tank models, for with such a stern much larger girthwise variations of boundary layer thickness are likely to occur on the model than on the ship. Thus fig. 14 shows wake contours calculated by Gadd's method /1/ at the plane of the flow deflectors. The deflectors on the ship were situated in the region of the 3, 5 and 7 m waterlines with their trailing edges on station 3/4. It can be seen that according to the calculations the deflectors near the 5 m waterline would be in a region of much lower flow speed on the model than on the ship, whereas there would

be much smaller differences for the 3 m and 7 m levels. Moreover at the 3 and 5 m waterlines the flow angles at the hull surface are predicted to be considerably different on the model from those on the ship, as can be seen from figs. 15 and 16. Thus the calculations suggest that the model scale flow deflectors at the 3 m and 5 m waterlines will behave differently from the full scale ones.

Experimental confirmation of theoretical predictions

At least at the model scale the theoretical predictions appear to be qualitatively correct. Thus the tracing of a photograph of flow directions in the towing tank, as indicated by tufts, in fig. 15, shows that these directions agree quite well with the predicted ones. Moreover one of the wind tunnel models referred to earlier was of this same hull form, and boundary layer profiles measured on this model are not too dissimilar from the predicted ones, as can be seen from fig.17.

Foreshortened models with correct afterbody shape

The above discussion has shown that it is hardly surprising that difficulties were experienced in correctly predicting the full scale behaviour of flow deflectors from tests on exactly scaled models. It would clearly better to use a model which, whilst having the correct afterbody shape where the deflectors have to be fitted, was distorted upstream in such a way that the boundary layer flowing over the deflectors approximated more closely in its thickness and flow angles to that on the full scale ship. This led to the consideration of a distorted double model as shown in fig. 18. (It is shown here in its final test configuration in a cavitation tunnel, as discussed below.) Ideally, the flow in the propeller plane of such a model should resemble that on the ship, but the natural unmodified flow might not do this, so that corrective

devices might have to be attached to the model. Any such devices would have to be placed well forward of the flow deflectors which it was required to test.

Calculations to assess whether flow corrective devices are likely to be required

To give a preliminary indication whether or not such corrective devices were likely to be needed, further calculations were made. Hull surface flow directions on the fore shortened model were predicted as in fig. 19 to be even more upwards at the plane of the flow deflectors than those on the full scale ship, suggesting that an artificial cross-flow in the boundary layer might need to be introduced. Propeller plane wakes were also calculated for comparison with those calculated for the undistorted model and ship. Such calculations are at best very crude, and as can be seen from fig. 20 they fail to predict the narrow but quite intense wake in the upper half of the propeller disc on the undistorted model. This narrowed wake can be associated with the streamwise vorticity generated by the bulbous stern, and although this in itself is predicted quite well (fig. 15), its effects on the wake are not. The prediction for the full scale case (fig. 21) appears to be even worse, though here we have only a scale-corrected wake with which to make comparison, and the validity of the correction procedure is perhaps open to question. Despite the inaccuracy of the predictions in figs. 20 and 21 however, the difference in character between these predicted wakes and that predicted for the foreshortened model in fig. 22 is sufficiently marked to reinforce the suggestion that corrective devices are necessary for the latter model. The comparative lack of streamwise vorticity in the afterbody flow has led to a wake which is wider at the top and narrower at the bottom than for the undistorted hull. In fact the predicted wake is not too unrealistic for the foreshortened model as can be seen from fig. 22: the measurements shown there were made in the course of the experiments described in the next section.

Wind tunnel experiments with foreshortened model

For the present investigation, where it was desired to establish whether or not the foreshortened model could give realistic results, it was intended from the outset that ultimately this model should be tested in the cavitation tunnel, as in fig. 18. This would enable fluctuation pressure levels to be measured with various flow deflector arrangements, for direct comparison with the full scale results. However it would have been very time, consuming to perform the necessary trial and error experimentation to find the appropriate flow correcting devices in the cavitation tunnel. A wind tunnel is much more convenient for such a purpose. Accordingly the model was tested in a wind tunnel fitted with an octogonal sleeve insert as in fig. 23. The sleeve simulated approximately the circular working section of the cavitation tunnel, thus ensuring that the model would operate at the same blockage ratio in the two facilities. It could therefore be assumed that any wake established in the wind tunnel would be duplicated in the cavitation tunnel.

For future applications of the foreshortened model technique, especially where results have to be obtained quickly, it may not be necessary to measure cavitation pressures. Instead, after establishing a realistic effective naked hull wake, it may well be sufficient to find deflector arrangements which significantly improve this wake. There would then be no need to test the wind tunnel model in the octogonal sleeve insert - it would simply be tested in the normal wind tunnel working section.

The first part of the present experiments in the wind tunnel consisted in attempt to modify the bare model wake so that it became close to the assumed full scale ship wake, shown on the right hand side of fig. 21. The first improvement involved fitting a perforated plate to the aft model support, as shown in fig. 18 for the final cavitation tunnel configuration. This made the flow steadier and slightly reduced the wake intensity,

perhaps due to an alleviation of the adverse effects of tunnel blockage in the rather constricted working section. The measured wake shown in fig. 22 was with this plate fitted, but it was clearly still far from the required one of fig. 21. The closest approach to this that could be obtained, after many trials of alternative arrangements, was with a pair of vortex generators, similar to but larger than the scaled flow deflectors, at station $1^1/2$ near the 3 m waterline, as in figure 18. These produced longitudinal vortices inducing an artificial cross-flow in the boundary layer to simulate more closely the required flow. The vortices were very concentrated for a short distance downstream of the generator tips, where they could be visualized by tufts which rapidly spun round. However vortex bursting then seemed to occur, with the vorticity becoming more widely diffused. This took place upstream of the flow deflector position. Thus it could be assumed that if the propeller plane wake was realistic, the boundary layer flow at the flow deflector plane would also be sufficiently similar to that on the full scale ship. This would mean that the flow deflectors could be expected to behave in a similar way on the model as on the ship.

The final effective naked hull wake achieved was not perfect, as can be seen from a comparison of fig. 24a with fig. 21, but it was certainly far better than without the upstream vortex generators. It was considered to be sufficiently realistic to proceed to the investigation of the additional modifications of the wake induced by the flow deflectors.

As mentioned above, two deflector arrangements were tried on the ship, one with the two lower pairs of deflectors sketched in figure 18, and the other, more successfully, with the additional upper pair as well. It was conjectured however that the two upper pairs of flow deflectors, or conceivably even the top pair alone, would also have been effective. Therefore it was decided to investigate these arrangements as well as the ones actually used on the ship.

The resulting wakes are shown in fig. 24. It can be seen that the biggest improvement over the wake with no flow deflectors is produced by the 3 pair configuration, as actually used on the ship, but the two upper pairs of deflectors give nearly as good a result. The two lower pairs give a significant, but more modest, improvement, and there is also some improvement with the upper pair alone.

Thus on the basis of the wind tunnel experiments it would be expected that the 3 pair or upper 2 pair arrangements of flow deflectors would be very beneficial for alleviating vibration and noise, that the two lower pair arrangement would be quite beneficial, and that the upper pair of deflectors alone would produce a small improvement.

Comparison with towing tank experiments on undistorted model

Different conclusions would however have been reached from tests on exactly scaled deflectors on a normal towing tank model. Fig. 25 shows that although the three deflector arrangement produces a significant, though less marked, improvement than that shown in fig. 24, the arrangement with the two lower pairs of deflectors actually makes the wake slightly worse. Thus it would be expected to be of no benefit at all on the ship.

Cavitation tunnel experiments with foreshortened model

Pressure fluctuation levels were measured in the cavitation tunnel at the reflection plane above the screw at conditions corresponding to ballast conditions on the ship at 115 and 123 rpm. Fig. 26 shows the harmonic components of the non-dimensional pressure fluctuation levels $K_p = p/\rho\, n^2 D^2$ for the various flow deflector arrangements.

The results broadly confirm the expectations of section: Wind tunnel experiments ..., page 5, as inferred from the measured wake flows of fig. 24, though the upper pair of deflectors alone appears in the pressure measurements to be about as good as the two lower pairs, whereas the latter arrangement would have been expected to be better than the upper pair alone, according to fig. 24.

Comparison with ship results

Results are available for the ship in ballast condition with no flow deflectors, with the two lower pairs, and with all three pairs, and in load condition with all three pairs of deflectors only.

Qualitatively the finding that in ballast draft the two lower pairs gave some improvement and the three pairs a big improvement is borne out by vibration levels measured at the stern gland (fig. 27). Pressure fluctuation levels were also measured and here the results are somewhat more confusing, as fig. 28 shows that the two lower pairs of deflectors seem to make a big improvement at 115 rpm but to make things worse at 123 rpm, despite the fact that the stern gland vibration level at that speed is reduced (fig. 27). At both speeds however the three pair configuration is a considerable improvement over the naked hull configuration.

The non dimensional pressure levels in fig. 28 are considerably larger than those measured in the model tests in fig. 26. These figures refer to the ballast condition. In the load condition, on the other hand, there is good agreement between the levels measured on the model and on the ship, as can be seen from fig. 29.

Possible causes of differences between model and ship results

One obvious possible explanation of the differences between figs. 26 and 28 is that the wake without flow deflectors on the model does not simulate sufficiently accurately that on the ship. Certainly the wake peak in fig. 24a is a little less sharp than that aimed at, shown in fig. 21. This might account for the lower pressure levels without flow deflectors in fig. 26 compared with fig. 28, and for the apparently excessive reduction in the pressure levels brought about by the 3 pairs of deflectors in fig. 26. However the ballast and load wakes are quite similar, so if such a deficiency in modelling the wake were the main cause of the discrepancies, it would be expected that the model tests for the load condition would also indicate pressure levels which are much too low. Fig. 29 shows that this is not the case. The scale of plotting here is different from that of figs. 26 and 28, it should be noted, and the model predictions are for a level not much different from those in the ballast case, fig. 26.

An alternative explanation for the discrepancies between figs. 26 and 28 is that in the ballast condition a great quantity of air bubbles is formed at the bulbous bow, which breaks the surface then. These bubbles may be carried along under the hull and may significantly affect the cavitation pressures. In the load condition the bulb is fully immersed and bubbles are not formed. The bow for this ship is closely similar to that for the ship discussed in /8/, where air bubble entrainment was considered to be one of the primary causes of the pressure fluctuations experienced in the ballast condition. The present cavitation tunnel tests do not attempt to simulate the effects of such entrained bubbles, and this may well be why the model scale pressure levels at ballast draft are lower than on the ship.

Be that as it may, even if quantitatively the results from the foreshortened model are judged to be in error, they give a qualitative picture of the effects of the various deflector

arrangements which is substantially correct. It is felt, therefore, that such a technique is a useful one to use in any future tests of flow deflectors for curing vibration problems, and as suggested, wind tunnel tests alone, with assessment of the resulting wakes, would probably be sufficient for this purposes.

Concluding remarks

The experiments described in the foregoing are examples of how useful the wind tunnel can be as an adjunct to the investigation of what at first sight my seem to be purely hydrodynamic problems.

Acknowledgements

This work was supported by the Ship and Marine Technology Requirements Board of the Department of Industry, HM Government, UK. Acknowledgement is also due to the industry sponsors of the recently completed PHIVE programme.

References

/1/ Gadd, G.E.: "A Simple Calculation Method for Assessing the Quality of the Viscous Flow over a Ship's Stern". Paper presented at the International Symposium on Ship Viscous Resistance, SSPA, Göteborg, Sweden, 1978.

/2/ Klebanoff, P.S.: NACA Report 1110, 1952

/3/ Bradshaw, P.: "Conditions for the existence of an inertial subrange in turbulent flow". Aeronautical Research Council R&M 3603, 1969.

/4/ Townsend, A.A.: "The structure of turbulent shear flow". 2nd edition, Cambridge University Press, 1976.

/5/ Odabasi, A.Y. and O. Saylan: "GEMAK-a method for calculating the flow around the aft-end of ships". 13th Symposium on Naval Hydrodynamics Tokyo, 1980.

/6/ Kline, S.J. and A. McClintock: "Describing uncertainty in single-sample experiments". Mechanical Engineering Dept Standorf University, Jan. 1953.

/7/ Gadd, G.E.: "Flow deflectors - a curve for vibration". The Naval Architect, No 6, 1980, p 238.

/8/ Takekuma, K.: "Effect of air bubbles entrained from bow on propeller induced pressure fluctuation". Mitsubishi Technical Bulletin No 140, June 1980.

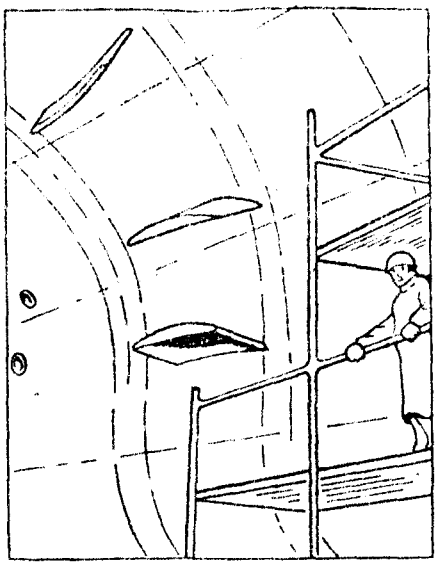

Fig. 13 SKETCH OF FLOW DEFLECTORS BEING FITTED TO SHIP

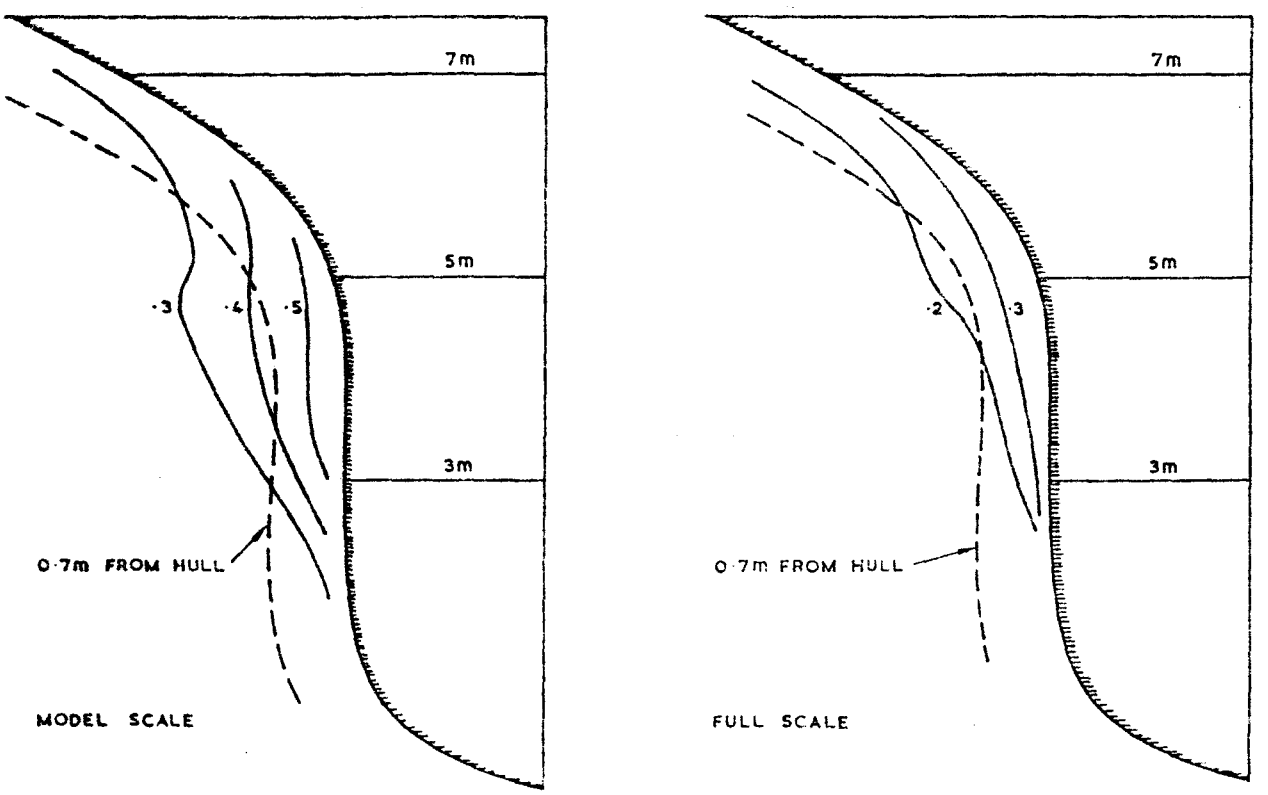

Fig. 14 PREDICTED WAKE CONTOURS AT PLANE OF FLOW DEFLECTORS

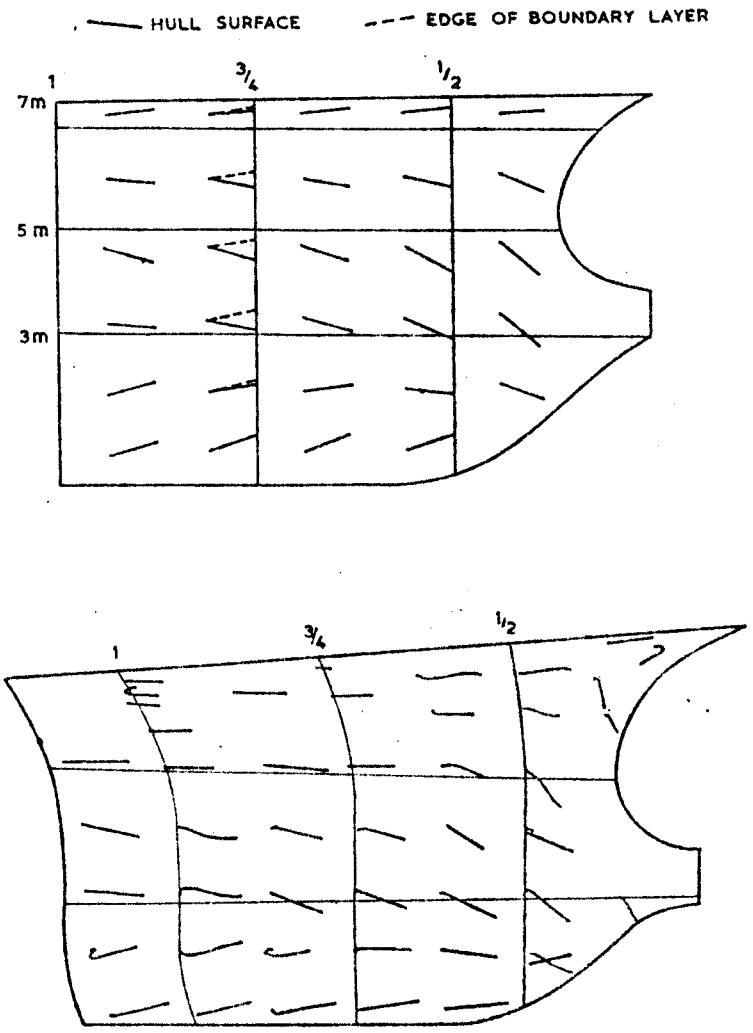

Fig. 15 CALCULATED AND MEASURED FLOW DIRECTIONS FOR MODEL IN BALLAST CONDITION

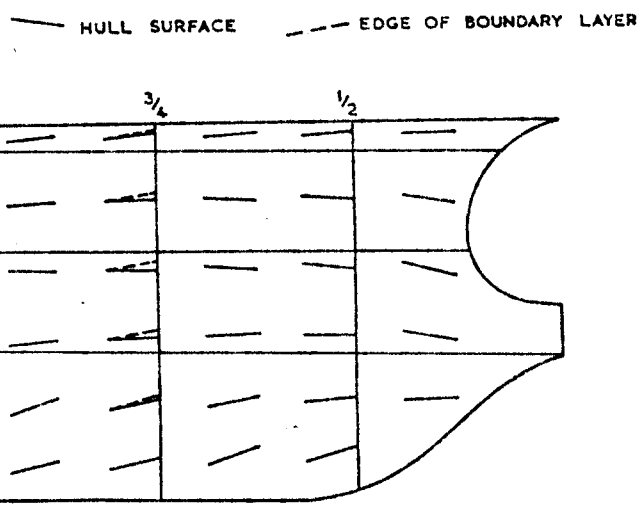

Fig. 16 CALCULATED FLOW DIRECTIONS FOR SHIP IN BALLAST CONDITION

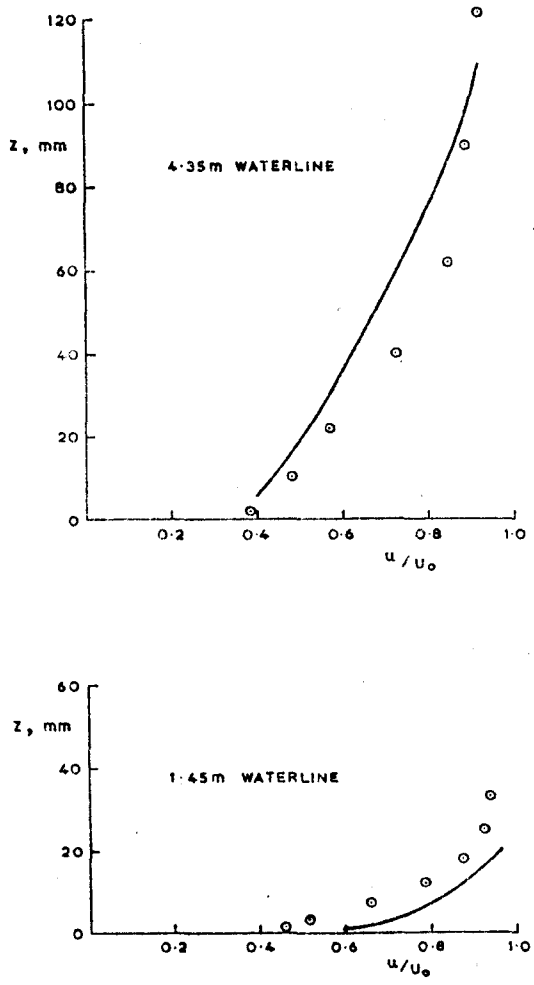

Fig. 17 CALCULATED CURVES COMPARED WITH MEASURED POINTS FOR BOUNDARY LAYER ON 1/30 SCALE MODEL AT STATION 3/4

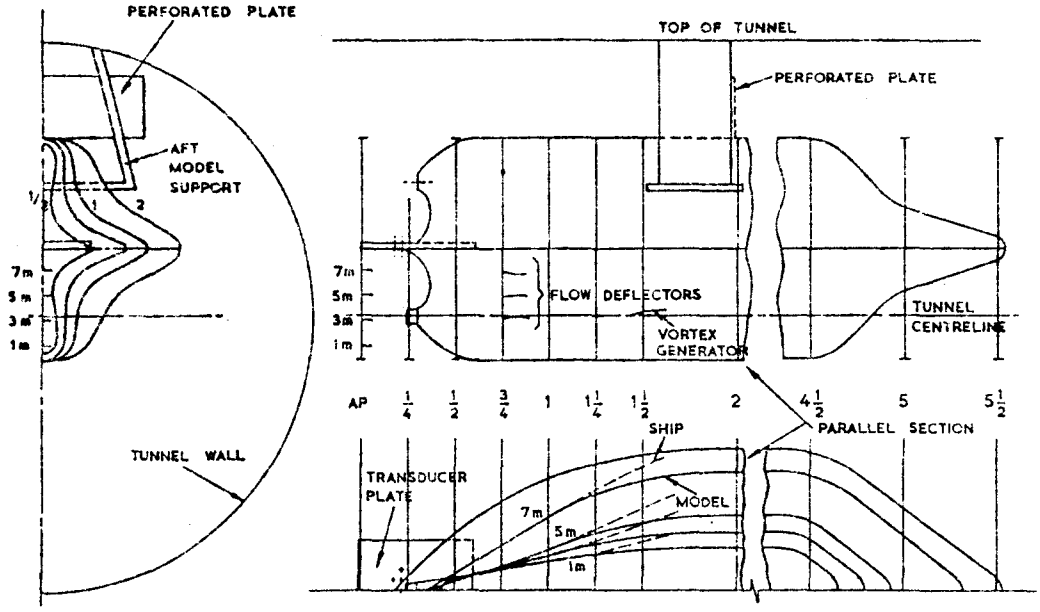

Fig. 18 DOUBLE HULL FORESHORTENED MODEL IN WATER TUNNEL

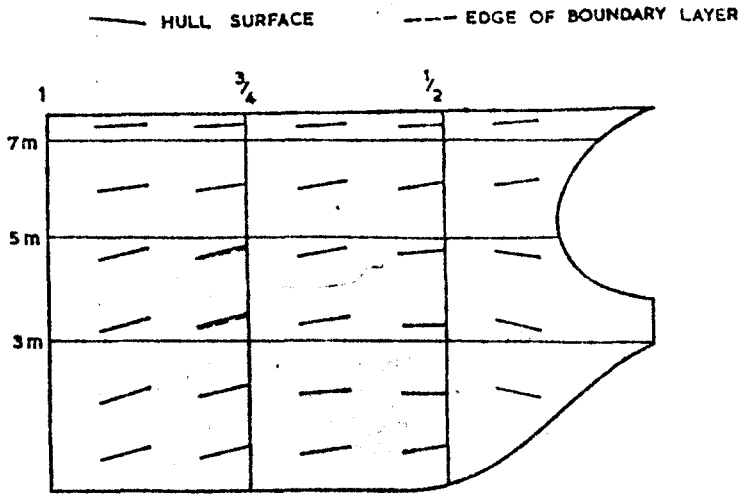

Fig. 19 CALCULATED FLOW DIRECTIONS FOR FORESHORTENED MODEL WITHOUT UPSTREAM VORTEX GENERATORS

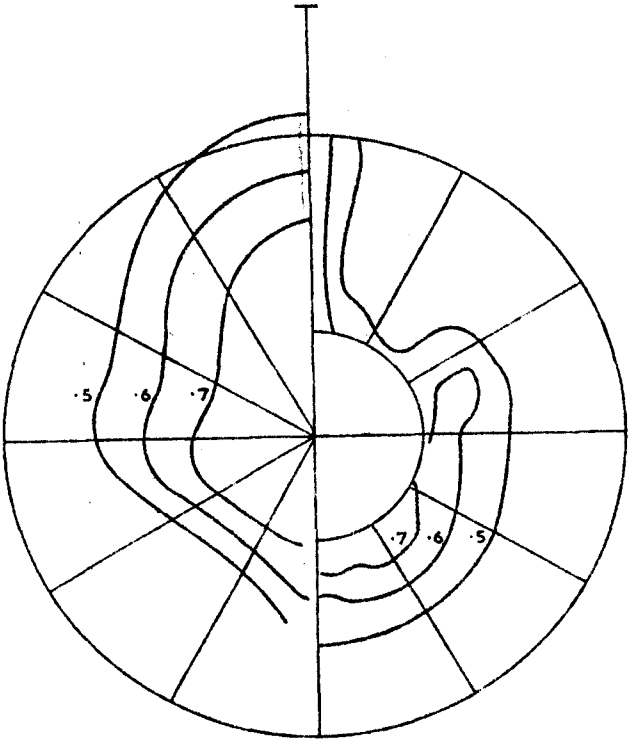

Fig. 20 PROPELLER PLANE WAKE CONTOURS AT MODEL SCALE: LEFT, PREDICTED : RIGHT, MEASURED

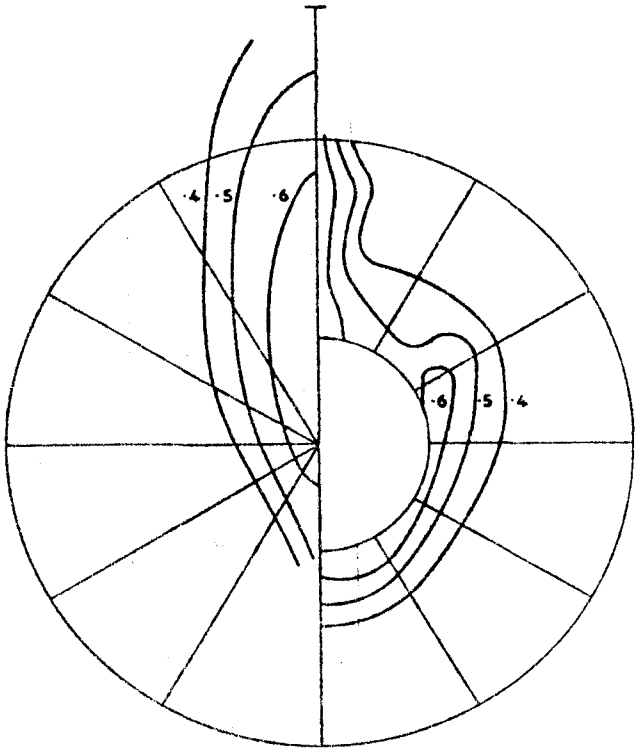

Fig. 21 PROPELLER PLANE WAKE CONTOURS AT FULL SCALE: LEFT, PREDICTED: RIGHT, INFERRED FROM MODEL SCALE MEASUREMENTS

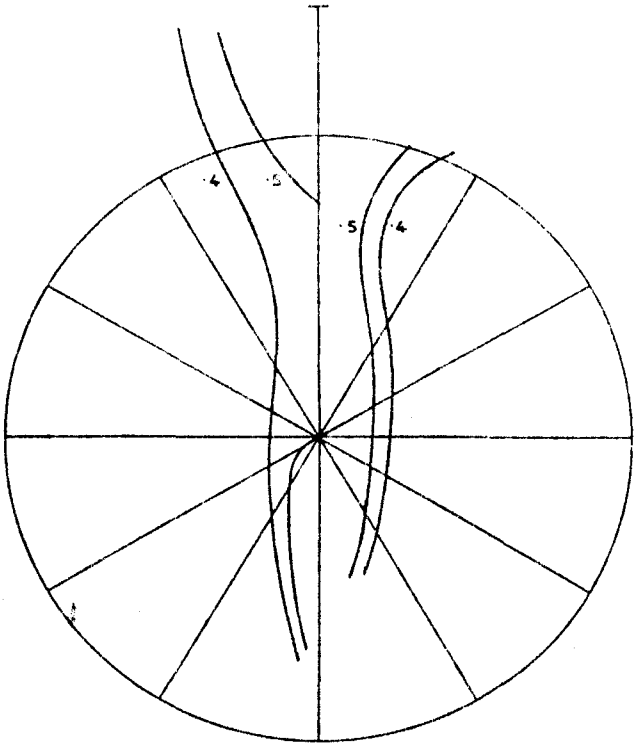

Fig. 22 PROPELLER PLANE WAKE CONTOURS FOR FORESHORTENED MODEL: LEFT, PREDICTED : RIGHT, MEASURED

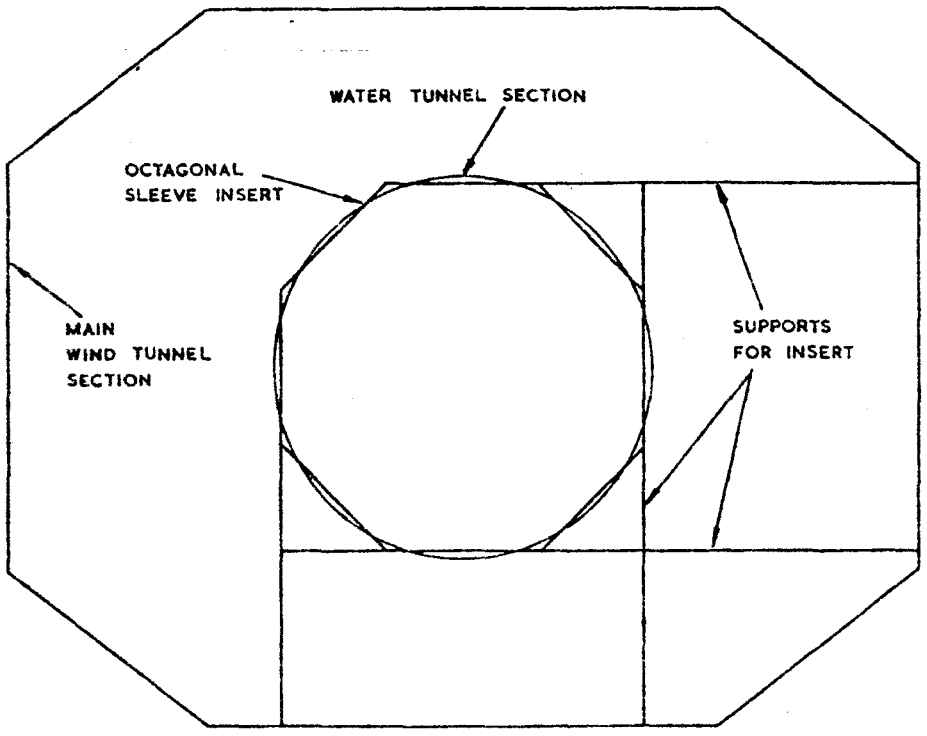

Fig. 23

OCTAGONAL INSERT TO WIND TUNNEL SIMULATING CAVITATION TUNNEL WORKING SECTION

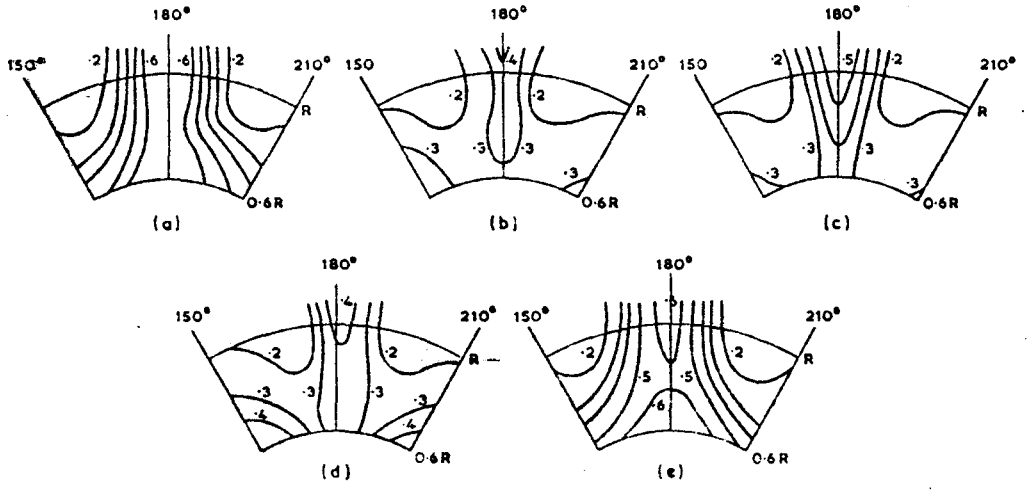

Fig. 24 WAKE CONTOURS IN UPPER PART OF PROPELLER DISC IN WIND TUNNEL
NUMBER OF PAIRS OF FLOW DEFLECTORS: a, NONE : b, 3 : c, LOWER 2 : d, UPPER 2 : e, UPPER 1

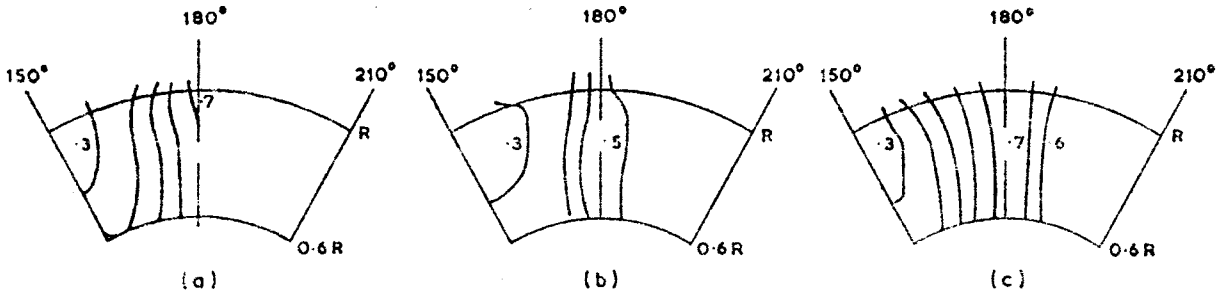

Fig. 25 WAKE CONTOURS IN UPPER PART OF PROPELLER DISC IN TOWING TANK
NUMBER OF PAIRS OF FLOW DEFLECTORS : a, NONE : b, 3 : c, LOWER 2

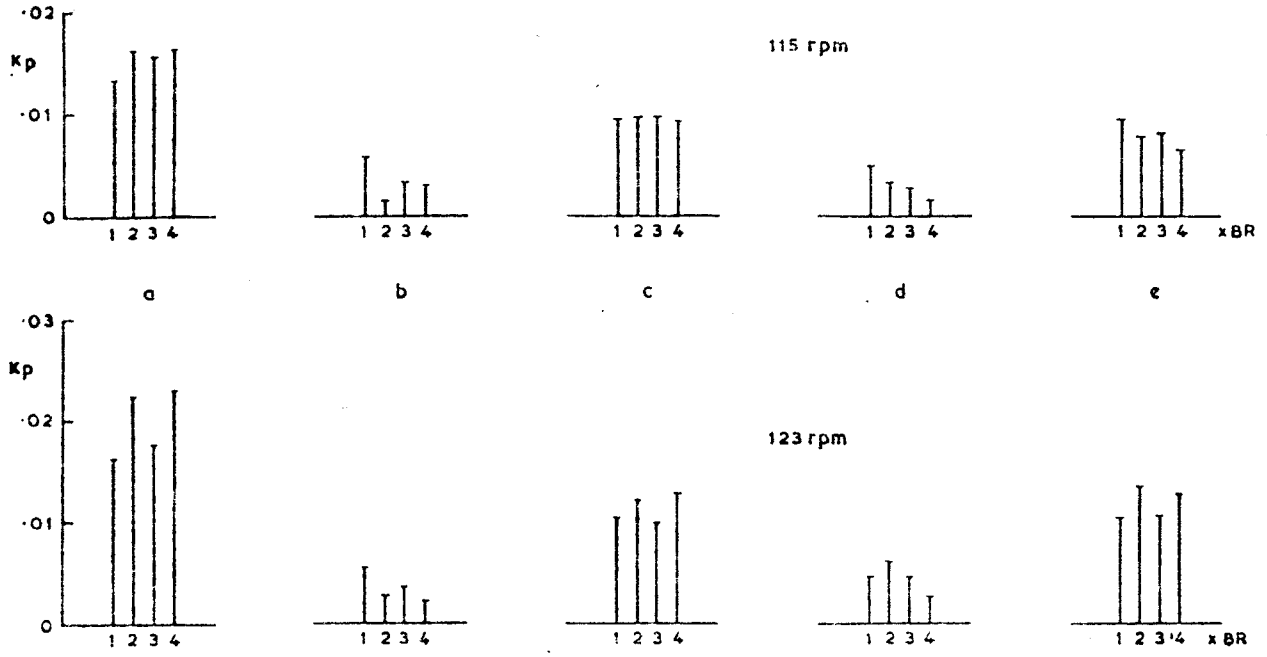

Fig. 26 PRESSURE MEASUREMENTS ON MODEL FOR BALLAST CONDITION
NUMBER OF PAIRS OF FLOW DEFLECTORS : a, NONE : b, 3 : c, LOWER 2 : d, UPPER 2 : e, UPPER 1

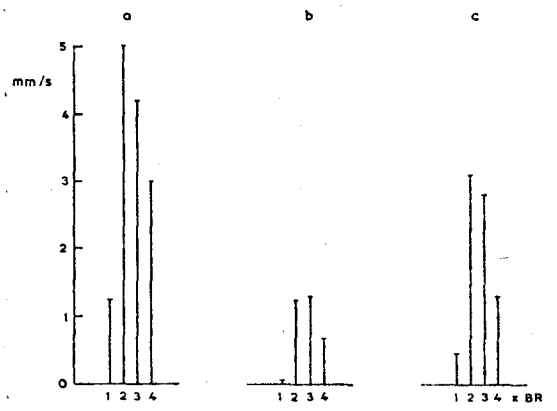

Fig. 27 PEAK VERTICAL VIBRATION VELOCITY AT STERN GLAND ON SHIP IN BALLAST CONDITION AT 123 rpm. NUMBER OF PAIRS OF FLOW DEFLECTORS: a, NONE: b, 3: c, LOWER 2

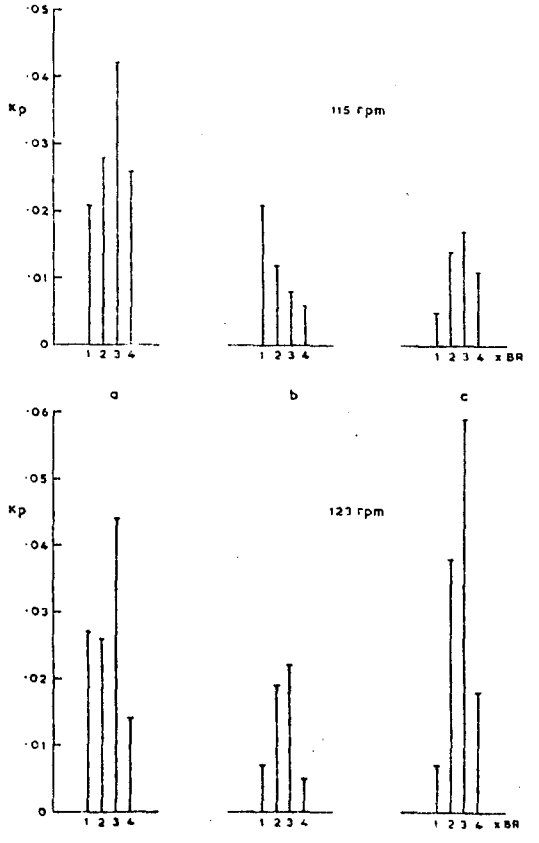

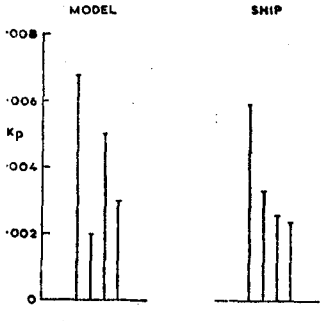

Fig. 29 PRESSURE MEASUREMENTS FOR LOAD CONDITION WITH 3 PAIRS OF FLOW DEFLECTORS AT 123 rpm

Fig. 28 PRESSURE MEASUREMENTS ON SHIP IN BALLAST CONDITION. NUMBER OF PAIRS OF FLOW DEFLECTORS: a, NONE: b, 3: c, LOWER 2